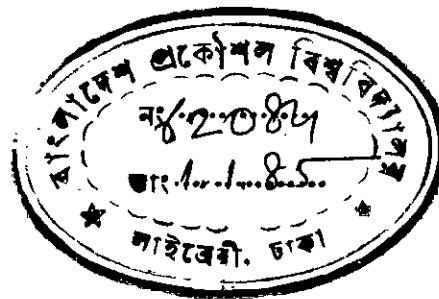AN INVESTIGATION OF LOCAL SCOUR

AROUND BRIDGE PIERS

A THESIS

BY

M.R. KABIR

IN PARTIAL FULFILLMENT OF THE REQUIREMENTS FOR

THE DEGREE OF MASTER OF SCIENCE IN ENGINEERING

(WATER RESOURCES)

BANGLADESH UNIVERSITY OF ENGINEERING AND TECHNOLOGY

DHAKA

AUGUST 1984.

BANGLADESH UNIVERSITY OF ENGINEERING AND TECHNOLOGY

DEPARTMENT OF WATER RESOURCES ENGINEERING
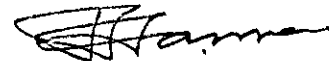
August 23,1984

WE HEREBY RECOMMEND THAT THE THESIS PREPARED BY

M.R. KABIR

ENTITLED <u>AN INVESTIGATION OF LOCAL SCOUR AROUND BRIDGE

PIERS</u> BE ACCEPTED AS FULFILLING THIS PART OF THE

REQUIREMENTS FOR THE DEGREE OF MASTER OF SCIENCE IN

ENGINEERING (WATER RESOURCES).

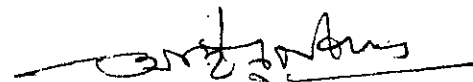|	
Chairman of the Committee	(Dr. M. Shahjahan)
Member	(Dr. A. Hannan)
Member	(Dr.M.K. Alam)
Member	(Dr. A. Nishat)
Head of the Department	(Dr. A. Hannan)

ABSTRACT

Scour around any obstruction is the lowering of a portion of the river bed below its natural level. This is caused due to the large scale eddy structures or a system of vortices which are develop near the obstructions. Though the mechanism of scour is difficult to quantify but its study gives considerable guidance in predicting the magnitude of scour around any hydraulic structure. The determination of scour depth is required for the design of any foundation of hydraulic structure for its safety.

This study was taken to predict the scour depth for different shapes of piers on different bed materials and flow conditions. Four different shapes of piers were used viz., rectangular, circular, round nose and sharp nose. Three sets of runs were conducted for each type of pier for three different bed materials. Field data of Hardinge bridge and East-West Interconnector were collected and analysed along with the experimental data and were compared with the potential predictors of scour depth.

It was observed that relative scour depth d_t/b (where d_t is the depth of scour from water level, b is the width of pier) increases with the increase of Froude Number, $F = V/(gy)^{\frac{1}{2}}$. In addition, it was evident that scour depth is higher for finer grade of bed material and vice versa. The ratio of scour depth to approach flow depth was found to be constant at a value of 1.95.

Empirical formulae of Inglis (1949) Blench (1962) and Shen-et al (1966) were used to predict the scour depth, using the field and laboratory data. Scour prediction by Blench (1962) formulae indicated better correlation compared to other formulae as this envelopes most of the data.

ACKNOWLEDGEMENT

The author gratefully acknowledges his deepest gratitude and indebtedness to Dr. Muhammad Shahjahan, Professor, Department of Water Resources Engineering, Bangladesh University of Engineering and Technology(BUET), Dhaka, under whose guidance, constant encouragement and co-operation throughout the experimental investigations, it was possible to complete this study.

The author extends his deep appreciation to Dr. Abdul Hannan, Professor and Head, Department of Water Resources Engineering, BUET. The author is also grateful to Dr. Ainun Nishat, Director, Institute of Flood Control and Drainage Research, and Dr. M.K. Alam, Associate Professor, Department of Water Resources Engineering, BUET, for their helpful comments and corrections.

Gratitude is expressed to all officials of Bangladesh Power Development Board and Bangladesh Railways who helped to obtain data and other relevant papers for the East-West Interconnector and the Hardinge Bridge.

The author also thanks to Mr.M.Mofser Ali and Mr.A.K.Azad for typing and drawing of figures of this thesis.

Finally, the author is indebted to his parents for their constant encouragement and support.

M.R.K.

TABLE OF CONTENTS

TABLE OF CONTENTS(Contd.)

TABLE OF CONTENTS(Contd.)

LIST OF FIGURES

LIST OF FIGURES (Contd.)

LIST OF FIGURES (Contd.)

LIST OF TABLES

NOTATION

SYMBOLS	DEFINITION	UNITS
b	Width of pier	ft
B	Width of channel	ft
c	Bed load charge	—
d_s	Scour depth below normal river bed	ft
d_t	Scour depth below water level	ft
d_e	Lacey mean depth	ft
d_b	Mean depth	ft
D	Particle diameter	ft
D_{50}	Median bed material size	ft
F	Flow Froude Number $= V/(gy)^{\frac{1}{2}}$	—
F_c	Critical Froude Number $= V_c/(gy)^{\frac{1}{2}}$	—
F_d	Particle Froude Number $= V/(gD_{50})^{\frac{1}{2}}$	—
F_{dc}	Critical Particle Froude Number $= V_c/(gD_{50})^{\frac{1}{2}}$	—
f_s	Blence side factor	
f_e	Lacey's silt factor	
g	gravitational acceleration	$ft/sec.^2$
h	height of the pier	ft
k	coefficient	
l	length of pier	ft
t	time	
V	Approach velocity	sec.
V_c	Critical velocity	ft/sec.
W_b	Blench regime width of channel	ft
W_e	Width of water surface	ft

NOTATION (Contd.)

SYMBOLS	DEFINITION	UNITS
Y	Approach flow depth	ft
Y_c	Critical approach depth	ft
γ_s	Specific weight of sediment	lb/ft^3
γ_f	Specific weight of fluid	lb/ft^3
ν	fluid kinematic viscosity	$ft^2/sec.$
ρ	fluid density	$lb\ sec^2/ft^4$
ρ_s	sediment density	$lb\ sec^2/ft^2$
τ_c	critical shear stress	lb/ft^2

INTRODUCTION
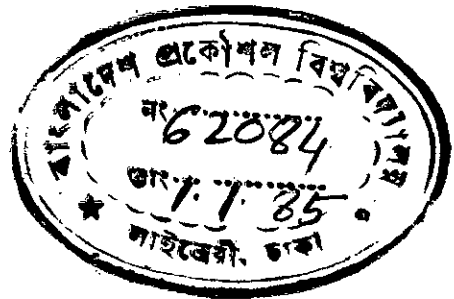
1.1.0 General:

Scour is defined as the change in elevation of the stream resulting from the erosive action of the flowing water over mobile bed (Fig.1.1). Scour can also occur in coastal regions as a result of the passage of waves. It is a consequence of sediment continuity and is generally aggravated by the presence of obstructions such as constricted waterway, piers, spurs, dikes etc.

In earlier days, hydraulic problems were avoided as far as possible by selecting bridge sites where channels were straight, banks were stable, and a square crossings could be arranged. Generous lengths of bridge were provided and occasional over topping of the approach roads by flood waters was tolerated. But as a result of a number of factors these policies have changed. These are, the increasing priority given to high standard road alignments and gradelines requiring acceptance of more difficult water crossing sites ; the increasing width, height and cost of bridges and the consequent need to keep their lengths to a minimum and public demands for a free flow of traffic at all times requiring the handling of reasonably predictable flood flows by the structure. Changes in location practices have resulted in the encroachment of road embankments into bodies of water where they too are subject to erosion. Thus, general practices in road

engineering make it necessary to give more attention to aspects
of hydraulic design, including the estimation of numerous hydra-
ulic parameters which determine the security of a structure
against scour and other actions of water.

In contrast of the scientific basis for structural
design of bridges there is no general theory available at
present which would enable the designer to estimate, with
confidence, the depth of scour at bridge pier and abutments.
This is due to the complex flow pattern around the embeded
structures. It can be seen that the scour depth depend upon
the properties of flow, the bed material in the stream and at
channel crossing (grading, layering, particle shape and size,
alluvial, cohesive or non-cohesive) and the obstruction geometry.
Because of the complexity in both the flow pattern and the
transport function, it often becomes necessary to undertake model
studies of the structure to be constructed.

In considering the importance of scour around bridge
piers many experiments and model studies have been made with
respect to specific structures. These have led to empirical
relationships between the scour and the various flow parameters.
However, when these are applied to a particular structure the
predicted depth of scour may vary widely. The reasons, therefore,
are probably due to different experimental conditions that may
not be appropriate to the particular hydraulic geometry to which
they were applied.

Knowledge of maximum depth of scour under various conditions especially around bridge piers for different types of bed materials of the stream, is essential for design of the bridge foundations as well as for proper maintenance of the bridge after its construction. The probable depth of scour mainly determine the depth below which the foundation of the bridge pier must be taken. This estimate of probable scour is important from the point of view of the safety of a structure, as well as economic design. An under-estimation of the scour will result in failure, while its over-estimation will increase the cost of the structures.

1.2.0 Importance of the Present Study:

A wide variety of empirical equations have been developed in the past to estimate the maximum scour depths around bridge piers. These equations have limitation in their use because, most of them were developed on limited data base either small or large scale.

Bangladesh is a land of rivers, interlaced by the numerous channels of the three mighty river systems of the world viz., the Ganges, the Brahmaputra and the Meghna. Many structures have been constructed across these river beds. The East-West Inter-connector and the Hardinge Bridge are the most important among these constructed structures from the hydraulic points of view.

The East-West Interconnector, Link between the east and west power grid system of Bangladesh crosses the river Jumna approximately between Aricha and Nagarbari. It consists of eleven caissons (Fig.1.2). The average depth of foundation of these caisson is 325 ft from the highest water level, which is considered one of the world's deepest foundation.

The Hardinge Bridge is a railway bridge over the river Ganges. It consists of sixteen piers. Piers of this bridge are sunk at a depth of 160 to 180 ft below water level.

These two examples show that enormous cost has been involved for large length of piers embedded beyond the scour depth. In future, there is probability of some more new structures across these river systems will be constructed and large sums of money will be involved. If scour depth is correctly predicted, then considerable amount of money can be saved. Therefore, it is felt that there is need to study scour phenomenon around bridge piers to obtain reliable data for evaluation of scour depth.

Considering the above fact, the present study has been undertaken to predict scour depth for different shapes of piers on variable bed materials and flow conditions. Field data of Hardinge Bridge and East West Interconnection will also be collected and analysed along with the experimental data and will be compared with the potential predictors of scour depth.

1.3.0 Objectives of the Study:

The safe and economical design of bridge pier, caisson etc. requires accurate prediction of the maximum expected scour depth of the stream bed around them. Hence the knowledge of probable maximum depth of scour under various conditions particularly on different types of bed materials is essential.

With this context the present study has been planned with the following objectives:

1. To observe the pattern and depth of scour at the upstream and downstream of the pier for the following conditions

    (a) For different shape of piers.

    (b) For different bed material sizes, and

    (c) For variable discharges.

2. To compare the scour depth data obtained in the laboratory with those of existing field data.

CHAPTER - II

REVIEW OF LITERATURE

2.1.0 Introduction:

Local scour around any obstruction to the flow is the lowering of a portion by erosion of the channel bed below an assumed natural level or other appropriate datum, tending to expose or undermine foundations that would otherwise remain buried. There are three important aspects of scour which must be considered when designing a foundation in an alluvial riverbed. The first is progressive degradation of the bed caused by changes in river regime. Typical causes of such changes of regime are channel improvements and construction of upstream dams and reservoirs. The second, is the temporary scour associated with the periodic rise in river stage during flood, or with the shifting of the thalweg of the stream. The third, is the local scour beyond natural riverbed level, caused by an obstruction placed in the stream. It is this last aspect of scour which is of primary interest in this study.

Two approaches to the problem of local scour prediction have been investigated. First, the experimental approach to deriving an analytical relationship which can be used for determining the maximum local scour depth is discussed and the factors affecting the flow and scour around such an obstruction are briefly described. The design formulae proposed by many of the investigators in this field are presented and discussed. Second, the appli-

cation of the empirical approach to the local scour problem is studied and discussed in a similar manner.

2.2.0 Mechanism of local scour:

Any obstruction like pier, caisson etc., placed transverse to the flow greatly distorts the flow pattern due to the concentration of stream lines around the obstruction. The dominant feature of this flow which develops near the obstruction is the large-scale eddy structure or the system of vortices. These vortex systems are the basic mechanism of the development of local scour and form an integral part of the flow structure. They also strongly change the velocity field around the obstruction.

Depending on the geometry of the obstruction and the pattern of the approaching flow, the eddy structure can be composed of any, all or none of the three basic systems (1969) namely the horseshoe vortex system, the wake-vortex system and the trailing-vortex system.

The horseshoe vortex is formed by the vortex filaments, transverse to the flow in the undisturbed velocity field which are concentrated by the presence of blunt nosed pier or caisson etc. In this, no vorticity is created by such obstructions. The pier serves as a focussing or concentrating device for the vorticity already present in the undisturbed stream. In fig.2.1, the ends of the vortex filaments composing the horseshoe vortex stretch

downstream is shown for a circular structure.

The wake-vortex system (Fig.2.2) is formed by the rolling up of the unstable shear layers generated at the surface of the pier. This vortex system acts like a vaccum cleaner in removing the bed material.

The trailing vortex system (Fig. 2.3) occurs only when the pier is completely submerged. It is composed of one or more discrete vortices attached to the top of the pier and extending downstream.

2.3.0 Classifications of Scour:

Whenever the rate of supply of sediment in a certain reach of a channel in alluvium is less than its transporting capacity, more sediment is picked up from the bed and banks resulting in enlargement of the section. This enlargement of the section toward bed is known as scour. Mathematically, it can be expressed as

$$\frac{dQ_s}{dt} = q_{s1} - q_{s2} \qquad \cdots \qquad \cdots \qquad \cdots \qquad (2.1)$$

where, $\frac{dQ_s}{dt}$ = the rate of scour in volume per unit time

q_{s1} = the capacity of the flow to transport sediment out of the scour hole in volume per unit time.

and q_{s2} = the rate at which sediment is supplied to the scour hole by the undisturbed flow.

Scour can be classified as general scour and local scour. General scour is the general lowering of the bed througout the width of channel in a considerable length of the reach local scour is the local lowering of the bed in the vicinity of a hydraulic structure, such as piers, caissons, spurs, dikes etc.

For the quantitative prediction of dpeth of scour, three classifications may be considered based on equation(2.1),

$$\frac{dQ_s}{dt} = q_{s1} - q_{s2}$$

(a) No scour, when $q_{s1} = q_{s2} = 0$

(b) Clear water scour, when $q_{s1} > 0$ and $0 \cong q_{s2} \ll q_{s1}$

and   (c) Scour with continuous sediment motion, when

$$q_{s1} \gg q_{s2} > 0$$

Only case (b) and (c) can cause abrupt changes in bed elevation near hydraulic structure like pier or caisson etc.

2.4.0 Causes of Scour:

A lowering of the stream bed in the vicinity of the obstructions can occur from a variety of causes. A useful distinction can be made by seperating the various causes into general categories (1) those characteristic of the stream itself, and (2) those due to the modification of the flow by the bridge crossing or any other structures.

The erosive power of flowing water on a channel boundary is determined primarily by the local shear stress or drag exerted

by the flow on the boundary, and by the associated velocities
and turbulent fluctuations of velocity near the boundary. The
relationship of local velocities to cross-sectional average
velocities is complex and depends on depth of flow, boundary
roughness, and channel geometry. Macroturbulent flow phenomena
such as eddies, helicoidal flow, rollers and surges may also be
important factors influencing scour. Average velocities and
depths therefore give at best a very rough indication of erosive
power, but calculations based on more refined measures are imprac-
ticable for the engineer in many cases. Fig. 2.4 illustrates the
relationships between velocities at different depths in a wide
stream of fairly regular depth (Neill,1973).

The factors which appear to have more effect on modifi-
cation of the flow are size of obstruction, shape of obstruction
and angle of attack. These factors also have effect on the scour
phenomenon.

2.5.0 Scour Protection:

The need for scour protection can be minimized by locating
hydraulic structures on stable tangential reaches of channels and
by placing foundations on non-erodible materials. But, such a
solutions is not always practicable, economical, or desirable
from an alignment standpoint of a structure.

Even, the choice among many protective works and other
alternatives, depends on several factors including load-bearing

requirements, sub-soil conditions actually encountered, economics, feasible construction methods and schedules, inspection procedures etc.

Having estimated the probable loest scour levels, several choices are open to the designer in selecting the type and elevation of the foundation. These are

(a) Place the bottom of the pier footing below estimated lowest scour levels, making allowance for local scour caused by the pier shaft and footing and including an approximate margin of safety. (Fig. 2.5a).

(b) Place the bottom of the pier shaft below estimated lowest general scour and provide protection against local scour effects (Fig.2.5b).

(c) Support the pier shaft or footing on piles or columns sunk well below lowest scour levels and designed to be secured when their upper parts are exposed by scour (Fig.2.5c) or protect the upper parts of piles or columns against exposure by bcal scour.

(d) Construct the pier in the form of a row of piles or columns without a footing or solid shaft, sinking these well below estimated scour levels and designing them to be secured when their upper parts are exposed by scour.

(e) Protect the spread footing or piles against under-
mining by means of a sheet pile skirting tied to the foundations.
The skirting must itself be designed against scour and less of
support.

2.6.0 Analytical design based on the experimental approach
2.6.1.0 Influence of various factors on scour:

The effects of the various factors upon scour can be
analyzed through experimental investigations. Among very many
factors some appear to have more effect on the scour phenomenon
than others, and the influence of these various factors are
discussed below.

2.6.1 Size of pier:

Laursen, Inglis, Blench,(1962), Shen et al (1971) Tarapore
and larras (Acres 1970) included the width of the pier as a
variable, in their experimentally derived relationships for
estimating local scour. From these, it is reasonably certain that
the depth of local scour depends on the width of the pier, the wider
the pier, the deeper the scour. It is also reasonably certain that
the depth of local scour will not continue to increase indefinitely
with pier width; a width will surely be reached at which the pier
will tend to act more like an abutment than a pier. There is no
experimental evidence to indicate the order of magnitude of pier
width at which this transition may take place.

The general lack of agreement among the various investigators on the effect of pier width on local scour indicated that the relationship between the two parameters is not yet fully understood.

All investigators do agree that the length of the pier does not affect the depth of local scour as long as the flow direction is parallel to the longitudinal axis of the pier.

2.6.1.2 Shape of Pier:

In respect of the effect of various pier nose shapes, all investigators agree that a significant reduction in the depth of local scour for a given pier width can be realized by streamlining the nose of the pier, the amount of reduction varying with the degree of streamlining.

2.6.1.3 Approach Depth of Flow:

Laursen(1962) states that the depth of local scour depends solely on the depth of approach flow, and the pier width. Shen et al (1969) and Blench (1962) derive relationships in which the depth of approach flow is an important parameter. Tarapore(Acres 1970) states that the depth of local scour depends upon the depth of approach flow for low depths of flow, but what constitutes a low depth of flow is not made clear.

Chitale(1962) Venkatadri et al and Bata(Acres 1970) found that the ratio of the maximum local scour depth to the approach flow, is a function of the Froude number and hence a function of depth of flow.

But unfortunately, the effect of depth of flow on local scour
is not yet fully understood. It might be possible when a large
number of field data are collected and subsequently analysed.

2.6.14 Approach Velocity of Flow:

Chabert and Engeldinger (Rao 1974) found that the depth of
scour varies almost linearly with the tractive force for clean
water and reaches a maximum at a value of the tractive force
necessary for continuous transport. They found that the depth of
scour varied in a similar way with the mean velocity as shown in
Fig. 2.6.

Laursenl (1962) summerised that Joglekar, Chitale, Thomas,
Ahmed, Blench and Bradley all infer that the depth of scour is
proportional to the two-thirds power of the discharge per unit
width which may be expressed in the following way

$$\text{Scour depth} \propto \frac{q^{\frac{2}{3}}}{F_b^{\frac{1}{3}}}$$

where, q is the discharge intensity and F_b is the appropriate
bed factor. Since the unit discharge is the product of velocity
and depth, then for a given depth of flow the depth of scour
should vary with velocity.

Laursen (1962) states that if there is no sediment supply
to the area of the pier, then the flow velocity and the grain size
of the sediment comprising the bed of the channel are important in
determining the depth of scour. However, under conditions of well
developed sediment movement, there is a constant supply of sediment
to the vicinity of the scour hole; as much material is supplied to
the hole as scouring can remove and hence the average river velocity
has little effect on the depth of the scour hole.

2.6.1.5 Angle of Attack:

Laursen(1962)Chabert and Engeldinger, and Varzeliotis
(Acres 1970) investigated the variation in the depth of local
scour with the angle of attack of the approaching flow and
concluded that the depth of scour increases as the angle of
attack of the approach flow increases. The scour pattern
around piers set at different angles to the direction of flow
are indicated in fig. 2.7 which shows the effect of the angle
of flow or attack on scour depth.

2.6.1.6 Time:

Researches conducted by the Iowa Research Laboratory
(Rao 1974) on models and proto-types on sandy bed bring out that
the scour changes with time. The depth of flow depends on the
adjustment of bed and silt carrying capacity of the water current
at different sections. As the scour hole increases in size, its
rate of formation decreases, the maximum depth of scour takes
place before the first mass of sediment settles in the scour
depression to induce condition of equilibrium. Coming to this
condition of equilibrium though takes time, will not last due
to the discharge in the stream being rarely constant for a
sufficiently long period. Scour can be clear water scour or the
scour with continuous sediment motion. The distinction between
these two types of scour and the definition of the equilibrium
depth of scour, d_{se}, are shown in Fig.2.8. With clear water

scour, the equilibrium depth of scour, d_{se} is approached asymptotically while there are periodic oscillation with continuous sediment motion.

2.6.1.7 Bed Material Size:

Shen et al (1969) present data which show no appreciable difference in scour depths for sands ranging from 0.24 mm to 3.0 mm mean diameter. Neill(1969) describes experiments which indicate that material of approximately 1.5 mm grain size was liable to deeper scour than either coarser or finear material. There is general agreement among all researchers that there is is definitely no dependence on sand size below 0.6mm.

2.7.0 Experimentally Derived Scour Depth Formulae:

Since the local scour phenomenon is very complex due to the involvement of numerous variables, it is almost impossible to study the effect of all the variables simultaneously. Many investigators in the past had studied the effect of one or more parameters on the magnitude of scour around hydraulic structures. Most experimental studies have resulted in forulae intending to predict the dimension of scour depth around bridge piers.

Inglis(1949) has developed a mathematical relationship from the experiments conducted at the Central Water Power Irrigation and Navigation Research Station, Poona, India in the

period of 1924-1942 with the objective to determining means of protecting the piers of the Hardinge Bridge, located on the river Ganges at Bheramara against scour. Geometrically similar models of Hardinge Bridge piers were set into the centre of the parallel sided channel having a bed of Ganges sand of mean diameter 0.29 mm. Model scales of 1:65 and 1:210 were used. From this experiment he obtained the equation of the following form:

$$\frac{d_t}{b} = 1.70 \ (\ \frac{q^{\frac{2}{3}}}{b} \ )^{0.78} \ \ldots \qquad \ldots \qquad (2.2)$$

where, d_t = total scoured depth below water level in ft.

  b = width of pier in ft.

  q = discharge per unit width of the approach flow in ft^3/s per ft. width.

As it was difficult to correlate this with the depth of scour at prototype piers, due to q (intensity of discharge per foot) depending upon the curvature of the river upstream which varies from river to river, it was considered desirable to study cases of actual scour in prototypes and work out a general, empirical relationship. Data were, therefore, collected for scour around bridge piers and a general relationship was proposed as follows

$$d_t = 2 \ [0.473 \ (Q/f_e)^{\frac{1}{3}}] \ \ldots \qquad \ldots \qquad (2.3)$$
$$= 2 \ d_e \ (Lacey)$$

Since Lacey's regime depth, $d_e = 0.473 \ (Q/f_e)^{\frac{1}{3}}$

where, Q is the maximum discharge in cusec; d_e is the maximum

depth of scour below highest flood level; f_e is equal to $1.76\sqrt{D_{50}}$.

Blench (1962) reviewed the model results reported by Inglis.
The data of severe scour around piers were for floods from,
30,000 cfs to 2,600,000 cfs. Blench has replotted the Inglis data
along with model data of Inglis, of his own data and of workers
at the University of Alberta, and stated that the formula
presented by Inglis (1949) could be reduced to the form

$$\frac{d_t}{y} = 1.8 \ (b/y)^{0.25} \qquad \dots \qquad \qquad \dots \qquad (2.4)$$

where y = normal approach flow depth in ft.
Blench did not elaborate on this formula, and it was not
immediately evident how he derived it from equation (2.2).

Chitale (1962) felt that the equation given by Inglis
cannot be adopted for general application because this
relation is not dimensionally correct.

Basic experiments were subsequently conducted in 1941 with the objective of testing the influence of upstream depth and sand diameter on scour around piers. The pier tested in these experiments was also 1/65 scale model of that of the Hardinge Bridge. It was rectangular in section, of length 1 ft, width 0.6 ft and semicircular cut and ease waters. The bed of the flume in these experiments was laid with sand of 0.32mm while the following materials were used just around the pier in succession

Sive number	Type of sand	Mean size, in mm
1	Screened dam sand	m = 0.16
2	White 'V' sand	m = 0.24
3	Nala sand	m = 0.68
4	Nala sand	m = 1.51

The sand around the piers was laid flush with the upstream bed level. A constant discharge of q = 1 cfs per ft was run and water level was adjusted to get a particular depth, the depths varying from 0.5 to 1.45 ft. Each experiment was continued until final maximum scour was obtained round the pier.

On the basis of the analysis of experimental data, he found that Froude number is a better criterion related to the maximum scour depth. The statistical equation obtained from the data is

$$\frac{d_s}{y} = -0.51 + 6.65F - 5.49F^2 \quad \ldots \qquad (2.5)$$

where, d_s = depth of scour below normal river bed in ft.

F = Froude Number.

Laursen (1962) carried out a very extensive series of
tests on models of a prototype pier. The prototype pier was
about 3.3 feet wide and the models were built at scales of
1:12 and 1:24. Five different sands were used of mean size
0.44mm to 2.25mm. Model velocities ranged from 1.0 fps to
2.5 fps. The velocity was maintained high enough to permit
general bed movement to be fully developed at all times.
Measurements of scour were made at the prototype pier during
the passage of three floods. Depths of water in the prototype
river were of the order of 10 feet. Fig.2.9 indicates the
degree of conformity obtained in Laursen's experiments, scour
depths in the model being considered to have geometric simi-
larity to the prototype and so being merely multiplied by the
appropriate scale ratio. While the model results indicate a
greater depth of scour than measured in the prototype, the two
results approach each other as the depth of flow increases.
Using both model and prototype data, and with due regard for
the reliability of such data, a basic design curve was drawn
for a square nosed pier parallel to the flow. Shape factors,
for variaus pier nose types, were given by Laursen to be
applied to the result obtained from the basic curve, assuming
the pier to be aligned with the flow. These factors have been
applied to the basic curve, and the resulting set of curves
is presented on fig.2.10.

The curves are meant to be conservative and Laursen emphasizes that the design curve presupposes the movement of the bed material as bed load. Caution is advised in the use of the design curves if a substantial fraction of the sediment transport is in the form of suspended load.

Shen, Schneider and Karaki (1969   ) conducted numerous sets of experiments at Colorado State University, USA. The flume used was 60 feet long by 6 feet wide and a cylindrical pier of 0.5 foot diameter was placed on a sand bed with mean bed material size of 0.24 mm. In addition to their experimental data the authors also incorporated in their analysis the data of Chabert and Ergeldinger, 1956,   for piers of 0.246 foot and 0.328 foot diameters respectively. They obtained the following relationship

$$\frac{d_s}{y} = 2 \left[F^2 (b/y)^3 \right]^{0.215} \quad \ldots \quad \ldots \quad (2.6)$$

The relationship is reproduced graphically on figure 2.11.

Ahmed (1962) conducted experiments on models of several bridge sites of West Pakistan. The experiments were carried out so that there was good general movement of the bed. The relationship of discharge intensity to total scoured depth, both around the piers and abutments and in bends, was investigated and he proposed a formula of the following type:

$$d_t = K.q^{\frac{2}{3}} \quad \ldots \qquad \ldots \qquad \ldots \qquad (2.7)$$

where the coefficient K is a function of boundary geometry
shape of pier nose or abutments, characteristics of bed
material and distribution of velocity in the channel section
at the piers.

Ahmed (1962) recommended that a value for K of 1.7 to
2.0 be adopted for use in predicting the total scoured depth
around piers, provided that guide banks at least equal to the
length of the river crossing were constructed to provide and
maintain straight channel flow characteristics in the vicinity
of the piers, thus precluding the development of severe channel
bends and the associated extreme scour depths in the critical
areas around bridge piers and abutments.

Arunachalam (1965) in his recent paper reviews several
of the more widely used methods of calculating local scour and
attempts to explain the major differences between them. He claims
that the different reference points used by past investigators for
measuring the depth of scour is the main cause of confusion surr-
ounding the relative effects of flow velocity and pier geometry
on local scour. He suggests that the total scoured depth below
water surface must be separated into the upstream flow depth,
which is a function of velocity or discharge and the depth of
local scour below the ambient stream bed which is a function
of only the depth of flow and pier geometry. He derives a
relationship for calculating the depth of local scour below

stream bed based on the Poona experiments on the Hardinge Bridge piers, but rewritten to express the discharge in terms of depth

His expression is

$$\frac{d_s}{b} = \frac{y}{b} \left[\frac{1.95}{(y/b)^{1/6}} - 1 \right] \quad \cdots \quad \cdots \quad (2.8)$$

Arunachalam recommends to use the 'lacey mean depth' for calculating the upstream flow depth.

Bata (Acres 1970) in 1960 reported results of a series of experiments on local scour around bridge piers. During this experiments the general bed movement existed. However, data on widths of flume, size of sand, depths and velocities of flow, and shapes and sizes of piers tested were not quoted.

Bata found that the influence of the Reynolds Number on local scour was negligible, as was the diameter of the sand particles. Finally he put forward the following expression for the limiting depth of local scour

$$\frac{d_s}{y} = 10 \left[\frac{V^2}{gy} - \frac{3D}{y} \right] \quad \cdots \quad \cdots \quad (2.9)$$

where, $D =$ diameter of sand particle (D_{50}).

Tarapore (Acres 1970) established a theoretical method of calculating local scour based on the potential flow around the obstruction in the channel. He attempted to verify his theoretical findings with a series of experiments conducted in a 12 inch wide flume, using a cylindrical pier two inches in diameter. Since his theoretical investigations took an advanced rate of bed load transport into account, it is assumed that his experiments were conducted with a fully active bed. He presents the relationship

$$d_s = 2.7 \left(\frac{b}{2}\right) \quad \ldots \qquad \ldots \qquad (2.10)$$

He claims, this equation is valid for large depths of flow. However, a criterion for determining wheather the depth is large is not given. For low depths of flow, the depth of local scour was found to be dependent on the depth of approach flow as well as the radius of the pier. Suspended load was found to have no effect on the depth of local scour.

Larras(Acres 1970) presents a formula for the depth of local scour at bridge piers based on the experimental results of chabert and Engledinger. The formula given is,

$$d_s = 1.42 \, b^{\frac{3}{4}} \quad \ldots \qquad \ldots \qquad \ldots \qquad (2.11)$$

Multiplying factors to be applied to the basic formula to account for pier nose shape and for angle of attack of the approach flow were given by larras, but are not elaborated by Neill who has described from the larras article written in French.

2.8.0 Empirical Approach of Analytical Design:

In this approach to predict the depth of local scour, a stable or regime depth of flow is estimated for the unobstructed river channel using an empirically derived formula and a multiplying factor then applied to this estimated depth to account for obstructions such as piers and abutments.

The following description is based on the approach by Lacey and Blench. Their formulae are based on the analysis of the numerous volume of data obtained from the operation of irrigation canals in India and Pakistan.

2.8.1 Lacey's Regime Depth Formulae:

Lacey's (Acres 1970) has given an expression for regime depth in rivers flowing in alluvium in 1929. The equation for regime width is,

$$W_e = 2.67 \ Q^{\frac{1}{2}} \quad \ldots \qquad \ldots \qquad \ldots \qquad \ldots \qquad (2.12)$$

and that for depth

$$d_e = 0.473 \left(\frac{Q}{f_e}\right)^{\frac{1}{3}} \quad \ldots \quad \ldots \quad (2.13)$$

where

W_e = width of water surface in feet.

Q = flood discharge in cfs

d_e = Lacey mean depth, feet

f_e = Lacey's silt factor, defined by $1.76 \sqrt{D_{50}}$.

Lacey proposed multiplying factors to be applied to the "Lacey mean depth" in order to calculate the maximum total scoured depth which could occur in stable reaches with no obstructions. Factors are

Condition		Factor
Maximum depth in a straight, stable reach	...	1.27
Moderate bend in the river	... ...	1.50
Severe bend in the river	... ...	1.75
Right angled bend	... ...	2.00

For reaches where the width of the river was artificially constricted, such as by guide banks, the "Lacey mean depth" becomes:

$$d_e = 0.9 \left(\frac{q^{\frac{2}{3}}}{f_e^{\frac{1}{3}}}\right) \quad \ldots \quad \ldots \quad \ldots \quad (2.14)$$

Same multiplying factors as used on an unconstricted reach are to be applied to obtain the maximum total scoured

depths.

These equations have apparently been checked against actual conditions at stable bridge sites in large sand bed rivers with good agreement.

2.8.2 Blench Regime Formulae:

Blench (1966) has replaced the silt factor in lacey's formulae and introduces the 'bed factor' and a 'side factor' Blench has differentiated the nature of channel bed and banks. His equations for a stable channel width and depth are:

$$W_b = \left(\frac{f_b}{f_s} \right)^{\frac{1}{2}} Q^{\frac{1}{2}} \quad \dots \quad \dots \quad \dots \quad (2.15)$$

$$d_b = \left(\frac{f_s}{f_b^2} \right)^{\frac{1}{3}} Q^{\frac{1}{3}} \quad \dots \quad \dots \quad \dots \quad (2.16)$$

where

W_b = Blench regime width of channel at half depth, feet.

f_b = Blench bed factor $= f_{bo} (1 + 0.12c)$

f_s = Blench side factor

$f_{bo} = 1.9 \sqrt{D_{50}}$

Q = discharge in, cfs

e = bed load charge, measured as dry weight per second of bed load divided by weight of water flow per second and reduced to parts per hundred thousand

d_b = Mean depth, equal to the cross-sectional area divided by W_b.

Blench suggested the values of f_s as follows:

Degree of Cohesiveness				f_s
Slight	...	...	...	0.1
Moderate	...	...	...	0.2
High	...	...	...	0.3

Where the river width is imposed by an artificial constriction, the depth equation becomes:

$$d_b = \frac{q^{\frac{2}{3}}}{f_b^{\frac{1}{3}}} \quad ... \quad\quad ... \quad\quad ... \quad (2.17)$$

where, q = unit discharge intensity per foot of width at half depth.

Blench proposed the following multiplying factors to be applied to the equation (2.15).

Condition	Factor
Maximum depth in a straight reach	1.5
Maximum depth in a bend of normal meander curvature	1.7

2.9.0 Summary:

An attempt has been made to review the currently available literature of local scour. which may be summerised as follows:

1. The depth of scour will increase with the increase of pier width but will not continue to increase indefinitely.

2. Significant reduction in the depth of scour for a given pier width can be realized by stream lining the nose of the pier.

3. For a given depth of approach flow the depth of scour will vary with the velocity.

4. The depth of scour increases as the angle of attack of the approach flow increases.

5. Lastly, on the basis of available design formula of local scours in alluvial rivers, design engineer should judge the work of any individual out of all studied, which is to be most thorough in scope and execution in considering the field problem.

CHAPTER - III

THEORETICAL CONSIDERATIONS

3.1.0 Introduction:

Local scour at bridge piers or near the embankment
is the result of vortex systems developed at the piers or
large wake vortices (or eddies) set up downstream of embank-
ments which scour downstream side of the embankments, the
river bank and the stream bed. The scouring is achieved due
to the resulting development of high velocity because of
partial blockage of the flow by the pier as seen commonly as
eddies.

The shape of the pier also significantly affects scour
depth because it reflects a strength of the horseshoe vortex at
the base of the pier as observed by Shen, Karaki et al(1969).
A blunt-nose pier will cause the greatest scour depth while
stream lining the front end of the pier will reduce the scour.
Moreover, streamlining the downstream end of piers will reduce
the strength of wake vortices.

In order to analyse the influence of pier shape it is
advantageous to consider the cross-sectional shape of the piers
and their positions relative to the direction of the flow. The
variables affecting depth and location of scour commonly used in

current practice are:

1. The geometric characteristics of the piers

   l = pier length parallel to the approach flow.

   b = pier width perpendicular to the approach flow.

2. The characteristics of the flow,

   Y = depth of approach flow

   V = velocity of approach flow

   d_t = depth of scour

3. The characteristic of the fluid and erodible bed material,

   ρ = fluid density

   ρ_s = sediment density

   ν = fluid Kinematic viscosity

4. Dynamic quantity involved in flow characteristics

   g = gravitational acceleration

   t = time.

3.2.0 Dimensional Analysis:

Mathematical theory and experimental data have developed practical solutions to many hydraulic problems. Important hydraulic structures are now designed and built only after extensive model studies have been made. Application of dimensional analysis and hydraulic similitude enable the engineer to organize and simplify the experiments and to analyze the results therefrom.

Where the number of physical quantities or variables equals four or more, the Buckingham P_i Theorem provides an excellent tool by which these quantities can be organized into the smallest number of significant, dimensionless groupings, from which an equation can be evaluated.

In this study, the problem can be written mathematically in the following way considering the variables involved in the system.

$$f(d_t, b, l, Y, V, \rho, \nu, D_{50}, \rho_s, g, t) = 0 \qquad (3.1)$$

This equation can be non-dimensionalized by using the Buckingham P_i Theorem.

Here, number of variables is twelve and the number of primary units is three. Therefore, number of dimensionless groups will be (11-3) or 8.

The equation (3.1) can be replaced by the equation

$$\emptyset(\pi_1,\ \pi_2,\ \pi_3,\ \pi_4,\ \pi_5,\ \pi_6,\ \pi_7,\ \pi_8\ ) = 0 \qquad (3.2)$$

The π - terms of this equation can be establish as follows:

$$\pi_1 = d_s^{a_1}\ b^{b_1}\ v^{c_1}\ \rho_s^{d_1} \qquad \ldots \qquad \ldots \qquad (3.2a)$$

$$\pi_2 = l^{a_2}\ b^{b_2}\ v^{c_2}\ \rho_s^{d_2} \qquad \ldots \qquad \ldots \qquad (3.2b)$$

$$\pi_3 = Y^{a_3}\ b^{b_3}\ v^{c_3}\ \rho_s^{d_3} \qquad \ldots \qquad \ldots \qquad (3.2c)$$

$$\pi_4 = \rho^{a_4}\ b^{b_4}\ v^{c_4}\ \rho_s^{d_4} \qquad \ldots \qquad \ldots \qquad (3.2d)$$

$$\pi_5 = \nu^{a_5}\ b^{b_5}\ v^{c_5}\ \rho_s^{d_5} \qquad \ldots \qquad \ldots \qquad (3.2e)$$

$$\pi_6 = D_{50}^{a_6}\ b^{b_6}\ v^{c_6}\ \rho_s^{d_6} \qquad \ldots \qquad \ldots \qquad (3.2f)$$

$$\pi_7 = g^{a_7}\ b^{b_7}\ v^{c_7}\ \rho_s^{d_7} \qquad \ldots \qquad \ldots \qquad (3.2g)$$

$$\pi_8 = t^{a_8}\ b^{b_8}\ v^{c_8}\ \rho_s^{d_8} \qquad \ldots \qquad \ldots \qquad (3.2h)$$

The dimensions in M.L, and T of the different variables of the equations (3.2a to 3.2h) can be substituted and the values of exponents may be **obtained** by equating the exponents of M.L and T. These values of the exponent can be substituted in the respective equation and following π - terms can be

obtained:

$$\pi_1 = \frac{d_t}{b} \; ; \qquad\qquad \pi_5 = \frac{Vb}{\nu}$$

$$\pi_2 = 1/b \; ; \qquad\qquad \pi_6 = \frac{D_{50}}{Y}$$

$$\pi_3 = \frac{Y}{b} \; ; \qquad\qquad \pi_7 = \frac{V}{(gy)^{\frac{1}{2}}}$$

$$\pi_4 = \rho / \rho_s \; ; \qquad\qquad \pi_8 = \frac{Vt}{b}$$

The new relationship in terms of π_1, π_2, ... π_8, is

$$f_1 \left(\frac{d_t}{b} \, , \, \frac{1}{b} \, , \, \frac{Y}{b} \, , \, \frac{\rho V^2}{g(\rho_s - \rho) D_{50}}, \frac{Vb}{\nu} \, , \, \frac{D_{50}}{Y} \, , \frac{V}{(gy)^{\frac{1}{2}}}, \, \frac{Vt}{b} \right) = 0 \quad (3.3)$$

Considering the effect of sediment density, ρ_s, in the parameter of submerged weight, $\gamma_s' = g (\rho_s - \rho)$, its inclusion as an independent parameter can be omitted. Therefore substituting γ_s' for $g(\rho_s - \rho)$, and solving for relative scour depth, $\frac{d_t}{b}$, equation (3.3) can now be written as,

$$\frac{d_t}{b} = f_2 \left(\frac{1}{b} \, , \, \frac{Y}{b} \, , \, \frac{\rho V^2}{\gamma_s' D_{50}}, \, \frac{Vb}{\nu}, \, \frac{D_{50}}{Y} \, , \, \frac{V}{(gy)^{\frac{1}{2}}} \, , \, \frac{Vt}{b} \right) \quad (3.4)$$

With the passage of time the dimension of a scour hole gradually increases and its growth is arrested when equilibrium condition is approached. In respect to the present laboratory set up, to measure the scour depth with time, the flow of water

has to be stopped for each time of scour depth measurement, so by stopping and restarting the flow, the stability of the flow will be disturbed. Therefore, the scour depth data with time was not possible to record with the present available instrumentation. Due to this the term $\frac{V_t}{b}$ has not been considered in this study. The term $\frac{V_b}{\nu}$ has not also been considered as the viscosity, has negligible effect on the scour process due to the flow being turbulent. Therefore the equation (3.4) can be reduced to

$$\frac{d_t}{b} = f_2 \left(\ l/b, \ Y/b, \ \frac{D_{50}}{Y}, \ \frac{V^2}{Y_s' D_{50}}, \ \frac{V}{(gy)^{\frac{1}{2}}} \right) \tag{3.5}$$

The particular form of $V/(gy)^{\frac{1}{2}} = F$, the Froude number of the approach flow is chosen because of the possible effects of surface waves on scour at approach-flow velocities. The term $\rho V^2/ Y_s' D_{50}$, is in effect also the square of the Froude Number in which D_{50} is the characteristic length, $\left[F_d = V/ (gD_{50})^{\frac{1}{2}} \right]$. F_d may be termed as the particle Froude number.

For particles of a given shape, for critical or incipient condition, shields obtained the following relationship:

$$\frac{\tau_c}{(Y_s - Y_f)D} = f \left(\frac{V_c \ D}{\nu} \right) \quad \cdots \quad \cdots \tag{3.6}$$

where, τ_c = critical shear stress = $V_c^2 \ \rho_f$

Y_s = specific weight of sediment

Y_f = specific weight of fluid

D = particle size

V_c = critical velocity.

Substituting $\tau_c = V_c^2\, \rho_f$ in equation (3.6), the expression becomes,

$$\frac{V_c^2}{(\gamma_s - \gamma_f)Y/\rho_f} = f\ \left(\frac{V_c\, D^2}{Y\, \nu}\right)$$

or, $$\frac{V_c}{(\gamma_s - \gamma_f)\, Y/\rho_f} = f\ \left(\frac{D}{Y}\quad \frac{V_c D}{\nu}\right)$$

or, $$\frac{V_c}{(gY)^{\frac{1}{2}}} = f\ \left(\frac{D}{Y}\quad \frac{V_c D}{\nu}\right)$$

From this expression it may be appreciated that $\frac{V_c}{(gY)^{\frac{1}{2}}}$ or F_c will be a function of D/Y and $\frac{V_c D}{\nu}$. Therefore, the relative sediment size $\frac{D_{50}}{Y}$, will be a function of F_c or $F_{dc} = V_c/(g\, D_{50})^{\frac{1}{2}}$. Thus the equation (3.5) can be written as

$$\frac{d_t}{b} = f_2\ (\quad l/b,\ Y/b, F_c, F\ ) \quad \ldots \quad \ldots \quad (3.7a)$$

$$\frac{d_t}{b} = f_2\ (\quad l/b,\ Y/b, F_{dc},\ F_d) \quad \ldots \quad \ldots \quad (3.7b)$$

The variations of relative scour depth with these independent variables of above two equations have been plotted and discussed in Chapter V.

CHAPTER - IV

LABORATORY SET UP AND MEASUREMENT

4.1.0 Introduction:

The present study was carried out in the Hydraulics
and River Engineering Laboratory of the Department of Water
Resources Engineering, Bangladesh University of Engineering
and Technology. The existing Flow Visualisation Tank with the
water supply system and measuring devices etc. were used in
this study. A brief description of the facilities and the
experimental procedure are given below.

4.2.0 Flow Visualisation tank:

The experiments were carried out in a recirculating
flow visualisation tank (Fig.4.1). The working section of the
tank was 13.25' x 2' x 0.67'. The tank was moulded from glass
fibre, with steel reinforcement to provide rigidity. It was
comprised of three parts - the inlet tank, the working section
and the reservoir tank. A droptight adjustable overshot weir
with upstream sand trap was accommodated within the discharge
tank. A perforated baffle plate had been incorporated into the
inlet tank which distributed the flow evenly across the width
of the flow table.

4.2.1 Water Supply System:

A centrifugal pump installed near the tail water tank of the flume was used to supply water to the test channels. Water was allowed to enter the inlet of the channel through a delivery pipe line from the pump, which after flowing through the channel entered into the tailwater tank. It was recirculated by means of the pump and the process was followed to have a continuous supply through the test channel.

4.2.2 Flow Measuring Device:

A flow meter fitted to the delivery pipe system was used to measure the volume of water flowing through the line. This meter was provided with the facility of taking the volume readings with an accuracy of one hundredth of a gallon. The volume of water passing through for 60 seconds was recorded and the discharge rate was calculated. The time was recorded by a stop watch.

4.2.3 The Tailwater Tank:

The tailwater tank at the downstream end of the flume was used as the source of supply of water for the pump. As the water was made to recirculate, this tank was provided for settling down the sediment carried from upstream. The tailwater level was more or less constant by supplying water from the main supply line of the laboratory.

4.2.4 Flow Entrance:

Water comming from the bottom of inlet tank through pump create waves at the flow entrance. As such, these waves produce initial thrust on the mobile bed during initiation of the test run. After several trials by stone pitching at the entrance, the initial thrust on the mobile bed was avoided. The trials indicated a 6" length stone pitching with one layer thickness of ½" and this specification was provided across the bed at the entrance to the channel (Fig. 4.2). Stone pitching also helped for slow transition of velocity from the entrance to the flume.

4.2.5 Initial Flume Bed:

The flume bed was filled up with sand for a depth of 3.5 inches. This depth was maintained for all the test runs even when one type of test sand was replaced by another. The bed was compacted properly for each run and approximately similar condition was maintained for other test runs. The general photographic view of the initial flume bed is shown in Fig. 4.3.

4.2.6 Bed Material:

Three different types of sand were used as bed material. Their median sizes were 0.19 mm, 0.40 mm and 0.94 mm. One sample of bed material ($D_{50} = 0.19$ mm) was collected from the Jamuna river near Aricha Ghat at which the East-West Interconnector crosses the river Jamuna. The wide variation in median sizes (D_{50}) of three bed material was choosen to observe clearly the effect of bed material sizes on scour depth. Size distributions of the three bed material samples were found out and were shown in Fig.4.4.

4.2.7 Discharge and Slope:

Different discharges for which test runs were conducted were 0.13cfs, 0.17 cfs, 0.20cfs and 0.24cfs. For each type of pier and bed material, slope and discharge were maintained constant for a particular test run.

4.2.8 Pier Shape:

Four different shapes of piers were used in the study. They were rectangular, circular, round nose and sharp nose Fig.4.5 shows the different shapes of pier.

The geometric characteric of piers are described by length, l width, b. The values of length-width ratio for four different piers are given below in the tabular form

Type of pier	Relative length, $= \frac{length, l}{width, b}$
Rectangular	3.00
Circular	1.00
Round nose	3.00
Sharp nose	3.00

4.2.9 Measurement of Scour Depth:

A moveable bridge with a point gauge mounted on it was used for taking measurements. The bridge was operated manually over a rail placed on the top of the two side railings. The point

the test run was continued until these readings were found
not variable.

When the test run achieved the stable condition,
one particular type of pier was placed in such a way that the
width of the pier was perpendicular to the flow. The location
of the pier was approximately middle of the working section.
After the pier was inserted into the bed, it took another one
to one and half hours to reach an equilibrium state. In this
state of equilibrium there was no appreciable activity in
sediment erosion or deposition in the scour hole. This was
confirmed through visual observations. Then the channel and
scour hole were carefully drained.

Contours within the scour hole and deposition region
were marked at 1 cm intervals, relative to the mean water level.
Mean water level was measured by a point gauge reading on three
different places marked earlier and was taken as the average
of the point gauge readings.

Three sets of runs were conducted for a particular
type of pier. Each set contained four test runs for four
variable discharges for a particular type of bed material.
Therefore, twelve sets of runs were conducted for four
different types of piers totalling forty eight test runs.

ANALYSIS OF DATA AND DISCUSSIONS

5.1.0 Introduction:

Phenomena involving scour around bridge piers have been studied in the laboratory and data collected from experiments have been plotted and analysed on the basis of the theoretical approach as described in the previous chater (Chapter IV).

The variations of relative scour depths, d_t/b with Froude number and relative depth, y/b were plotted and studied. The scour pattern around different shapes of pier for different bed material types and discharges were plotted.

Field data of Hardinge Bridge and the East-West Interconnector have also been collected and plotted on the basis of empirical equations forwarded by Inglis (1949), Blench (1962), Shen and Others (1966).

5.2.0 Collection of Data:

(a) Laboratory Tests: Data observed from the fourth eight laboratory test runs by placing four different piers (rectangular, circular, round nose and sharp nose) on different bed materials and discharges were collected. The mean diameter (i.e. D_{50}) of the various types of bed material chosen for the study were 0.19mm (the Jamuna river bed near Aricha), 0.40mm and 0.94mm.

Different discharges for which test runs were conducted ranged
between 0.13 cfs and 0.24 cfs. The flow conditions for the
various runs and the results obtained in these test are summari-
zed in Tables 1 to 4.

(b) Field Data: Data of Hardinge Bridge and the East-West
Interconnector were been collected. The Hardinge Bridge
($1\frac{1}{2}$ miles long) is a railway bridge link between the Pakshi
(Pabna) and Bheramara (Kushtia) over the river Padma. The
scour data around bridge piers had been taken from the records
of three consecutive years viz., 1976, 1977 and 1978 as shown
in Table -5. Observations around piers of the bridge shown in
Fig. 5.1(a) were made with the sounding method. Sounding and
surface velocity data were also taken at five different points
in between the two piers as shown in Fig.5.1(b). The shape of
the piers were round nose.

The East-West Interconnector crossed the river Jamuna
approximately in between Aricha and Nagarbari. It consisted of
eleven circular caissons and all were not located in the main
river. So, scour data were available only for six caissons.
These are shown in Table-6. Bed material samples had been
gathered ($D_{50} = 0.19$mm) and their size distributions shown
in Fig. 4.4.

5.3.0 Analysis and Discussions:

The effect of Froude number, F, bed material, D_{50}, relative approach depth, y/b and shape of pier on relative scour depth as observed from the laboratory test runs are described in the following sections.

5.3.1 Effect of Froude number on Scour Depth:

To study the effect of Froude number on relative scour depth, the variations of relative scour depth d_t/b was plotted against Froude Number in Figure 5.2. The relative length of the pier, l/b was also indicated for each type of pier.

The relative scour depths, $\frac{d_t}{b}$ were plotted against flow Froude number, $F [= V/(gy)^{\frac{1}{2}}]$ in Figure 5.2 and Figure 5.3 show the plots of relative scour depth $\frac{d_t}{b}$ against the particle Froude number, $F_d [= V/(gD_{50})^{\frac{1}{2}}]$. Figure 5.2 (for four different shapes of pier) show that relative scour depth, $\frac{d_t}{b}$ increases with the increase of Froude Number, F (or velocity). This can be explained in the following way. If the stream velocity is increased, then the strength of the scour mechanism increases, that is, the sediment transport rate into the hole is less than sediment removal from the hole. As a consequences the depth of scour is gradually increasing with the increase of flow Froude Number. Fig. 5.2 also show that for an increase of 0.1 in the value of Froude

Number, the relative Scour depths d_t/b also increase by 0.3, 0.5 and 0.56 for coarse (D_{50} = .94 mm) medium (D_{50} = 0.4mm) and fine (D_{50} = 0.19mm) sand respectively. The increase in the relative scour depth d_t/b for fine sand is maximum (i.e., 134% compared to the coarse sand. While the increase in the medium sand is only 78%). Thus, the relative scour depth, d_t/b is higher for finner size of bed material and gradually decreases as the coarseness of the bed material increases. This is also seen for other shapes of pier as shown in Fig. 5.2. Jain-et al (1980) also found similar trend in their experimental results.

To observe the effect of particle Froude number, F_d on the relative scour depth d_t/b Figure 5.3 have been plotted. From these plots it has been observed that relative scour depth, d_t/b increases with the increase of particle Froude number. Considering fig. 5.3 it is seen that the relative scour depth, d_t/b increases by a value of 0.2 for coarse material, 0.24 for intermediate material and 0.26 for coarsen material for a change of the particle Froude number value of 0.50. It is evident from this that the rate of increase in relative scour depth is lesser for finer material and gradually increases as the coarseness of the bed material increases. This is also seen for other shapes of pier as shown in Fig 5.3.

The relative scour depths, d_t/b were plotted against critical Froude number, $F_c = V_c/(gy)^{\frac{1}{2}}$ in Figure 5.4. Considering this figure, it has been observed that for 0.05 increase of critical Froude number, the relative scour depth, d_t/b increases by 0.34 for coarser material, 0.46 for intermediate material and 0.52 for finer material. Therefore, the effect of critical Froude number is more in case of finer bed material compared to intermediate and coarser bed material.

Fig. 5.5 show the plot of relative scour depth, d_t/b against the particle critical Froude number, $F_{dc} = V_c/(gD_{50})^{\frac{1}{2}}$ This plot shows that the relative scour depth, d_t/b also increases with the increase of critical particle Froude number, F_{dc}.

5.3.2 Effect of Approach depth on Scour Depth:

The variations of relative scour depth, d_t/b against the relative approach depth, y/b for four different shapes of pier are shown in Figure 5.6. The relative scour depth increases with the increasing relative approach depth. Referring to the Fig. 5.6 it has been observed that the relative scour depth, d_t/b increases by 0.24, 0.24 and 0.28 respectively for finner, coarser and intermediate bed material sizes for 0.1 increase of relative approach depth. From these values it may be inferred that the relative approach depth has considerable effect on relative scour depth.

The ratio of maximum scour depth to the approach depth for all shapes of pier for the present study range between 1.30

and 2.33 and the average value is 1.95. This relation of scour depth, d_t and the approach depth, y is very close to the relation earlier given by Inglis (1949) as, $d_t = 2y$. There is a discrepancy of only 2.5% between the value given by Inglis and the average value obtained from the data of the present study.

5.3.3 Effect of Piers Shape on Scour Depth:

Four different shapes of piers such as rectangular, circular, round nose and sharp nose (Fig.4.5) were used in this study. Figs. 5.7 to 5.18 show the scour pattern around the different shapes of pier for specific discharges and bed material.

The maximum scour depth, d_t has been observed as 0.33 ft in case of rectangular pier embedded in finer material (D_{50} = 0.19mm) for a dishcarge of 0.24 cfs whereas for the same discharge and in the same bed material, the minimum scour depth has been observed as 0.24 ft in case of sharp nose pier. Thus it may inferred that the sharp nose pier can be considered as quite efficient from the hydraulic point of view. For circular pier, the scour depth is lesser than the rectangular and it is higher for the round nose compared to the sharp nose pier.

For rectangular piers the development of scour covered in area approximately 1 x $\frac{1}{2}$l from the upstream end of the pier, where l is the length of the pier. Laterally the scour spread over a distance equalled to the length of the pier while along the flow direction the spread is only $\frac{1}{2}$l.

Deposition has been observed in the downstream end of the pier. This deposition sometimes has been observed in a distance of 1-2cm from the trailing end of the pier. A typical plot of scour depth contours for rectangular pier is shown in Fig. 5.11. Scour patterns for circular, round nose and sharp nose are also shown in Figs. 5.13 and 5.10 respectively. In case of circular pier the scour in plan form covers approximately 1.5 times the pier diameter around the pier. For round nose, area coverage is approximately half of the pier length in upstream and lateral directions from the pier face and full length of pier along the downstream direction from the upstream face of the pier. Deposition has also been observed in the downstream side from the trailing end of the pier. In case of sharp nose pier, scour coverage area is one third of the pier length in upstream side and seven-eight length of the pier in the downstream direction from the upstream face of the pier. Laterally, it covers approximately a distance of half the pier length. Little deposition has been also observed in the downstream side of the pier.

The maximum equilibrium depth of scour for all types of pier is observed at both upstream and downstream side of each pier type. Several photographs showing scour patterns around piers are also shown in Figs. 5.19 and 5.20.

5.3.4 Comparison of Field Data:

The scour data for Hardinge bridge and East-West Interconnector are plotted in Figs. 5.21 to 5.26 on the basis of the analysis given by Blench (1962), Inglis (1970) and Shen et al (Acres 1970). This has been done to compare the field data with their respective similar equations. Figs. 5.21 to 5.23 and Figs. 5.24 to 5.26 are plotted for Hardinge bridge and East-West Interconnector data respectively and the statistical equations obtained from these are given below in the tabular form

Name of the Investigator	Equations	Relationships obtained on the basis of present field data	
		Hardinge Bridge	East-West Interconnector
Blench (1962)	$d_t/y=1.8(b/y)^{0.25}$ ... ...(2.4)	$d_t/y=1.82(b/y)^{0.75}$ ... ... (5.1)	$d_t/y=1.38(b/y)^{0.312}$ ... (5.4)
Inglis (1949)	$d_t/b=1.70$ $(q^{\frac{2}{3}}/b)^{0.78}$ ...(2.2)	$d_t/b=1.34(q^{\frac{2}{3}}/b)^{1.07}$ ... ... (5.2)	$d_t/b=1.23(q^{\frac{2}{3}}/b)^{0.53}$ ... (5.5)
Shen et al(1969)	$d_s/y=2\left[F^2(b/y)^3\right]^{0.215}$ ...(2.6)	$d_s/y=8.91\left[F^2(b/y)^3\right]^{0.25}$ ... (5.3)	$d_s/y=1.768\left[F^2(b/y)^3\right]^{0.37}$ ... (5.6)

Though there are differences in views regarding the effect of sediment size on scour but comparing equation (5.1) with (5.4) it is evident that the scour depth has a significant effect of sediment size. Garde and Raju (1978) in their studies also showed a significant effect of sediment size on scour depth. Putting q = 369.93 cfs/ft., b = 37 ft. and y = 44.5 ft., in equations 5.1 and 5.4, the scour depths for Hardinge Bridge and East-West Interconnector turn out as 1.58 ft (Eqn.5.1) and 1.30 ft (Eqn.5.4) respectively and the observed scour depth, d_t/y = 1,60. The mean diameter, D_{50} of Hardinge bridge is 0.14mm (Personal communication with Dr.A. Nishat) and for East-West Interconnector is 0.19. From this it is evident that scour depth is more in finer material compared to the coarser material.

Equations (5.1), (5.2) and (5.3) are for Hardinge bridge while equations (5.4), (5.5) and (5.6) are for East-West Interconnector and shown similarity to equations (2.4), (2.2) and (2.6). Only differences are in constants and in the value of the index power. Comparing equation (5.2) and (2.2), it is found that the variations are 21% and 37%)in the values of the coefficient and index power respectively. Similarly, comparing equation (5.4) and (2.4), the variations are found 23% and 19% in the values of the coefficient and index power respectively. Figs. 5.21 to 5.26 also show the trend of deviation with equation (2.4), (2.2) and (2.6). These deviations may be due to the following reasons:

(a) Development of the empirical formulas from the small scale laboratory investigations where many parameters were kept constant, while the conditions differ under field conditions.

(b) Conditions and nature of bed material may vary considerably at different points and depths, data for which need to be monitored carefully.

(c) The scour also depends on the skewness of the flow and on the state of flow i.e., whether the flood is rising or falling. Precise observations regarding direction of current and state of flood should be recorded properly.

5.3.5 Comparison of Field and Laboratory Data:

Empirical formulas of Blench (1962), Inglis (1949) and Shen et al (1966) have been used to predict the scour depth (using the field and laboratory data). Observed scour depth in field and laboratory has been compared with the predicted scour depth by various formulas mentioned above. Figs. 5.27 to 5.32 are the plots of observed scour depths and the predicted scour depth. This study has been possible for round nose (Hardinge Bridge) and circular pier (East-West Interconnector), as the field data for other types of pier were not available.

5.3.5.1 Round-nose Piers:

The observed scour depths and the scour depths predicted by various formulas for round-nose piers are shown in Figs. 5.27 through 5.29. Blench's relation (Fig.5.27) mostly overpredicts the field data while the experimental data shows good correlation though the data cluster round a small zone.

Fig.5.28 shows the Inglis's relation, where all the experimental data were underpredicted whereas the field data were evenly distributed along the line of perfect agreement.

Fig. 5.29 shows the Shen et al's relation, where all the experimental data were overpredicted and among the field data few were on the line of perfect agreement and the remaining were distributed on the both sides of line of perfect agreement.

By comparing these figures, it may be concluded that the scour formula by Blench (1962) is the best predictor among those compared in this study for round-nose piers, as this envelopes most of the data, having higher values of linear correlation coefficient, r between the observed and predicted scour depth.

5.3.5.2 Circular Piers:

Figs. 5.30 through 5.32 shows the comparison between the observed scour depths and the scour depths predicted by various formulas for circular piers.

Blench's relation (Fig. 5.30), overpredict the most of the field data and under predict the most of the experimental data. Fig. 5.31 shows the Inglis's (1949) relation, where all the experimental data were underpredicted irrespective of the mean grain size. Field data were evenly distributed along the line of perfect agreement. In Shen et al's (1966) relation (Fig. 5.32), all the experimental data were overpredicted whereas only few of the field data were in the underperdicted zone.

Blence (1962) relation (Fig. 5.30) in case of circular piers also found to be the best predictor among those compared in this study as the point in this plot were less scattered compared to others.

CHAPTER - VI

CONCLUSION AND RECOMMENDATION

6.1.0 Conclusions:

The analysis of the Laboratory and field data on scour around bridge piers for different shapes and flow conditions as reported in the present study gives considerable support to the following conclusions:

1) The maximum depth of scour is developed in rectangular type of pier followed by circular, round nose and sharp nose. Similarly, the maximum area of scour in plan form follow the same sequence as the scour depth. Since the scour depth and area of scour in plan form are minimum for sharp nose piers, their use may be considered most beneficial from the hydraulic considerations.

2) The maximum scour depth may occur either at the upstream or at the downstream of the pier depending on the shape of pier.

3) The scour depth is higher in case of finer hed material and gradually decreases as the coarseness of the bed material increases. Thus, sediment size has considerable effect on the depth of scour.

4) The relative scour depth, d_t/b increases with the relative approach depth, y/b. In average, the ratio of maximum scour depth to the approach depth for all types of pier has been found to be 1.95.

5) Though there are differences in the values of the coefficient and index power for the equations of the form $y = ax^b$ (where Y and X are variables, a is the coefficient and b is the index power) but the equations derived from field data are almost identical with those derived by Inglis, Blench and Shen-et al. The change in the values of the coefficient, a and index power, b is due to various factors involved in the flow phenomenon around piers together with the constraints in the range of data.

6) Scour prediction by Blench formula indicates better correlation compared to other formulae .

6.2.0   Recommendations for future study:

The study of scour phenomenon around bridge pier may be extended by incorporating the following:

1. In the present study, the scour phenomenon around bridge piers in different bed materials were observed and the bed slope were kept constant. Therefore, the effect of bed slope on scour depth may be studied.

2. Small scale laboratory study has been conducted in cases of circular and round nose type of piers and the results have been compared with the circular and round nose piers of the East West Interconnector and the Hardinge Bridge respectively. Small scale studies for wider range of discharge in a broader tilting flume may be conducted to compare the field data of scour under similar conditions.

3. The effect of the flow direction with respect to the pier shape and position may be studied.

REFERENCES

Acres International Limited, 1970, _Design Transmittals_, East-West Interconnector Project of Bangladesh Power Development Board, Dhaka.

Ahmad, M., 1962, Discussion on scour at bridge crossings by Laursen, E.M., Trans., ASCE, Vol.127, Part-I.

Arunachalam, K., 1965, Scour around bridge Piers, Journal of Indian Road Congress, Vol. 29, No.2, PP.189-210.

Bangladesh Power Development Board, 1983, _Inspection and Maintenance_, printed reports on East-West 230KV Interconnector Jamuna river crossing of Bangladesh Power Development Board, Dhaka.

Bangladesh Power Development Board, 1980, _Progress Report East-West Electrical Interconnector Project_, Dhaka.

Bauer, W.J., 1962, Dsicussion on scour at bridge crossings by Laursen, E.M., Trans., ASCE, Vol. 127, Part-I.

Blaisdell,F.W. and Hebaus, G.G., 1981, Ultimate Dimensions of local scour, Journal of Hydraulics Divn., Proc. ASCE Vol.107, No. HY3, March.

Blench,T., 1962, discussion on scour at bridge crossings, by Laursen, E.M., Trans., ASCE, Vol. 127, Part-I.

Blench,T., 1966, Mobile Bed Fluviology, Department of Technical Services, University of Alberta, Canada.

Bradley, J.N., 1962, discussion on scour at bridge crossings by Laursen, E.M., Trans., ASCE, Vol.127, Part-I.

Carstens, M.R., 1966, Similarity Laws for localized scour, proc., ASCE Vol. 92, No. HY3, Paper 4818, PP. 13-36.

Chitale, S.V., 1962, discussion on scour at bridge crossings by Laursen, E.M., Trans., ASCE, Vol.127, Part-I.

Farhoudi, J and Smith, K.V.H, 1982, Time scale for scour downstream of hydraulic jump, Journal of the Hyd. Divn.ASCE Vol.108, No. HY10, Paper 17393, PP. 1147-1162.

Garde, R.J. and Raju. R., 1978, Mechanics of Sediment Transportation and Alluvial Stream problems, Wiley Eastern Ltd. New Delhi, India.

Giles, R.V., 1962, Schaum's outline of theory and problems of fluid mechanics and hydraulics, Schaum Publishing Co., Second Edition, New York, USA.

Gill, M.A., 1972, Erosion of sand beds around spur dikes, Proc., ASCE Vol. 98, No. HY9, Paper 9198, PP 1587-1602.

Indian Road Congress, 1977, Standard specifications and code of practice for road bridges, Section-I, General features of design, New Delhi, India.

Inglis, C.C., 1949, The behaviour and control of rivers and canals (with the aid of models), Part-II, Central Waterpower Irrigation and Navigation Research Station, Research Publication No. 13, Poona, India.

Jain, S.C., and Fischer, E.E., 1980, Scour around bridge piers at high flow velocities, Journal of hydraulics Divn., ASCE Vol.106, No. HY11, PP. 1827-1842.

Jain, S.C., 1981, Maximum clear water scour around circular piers, Journal of the hydraulics Divn., ASCE Vol.107, No.HY5, PP.611-626.

Joglekar, D.V., 1962, discussion on scour at bridge crossings by Laursen, E.M., Trans., ASCE, Vol.127, Part-I.

Jogleker, D.V., 1971, Mannual on River Behaviour Control and Training, Central Board of Irrigation and Power, Publication No.60, New Delhi, India.

Khan, A.O.A., 1983, An experimental investigation of the effect of location and projection of single groin in a bend, M.Sc.Thesis presented to the Department of Water Resources Engineering,BUET,Dhaka.

Komura,S., 1966, Equillibrium depth of scour in ong constrictions, Proc., ASCE, Vol. 92, No. HY5, Paper 4898, PP.17-37.

Laursen, E.M., 1962. Scour at bridge crossings, Trans., ASCE, Vol. 127, Part-I, Paper 3294.

Laursen,E.M., 1963, An analysis of relief bridge scour, Proc. ASCE, Vol. 89, No. HY3, Paper 3516, PP. 93-118.

Nagler, F.A., 1917, Obstruction of bridge piers to the flow of water, Trans., ASCE, Vol.82, paper 1409.

Neill,C.R., 1969, discussion on local scour around bridge piers by Shen,H.W, Schneider,V.R. and Karaki,S., Proc., ASCE, Vol.95, No. HY6, June.

Neill, C.R., 1973, Guide to bridge hydraulics. Project committee on bridge hydraulics, Roads and transportation association of canada, University of Toronto Press,Canada.

Pandey, U.S., 1980, Scour near railway bridge at Mokameh across river Ganges, Proc., International Workshop on alluvial river problems, University of Roorkee, India.

Raina, R.M. and Manglik, S.K., 1980, Feasibility study for location of a road bridge on Ganga in eastern Bihar, Proc., International Workshop on alluvial river problems, University of Roorkee, India.

Rao, B.B. and Muthuswamy, C., 1974, Considerations in the design and sinking of well foundations for bridge piers, Paper No. 238 of the Indian Road Congress, India.

Raudkivi, A.J. and Ettema, R., 1983, Clear-water scour at cylindrical piers, Journal of hydraulics Engg., Vol. 109, No.3, PP. 338-350.

Romita, P.L., 1962, discussion on scour at bridge crossings by Laursen, E.M., Trans., ASCE, Vol. 127, Part-I.

Shen, H.W., Schneider, V.R. and Karaki,S., 1969, Local scour around bridge piers, Proc., ASCE, Vol.95, No.HY6, Paper 6891, PP. 1119-1140.

Shen, H.W., 1971, Scour near piers, River Mechanics II, Shen H.W., ed., W.R.P., Fort Collins, Colorado, USA.

Simons, D.B. and Senturk,F., 1977, <u>Sediment transport technology,</u> Water resources publications, Fort Collins, Colorado, USA.

Singh, B., 1979, <u>Fundamentals of Irrigation Engineering,</u> Sixth edition, Nem Chand and Bros., Roorkee, India.

Thomas, A.R., 1962, discussion on scour at bridge crossings by Laursen, E.M., Trans., ASCE, Vol. 127, Part-I.

Tison, L.J., 1962, discussion on scour at bridge crossings by Laursen, E.M., Trans., ASCE, Vol.127, Part-I.

Varshney, R.S., Gupta, S.C. and Gupta, R.L., 1977, <u>Theory and Design of Irrigation Works,</u> Third edition, Nem Chand and Bros., Roorkee, India.

CIRCULAR CAISSON

b

FLOW

y

d_t

d_s

SAND
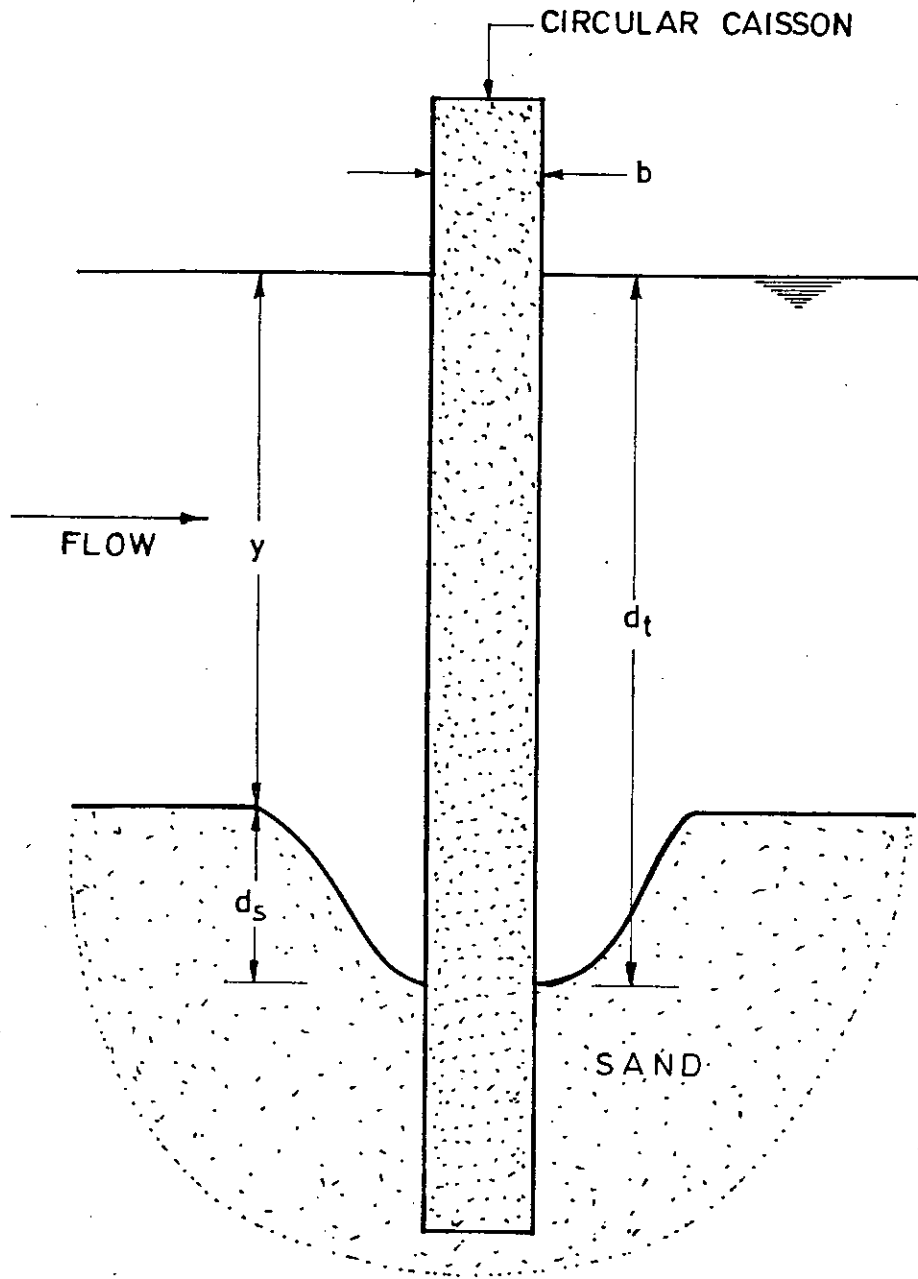
FIG. 1·1 DEFINITION SKETCH
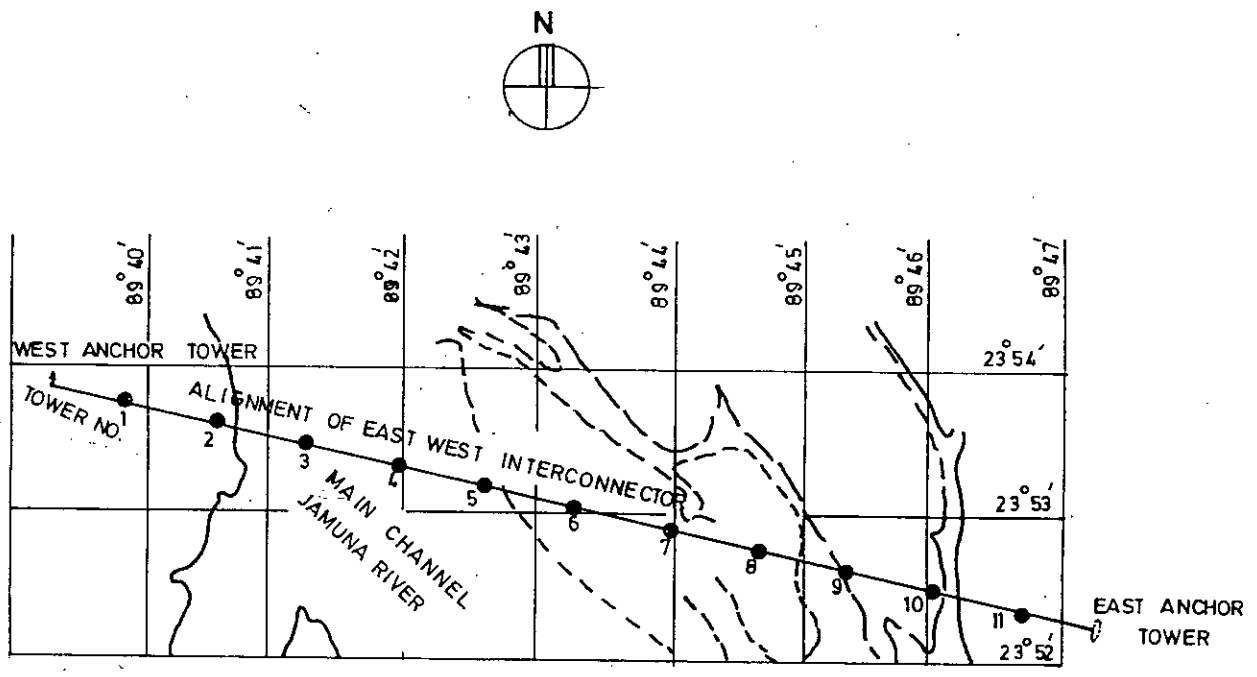
FIG. 1·2 JAMUNA RIVER CROSSING PLAN
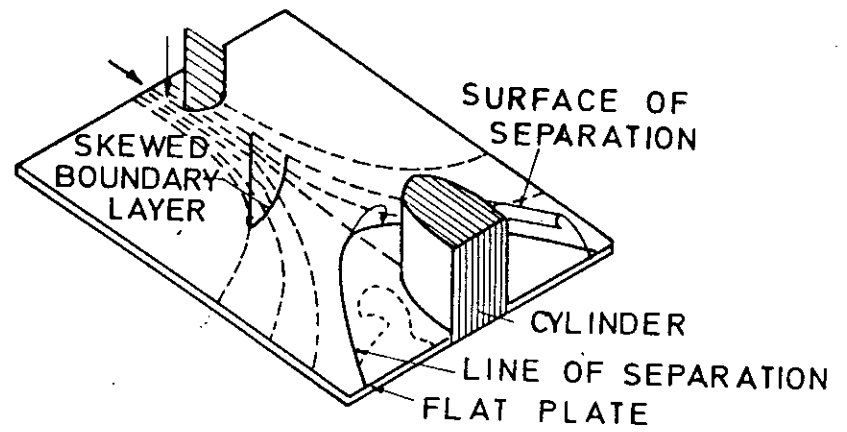
FIG. 2·1   HORSE-SHOE VORTEX SYSTEM
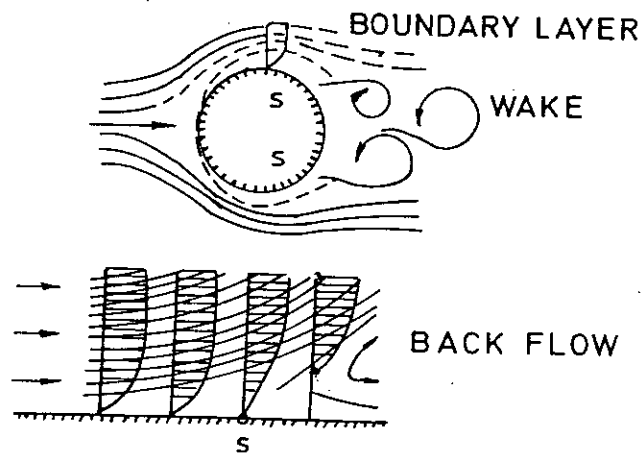
FIG. 2,2   WAKE VORTEX SYSTEM
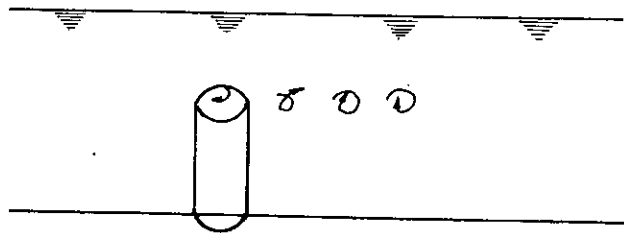
FIG. 2·3   TRAILING VORTEX SYSTEM
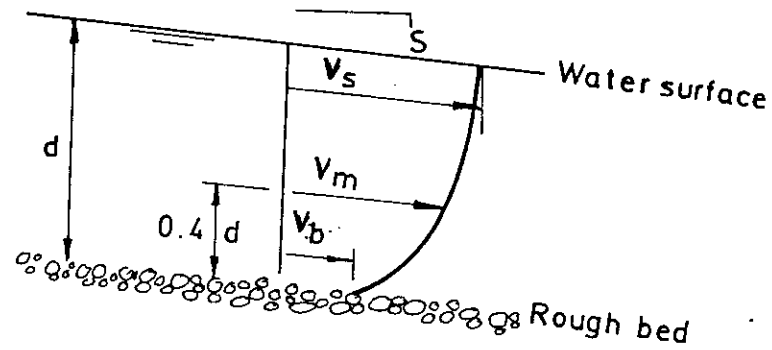
Fig. 2·4 The vertical velocity profile and approximate velocity ratios in a wide straight channel with a rough bed. The time average bed shear stress ΥdS where Υ is the unit weight of water. The surface velocity V_s is about 1·1·1·2 times the mean velocity V_m. The bottom velocity V_b is usually in the range 0·3 – 0·7 times V_m. The bottom velocity (time average value) is somewhat ill defined because of the steep velocity gradient and the strong turbulent fluctuations Particles on the bed experience fluctuating lift and drag forces even when the surface velocity is fairly steady.
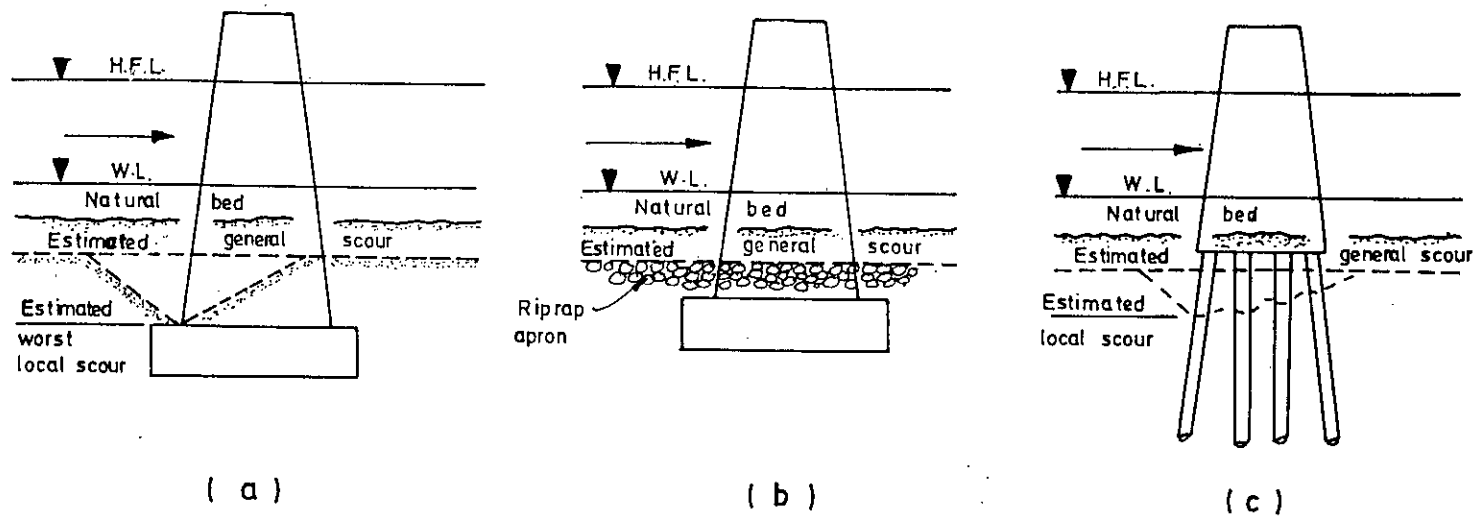
Fig. 2·5 Various ways of catering for scour in the design of pier foundations.

    (a) bottom of footing placed well below the estimated lowest scour level

    (b) footing placed below the general scour level and protected by riprap apron against local scour

    (c) pier supported on piles designed to withstand the exposure of their upper parts, with alternatives.
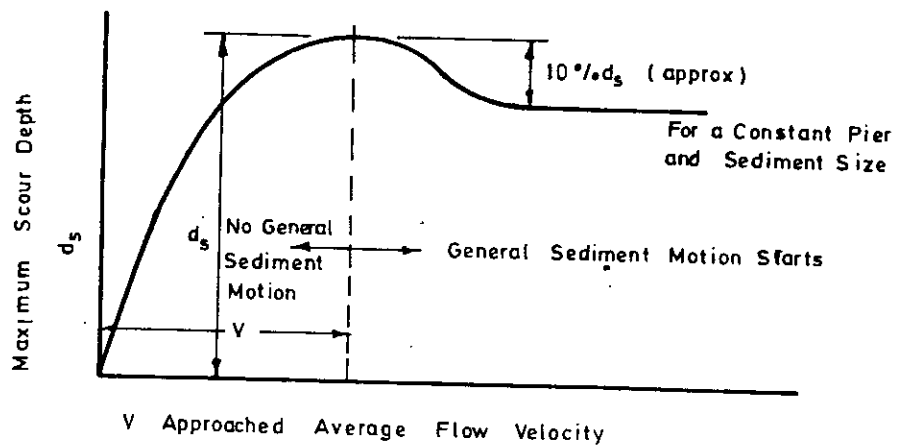
FIG. 2.6 <u>VARIATION OF SCOUR DEPTH WITH VELOCITY</u>
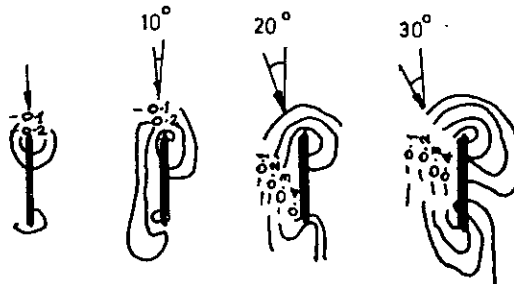
Fig. 2·7 Scour patterns around piers with stream flow at different angles to its alignment. Depth of flow as unity.
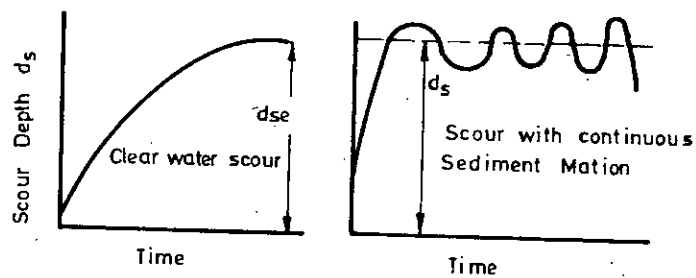
FIG. 2.8 <u>TIME VARIATION OF SCOUR DEPTH</u>
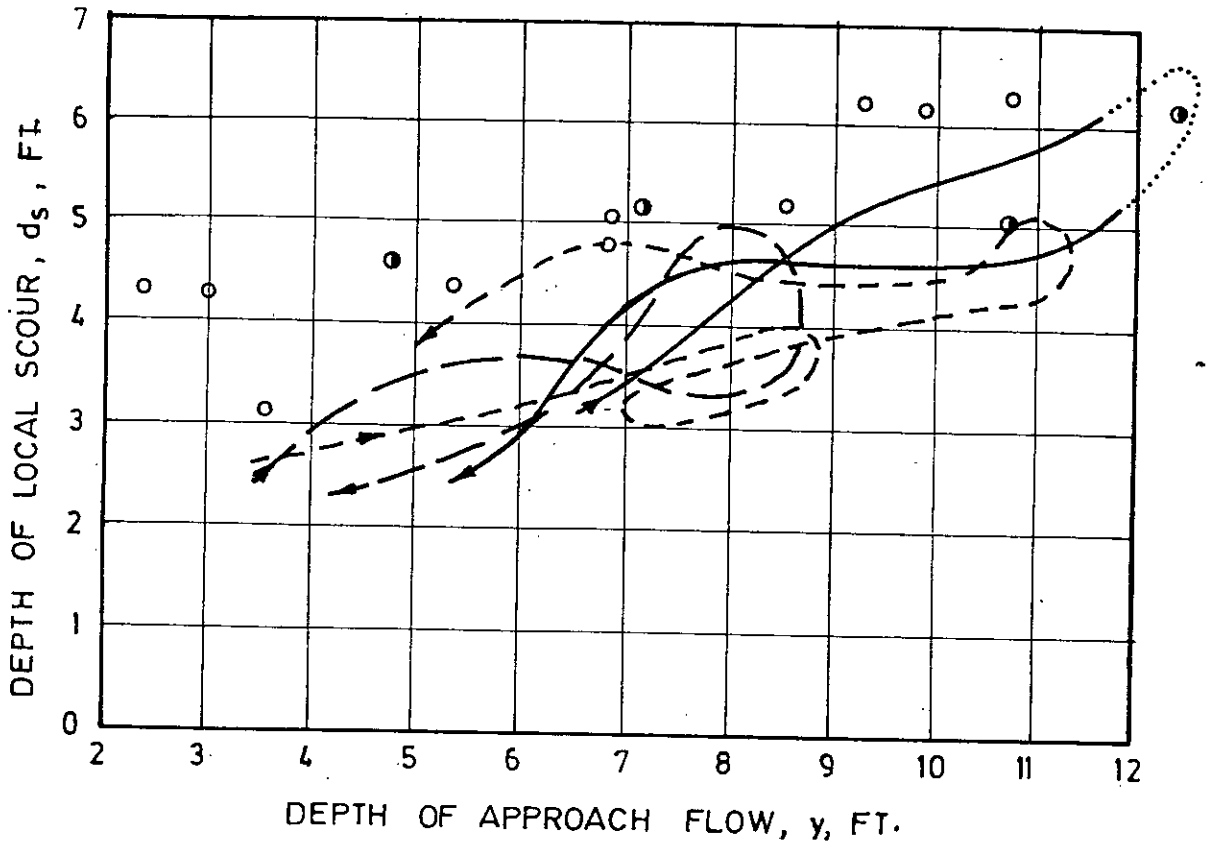
FIG. 2·9 MODEL-PROTOTYPE CONFORMITY FROM LAURSEN'S INVESTIGATION
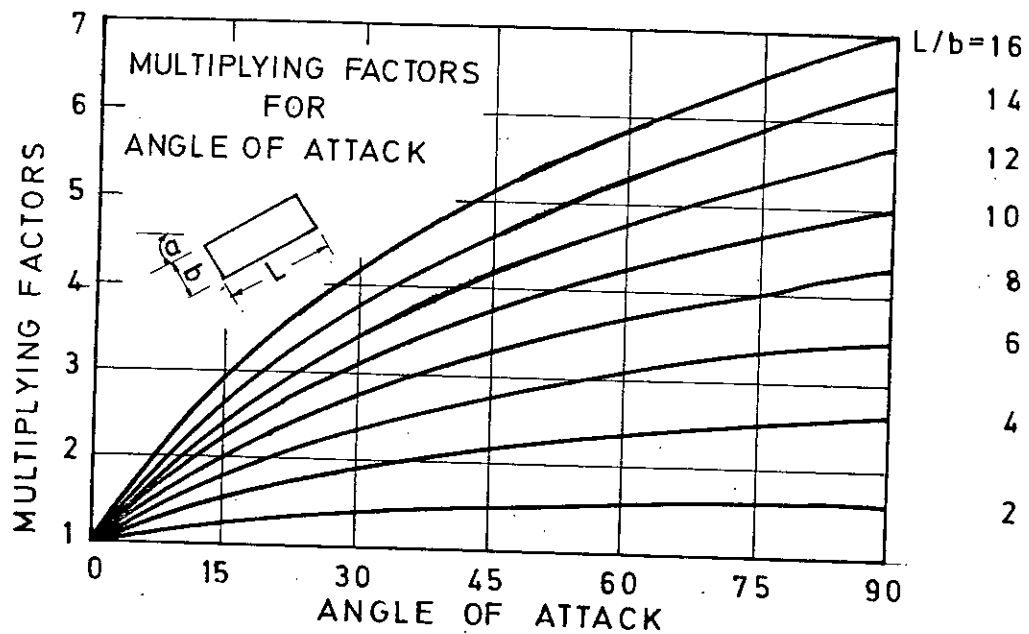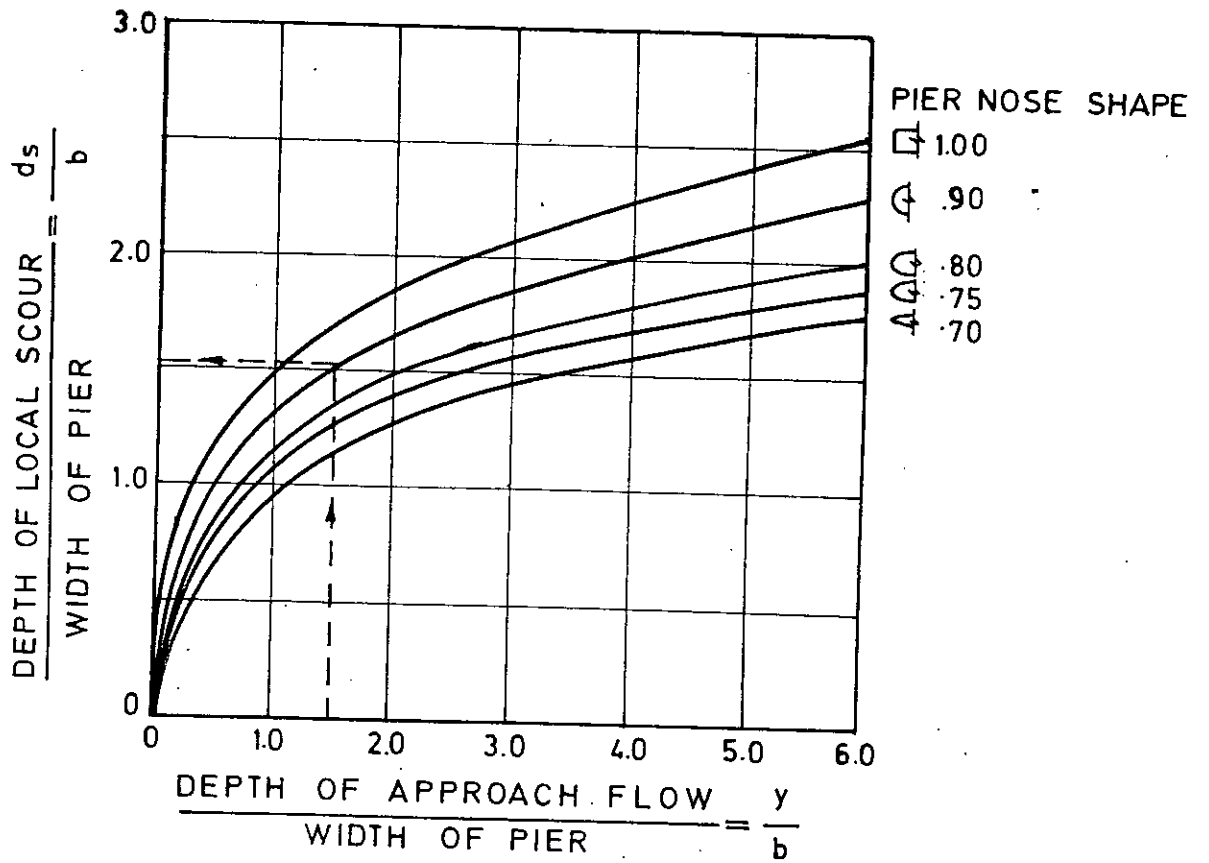
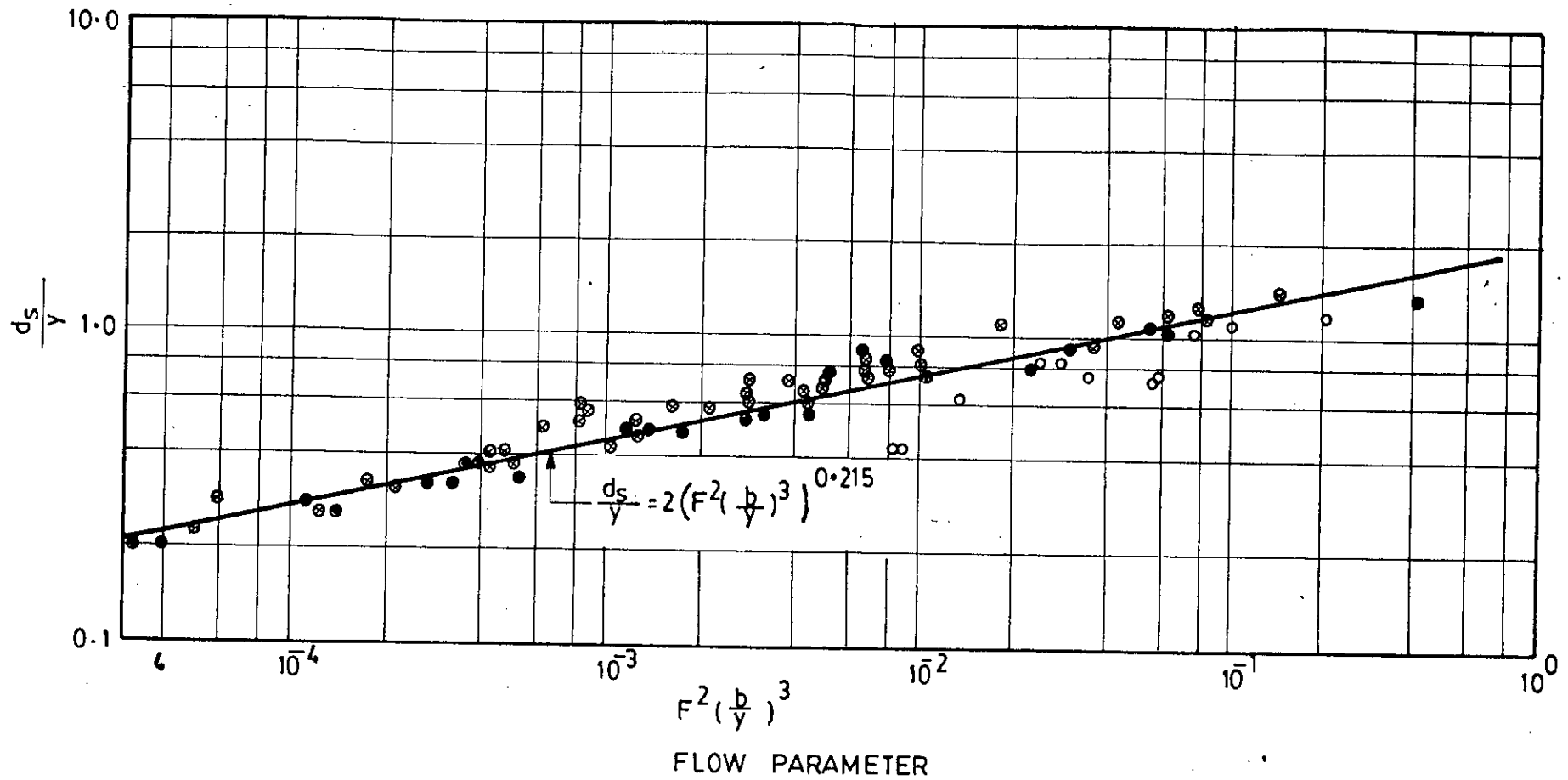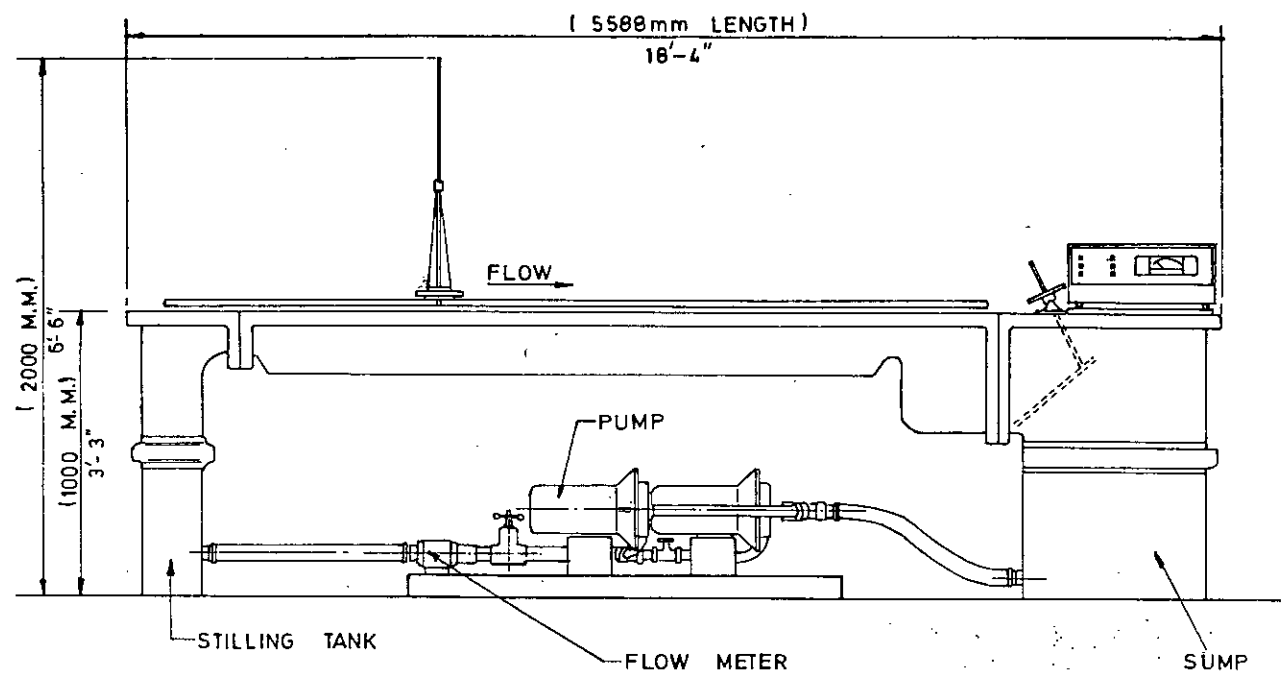FIG. 2.10. DESIGN CURVES FOR CALCULATING DEPTH OF LOCAL SCOUR AT BRIDGE PIERS.

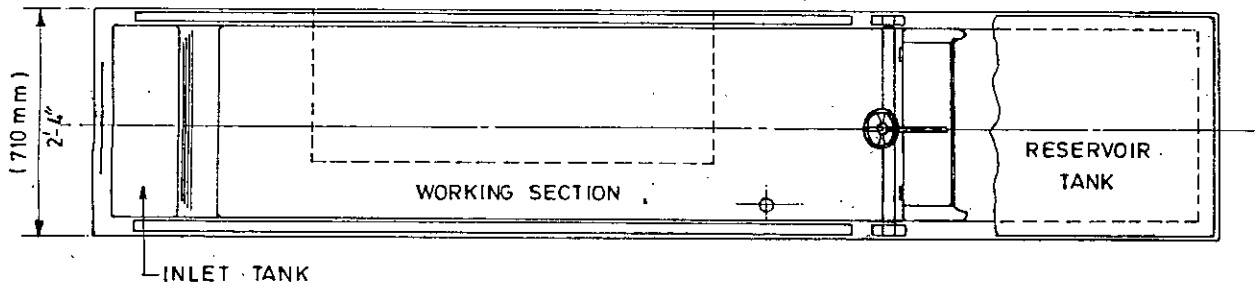FIG. 2.11 DESIGN CURVE FOR
CALCULATING DEPTH OF
LOCAL SCOUR AT BRIDGE
PIERS

LEGEND

	SOURCE	SAND SIZE D_{50} mm
o	COLORADO STATE UNIVERSITY	0·24
●	CHABERT AND ENGELDINGER	0·26
⊗	CHABERT AND ENGELDINGER	0·52

(5588mm LENGTH)
18'-4"

(2000 M.M.)

6'-6"

(1000 M.M.)
3'-3"

FLOW

PUMP

STILLING TANK

FLOW METER

SUMP

FLOW VISUALISATION TANK

(710 mm)

2'-4"

WORKING SECTION

RESERVOIR TANK

INLET TANK
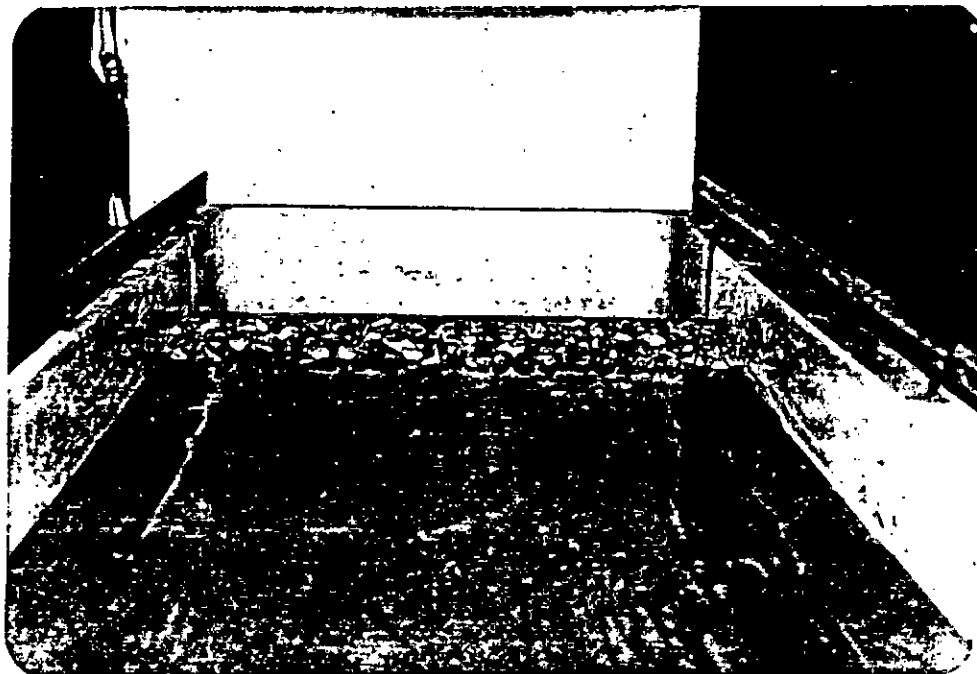
PLAN OF VISUALISATION TANK

FIG, 4.1 FLOW VISUALISATION TANK

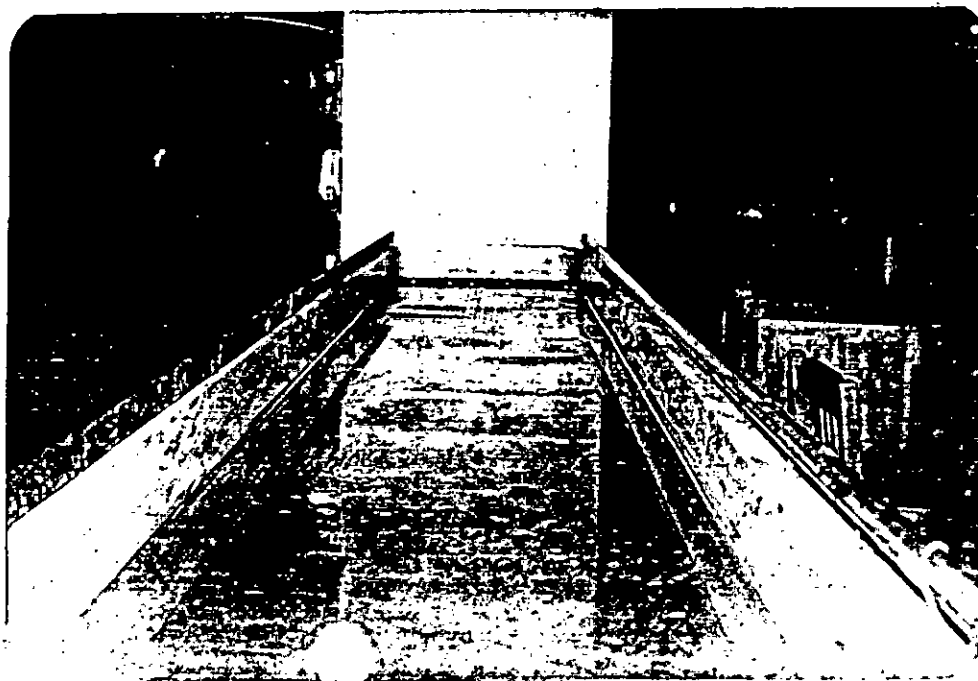FIG. 4·2 PHOTOGRAPH OF STONE PITCHING
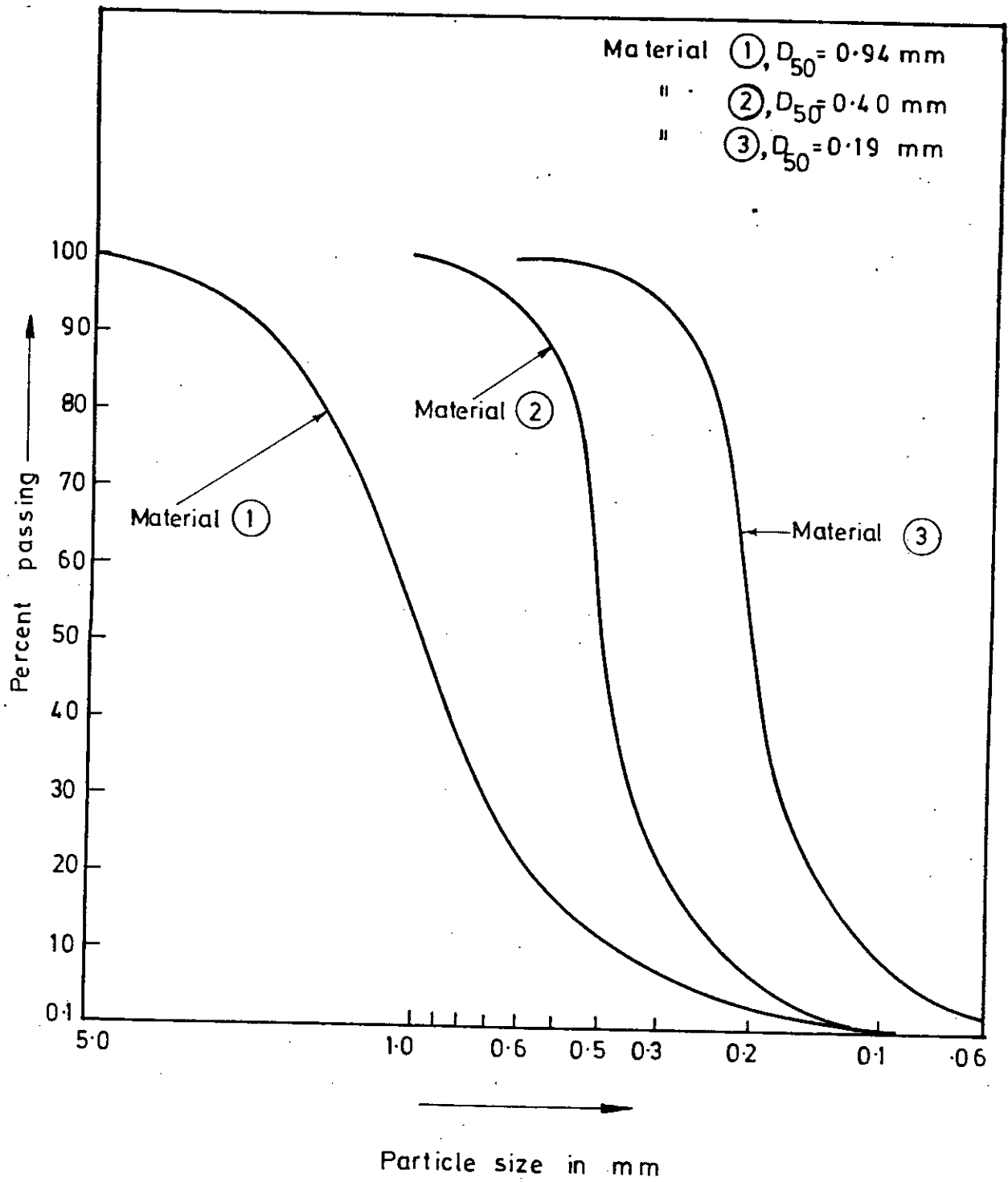

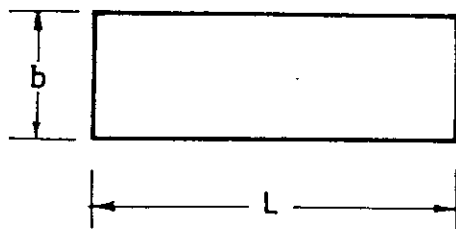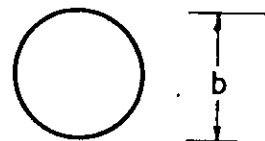
FIG. 4·3 GENERAL VIEW OF FLUME BED

FIG. 4·4 GRAIN SIZE DISTRIBUTION

L, LENGTH OF PIER =0·492 ft
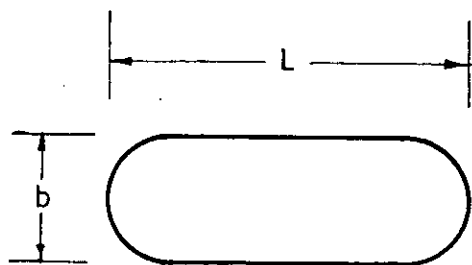
b, WIDTH OF PIER =0·164 ft

a) RECTANGULAR

b) CIRCULAR

c) ROUND - NOSE
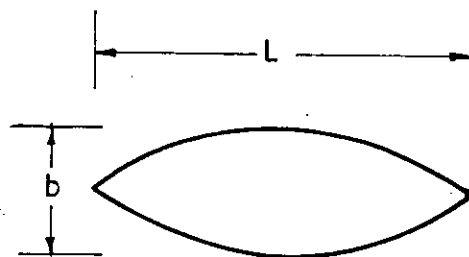
d) SHARP - NOSE

FIG. 4·5 DIFFERENT SHAPES OF PIER
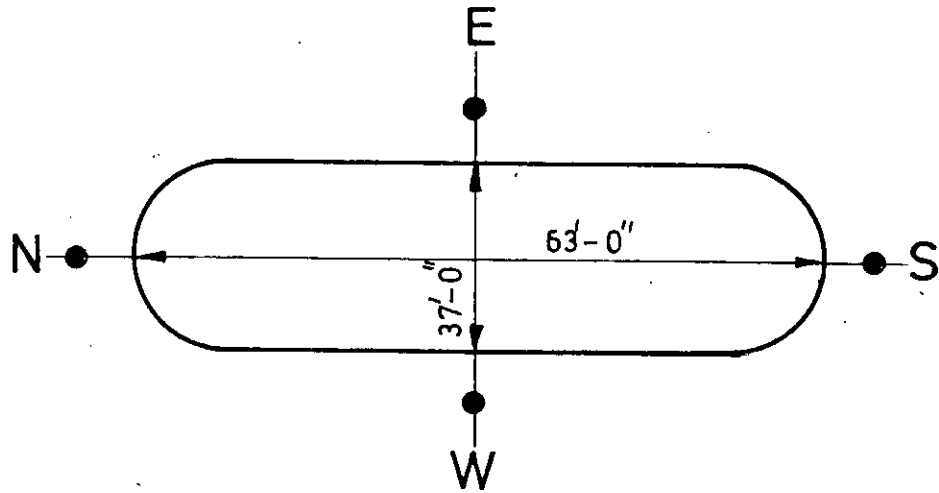
FIG. 5·1 (a) SCOUR OBSERVATION POINTS AROUND A PIER
OF HARDINGE BRIDGE
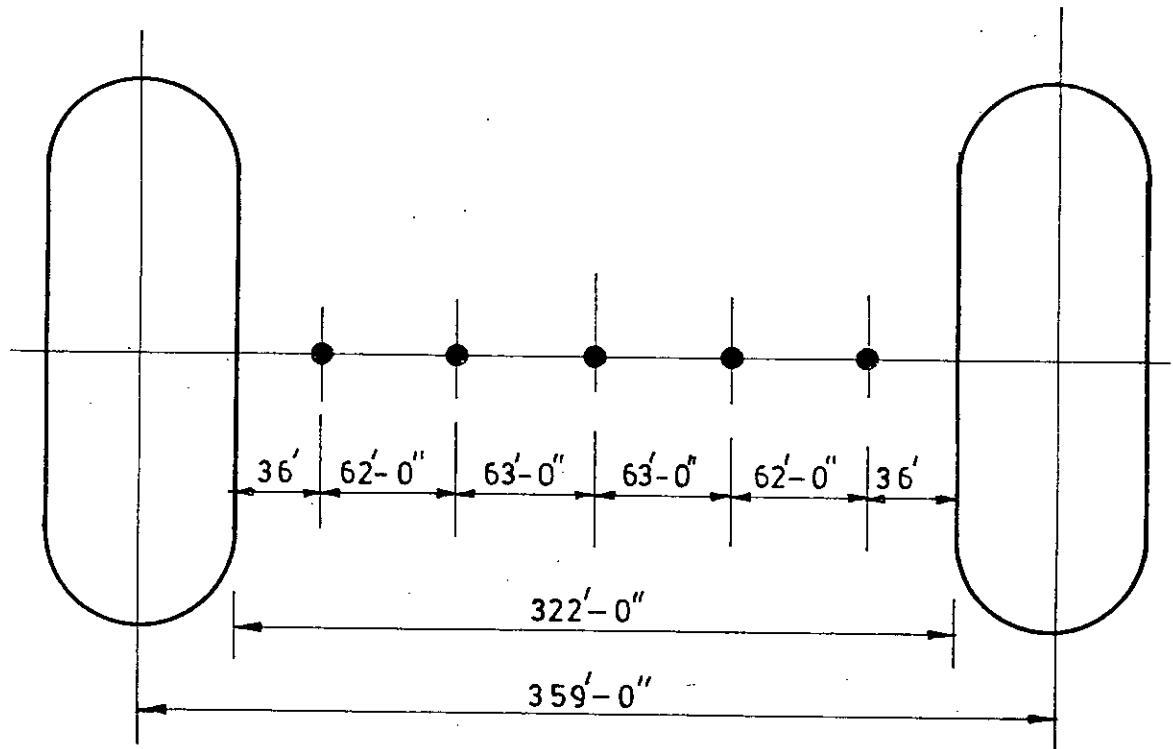
FIG. 5·1 (b) VELOCITY AND DEPTH OBSERVATIONS IN BETWEEN
TWO PIER OF HARDINGE BRIDGE
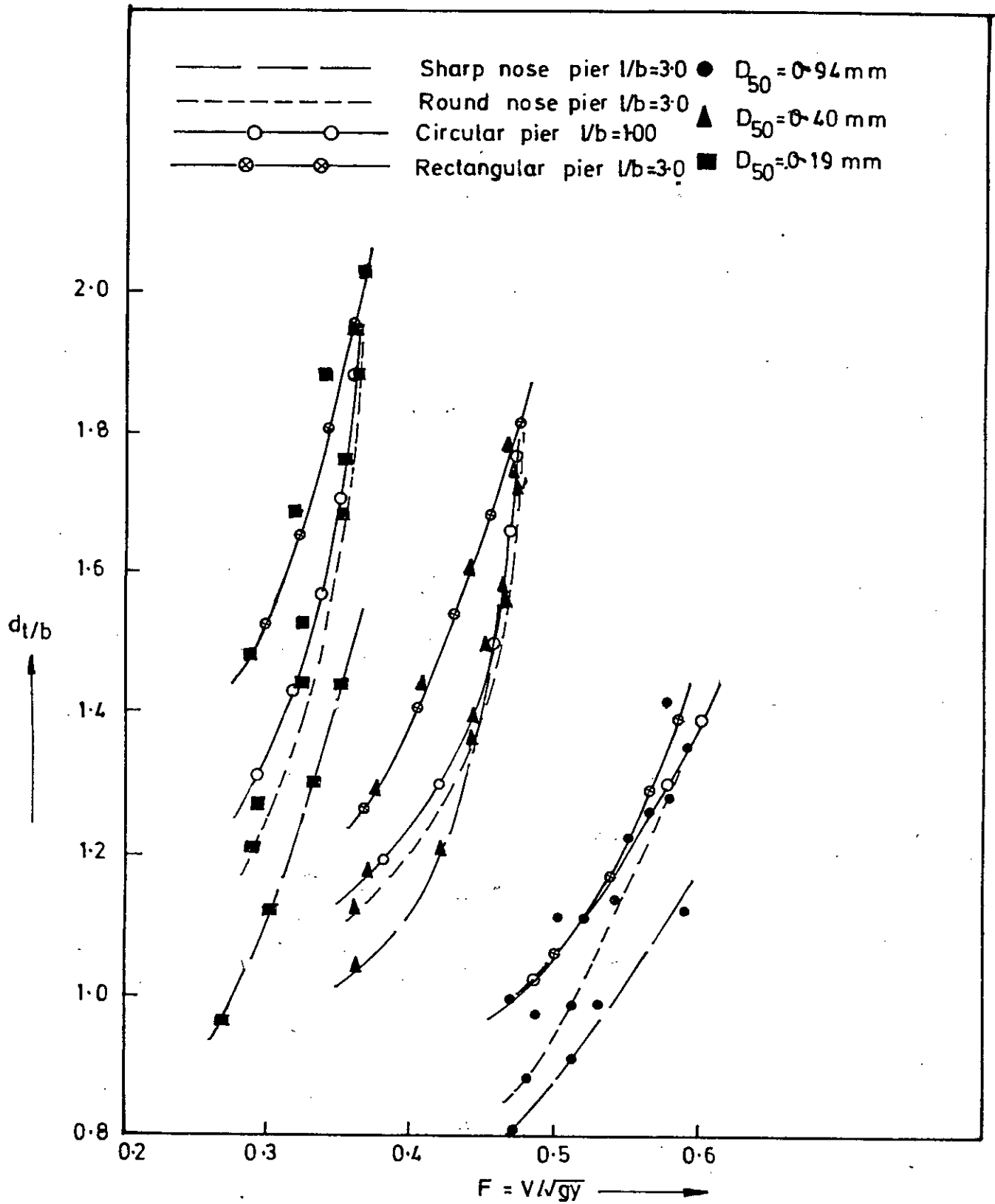
FIG. 5·2 SCOUR DEPTH VERSUS FLOW FROUDE NUMBER
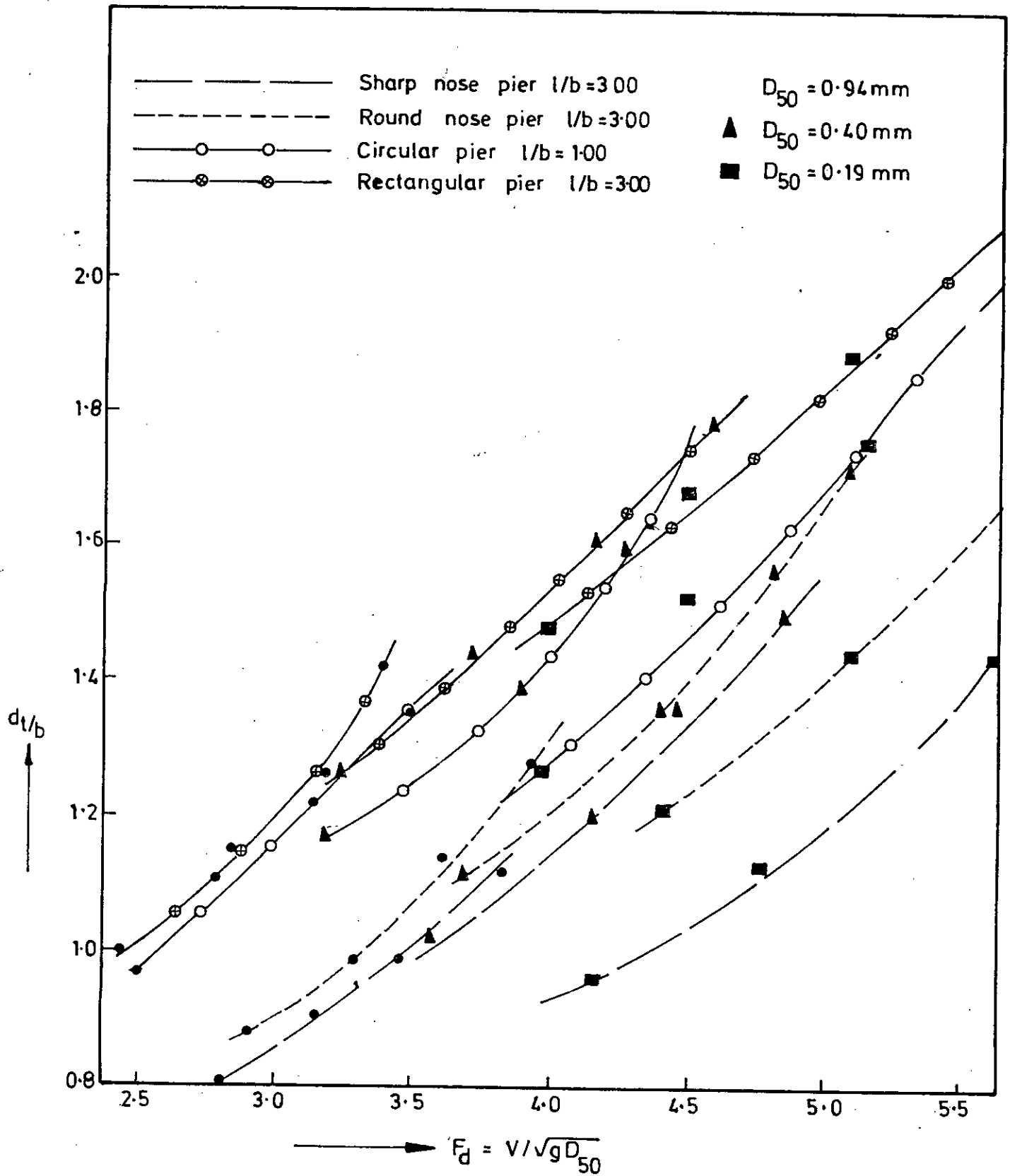
FIG. 5·3 SCOUR DEPTH VERSUS PARTICLE FROUDE NUMBER
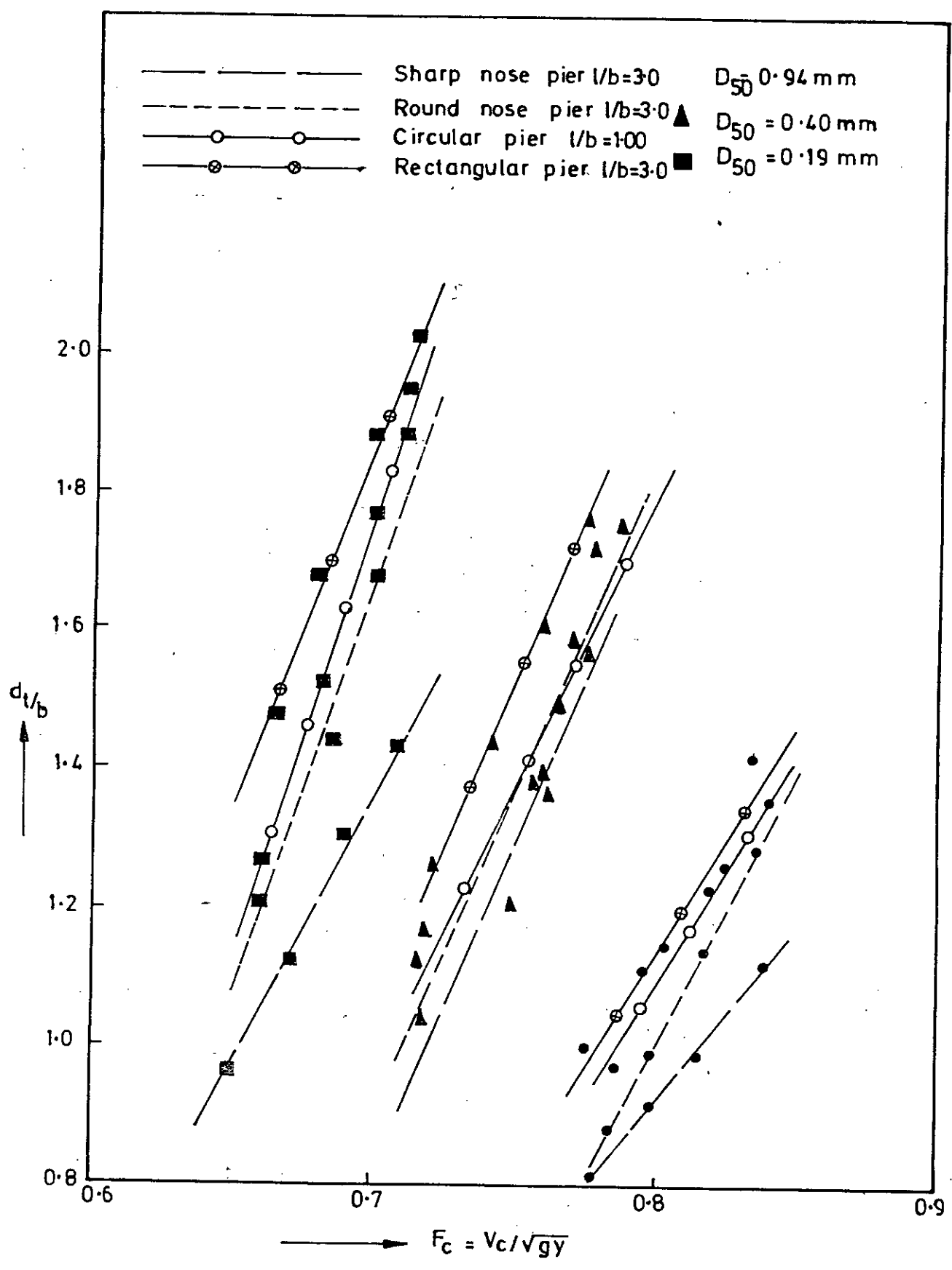
FIG. 5·4   SCOUR DEPTH VERSUS CRITICAL FLOW FROUDE NUMBER
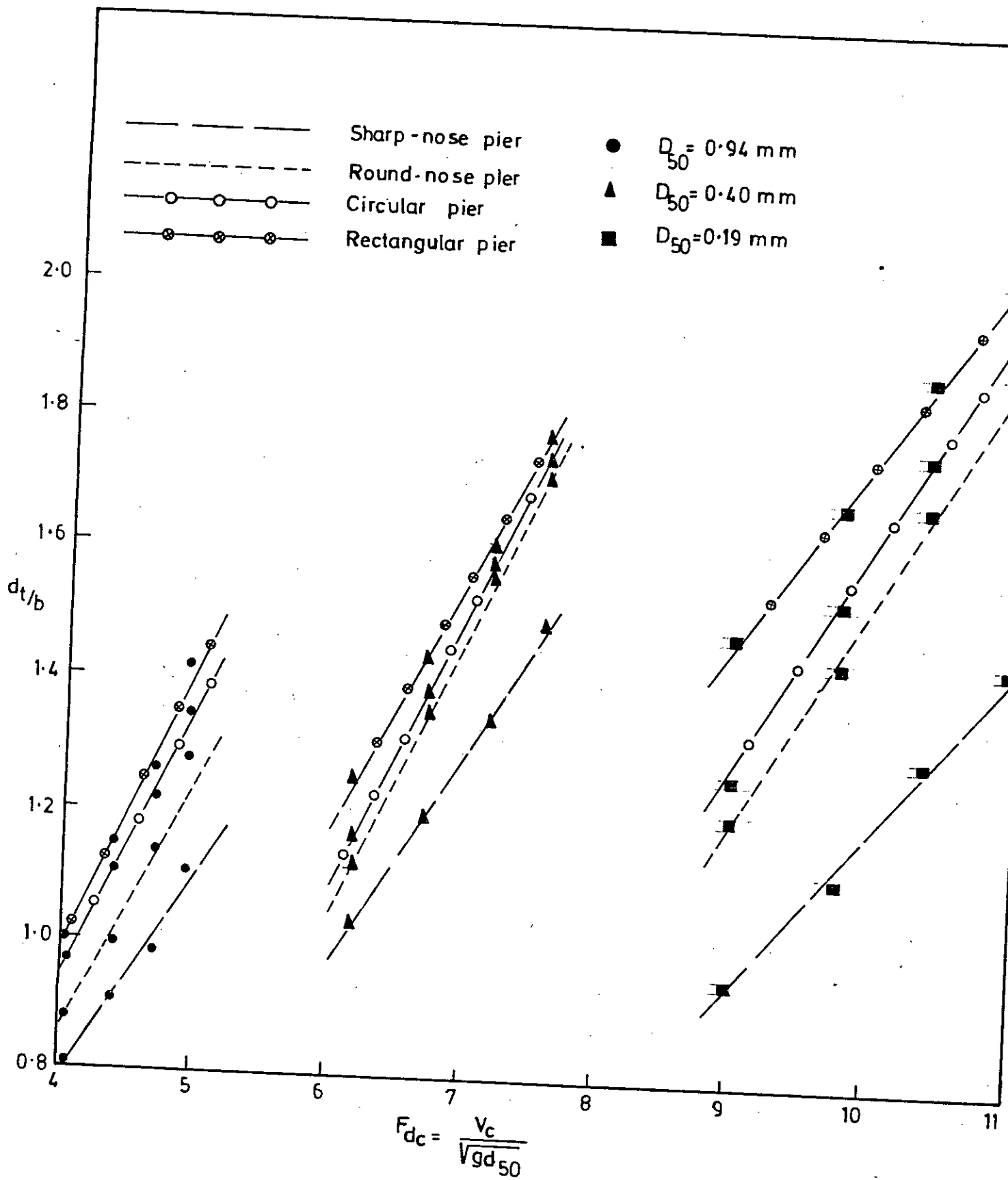
FIG. 5·5 SCOUR DEPTH VERSUS PARTICLE CRITICAL FROUDE NUMBER
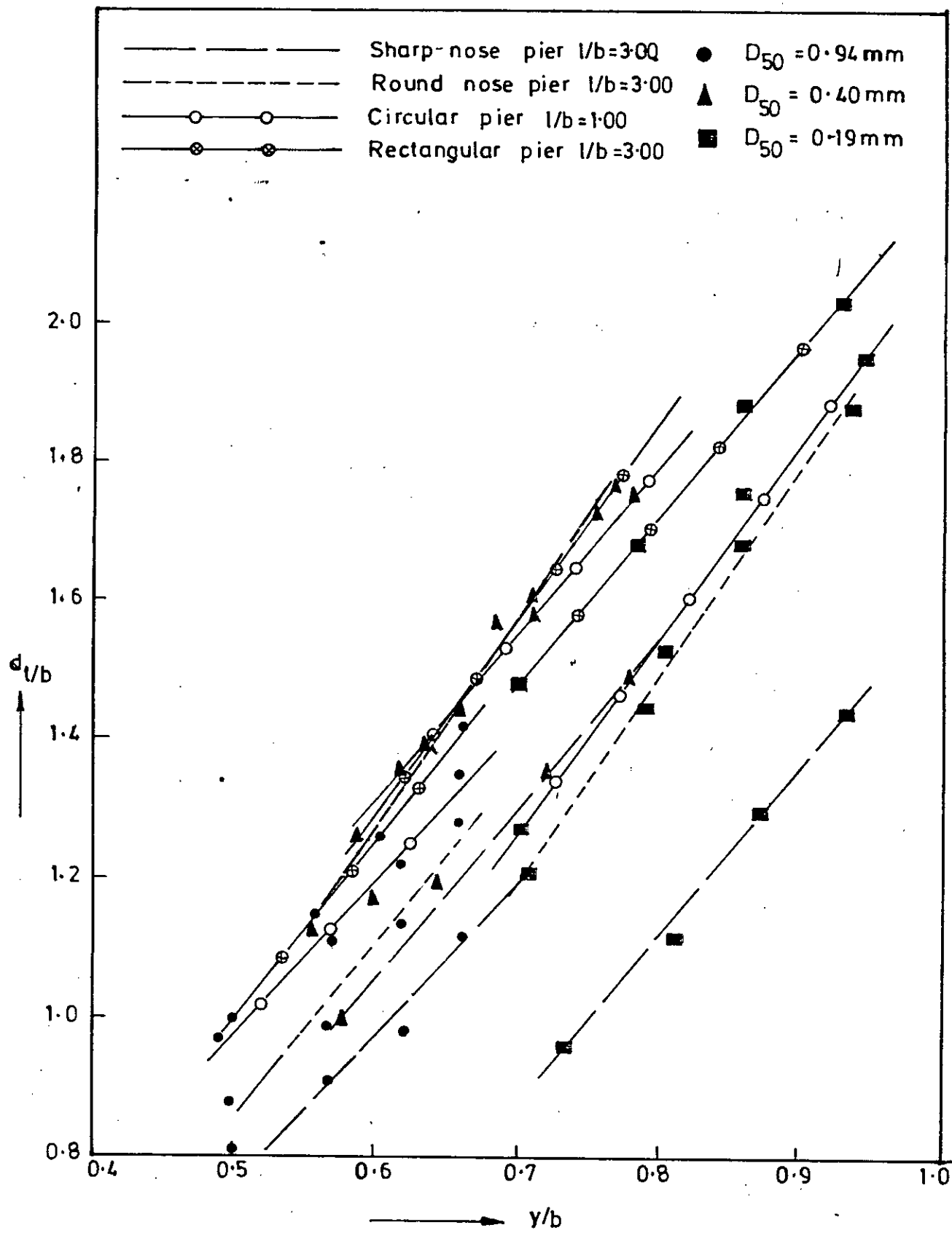
FIG. 5·6   SCOUR   DEPTH   VERSUS   APPROACH   DEPTH   OF   FLOW
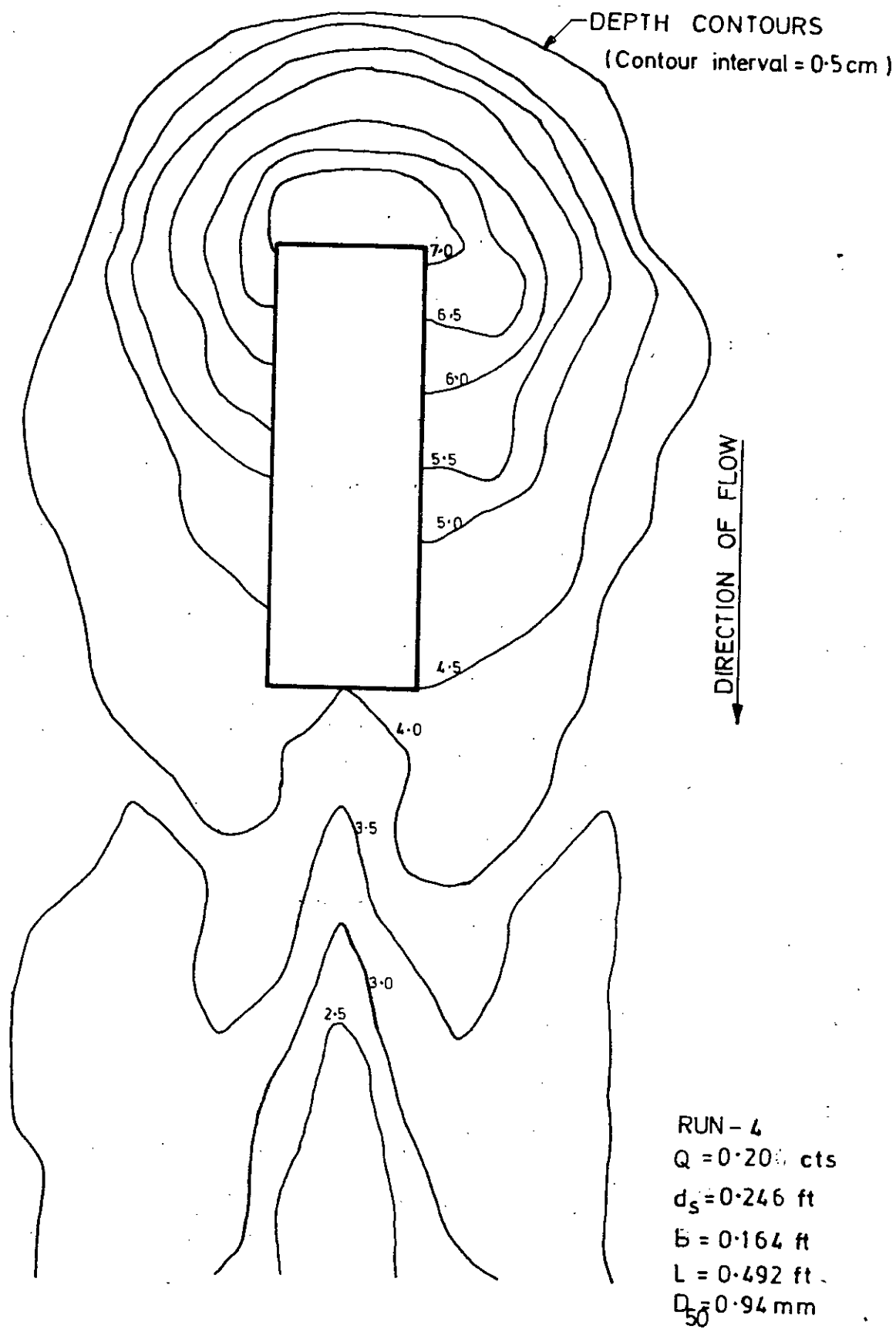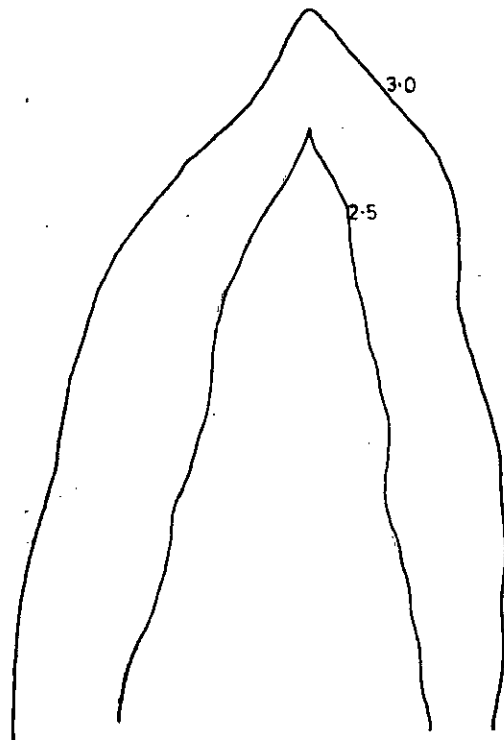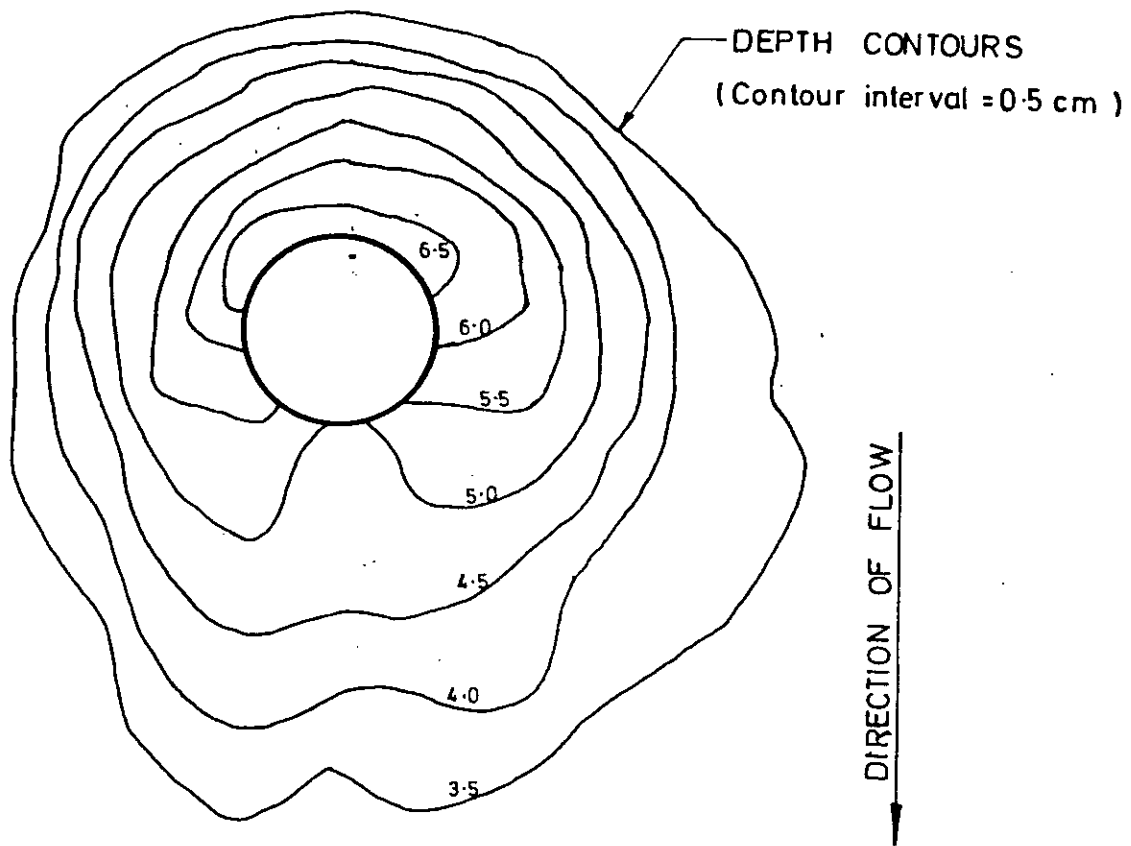
DEPTH CONTOURS
(Contour interval = 0·5 cm)

DIRECTION OF FLOW

7·0

6·5

6·0

5·5

5·0

4·5

4·0

3·5

3·0

2·5

RUN – 4

$Q = 0·20$ cts

$d_s = 0·246$ ft

$b = 0·164$ ft

$L = 0·492$ ft

$D_{50} = 0·94$ mm

FIG. 5·7 SCOURE PATTERN AROUND RECTANGULAR PIER
(Scale 1:2)

FIG. 5·8 SCOUR PATTERN AROUND CIRCULAR PIER
(Scale 1:2)

DEPTH CONTOURS
(Contour interval = 0·5 cm)

DIRECTION OF FLOW

6·5
6·0
5·5
5·0
4·5
4·0
3·5

3·5   3·0   3·0   3·0   3·5

Run - 11

Q = 0·20 cts

d_t = 0·21 ft

b = 0·164 ft

L = 0·492 ft

D_{50} = 0·94 mm

FIG. 5·9 SCOUR PATTERN AROUND ROUND NOSE PIER
(Scale 1:2)

DEPTH CONTOURS
(Contour interval 0·5cm)

DIRECTION OF FLOW

6·0

5·5

5·0

4·5

4·0

3·0

3·5

3·0

3·5

3·0

Run -15

Q = 0·20 cts

d_s = 0·2165 ft

b = 0·164 ft

L = 0·492 ft

D_{50}= 0·94m m
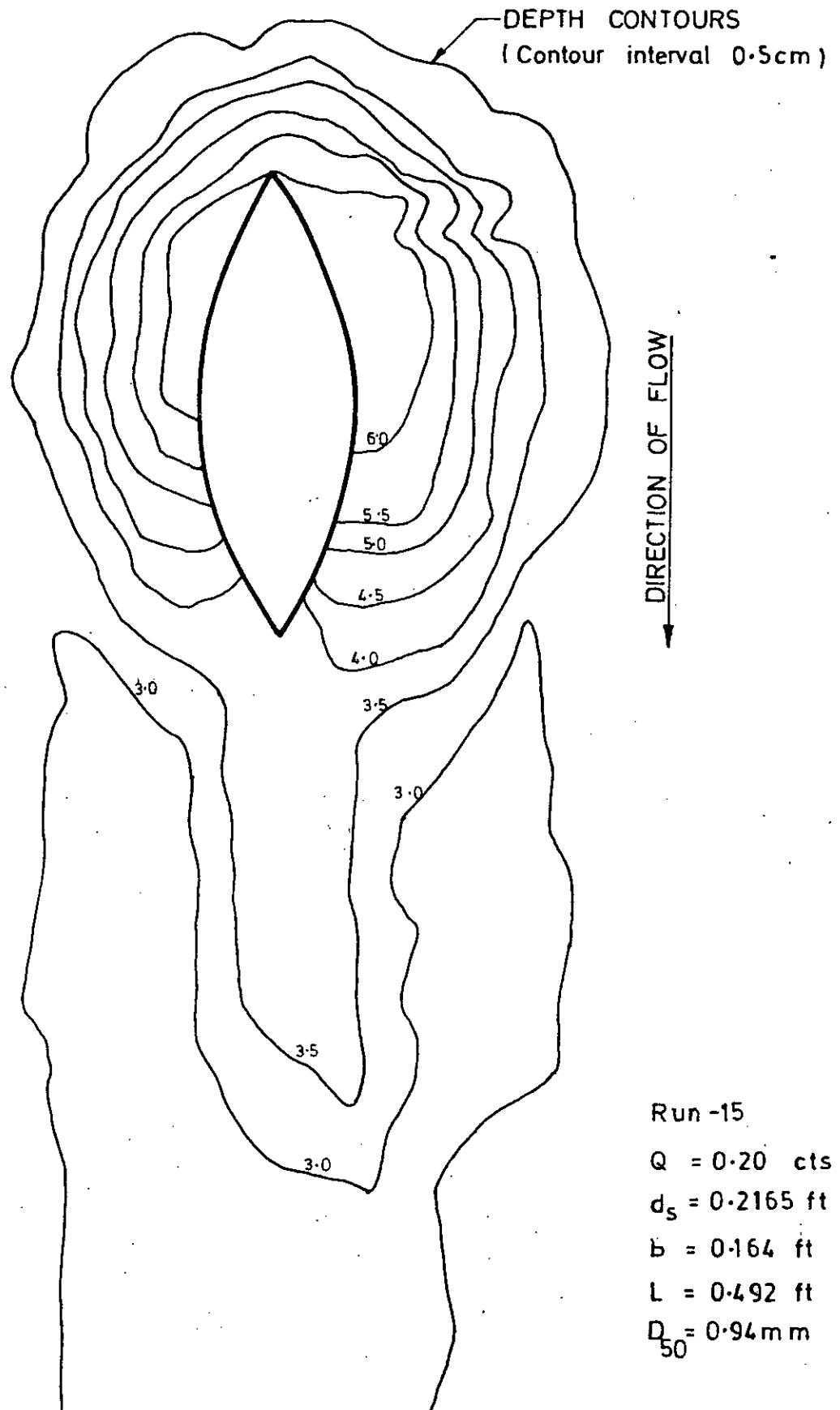
FIG. 5·10 SCOUR PATTERN AROUND SHARP- NOSE PIER
(Scale 1:2)

DEPTH CONTOURS
(Contour interval = 0·5 cm)

DIRECTION OF FLOW

Run - 20

Q = 0·24 cts

d_t = 0·29 ft

b = 0·164 ft
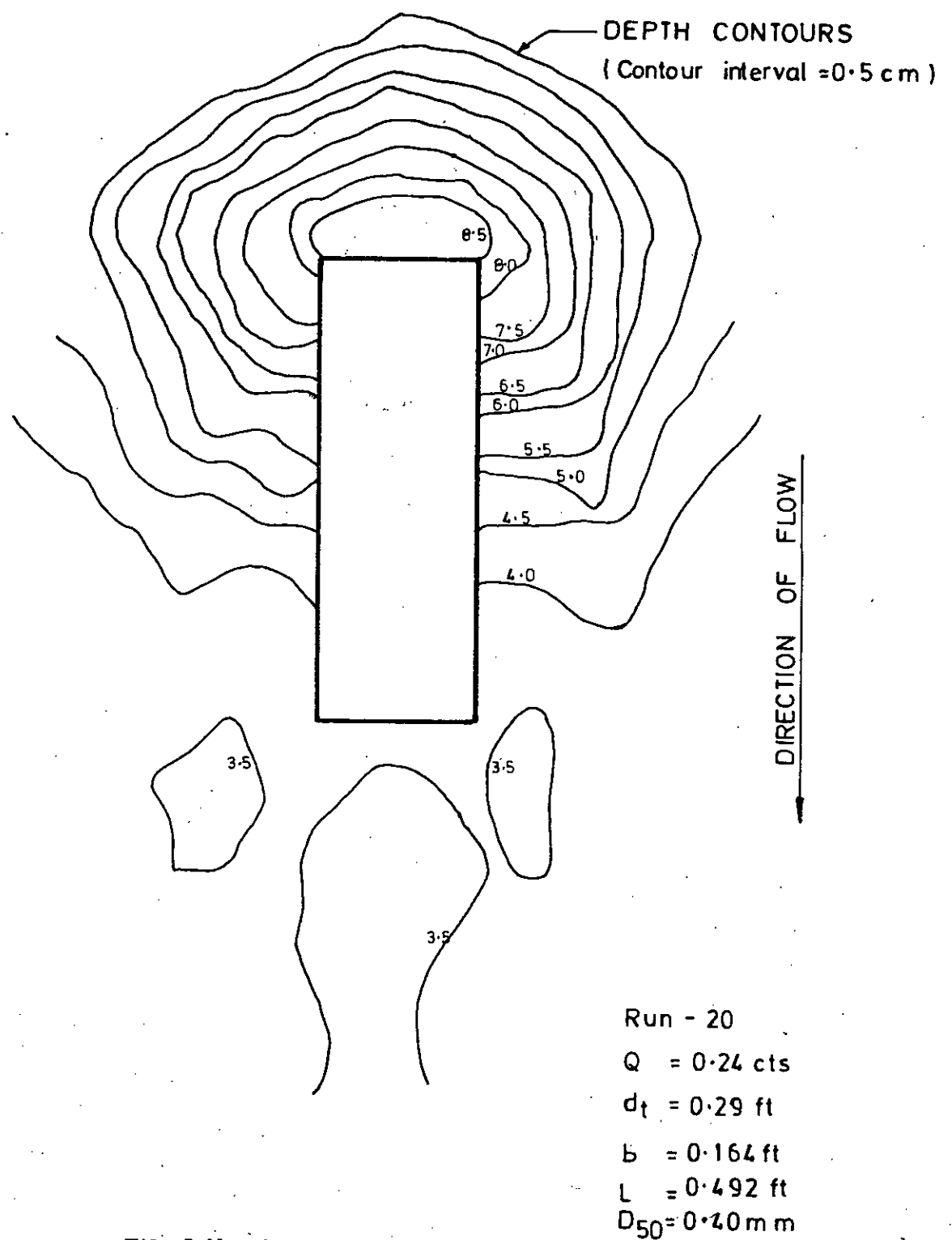
L = 0·492 ft

D_{50} = 0·40 mm

FIG. 5·11 SCOUR PATTERN AROUND RECTANGULAR PIER
(Scale 1:2)
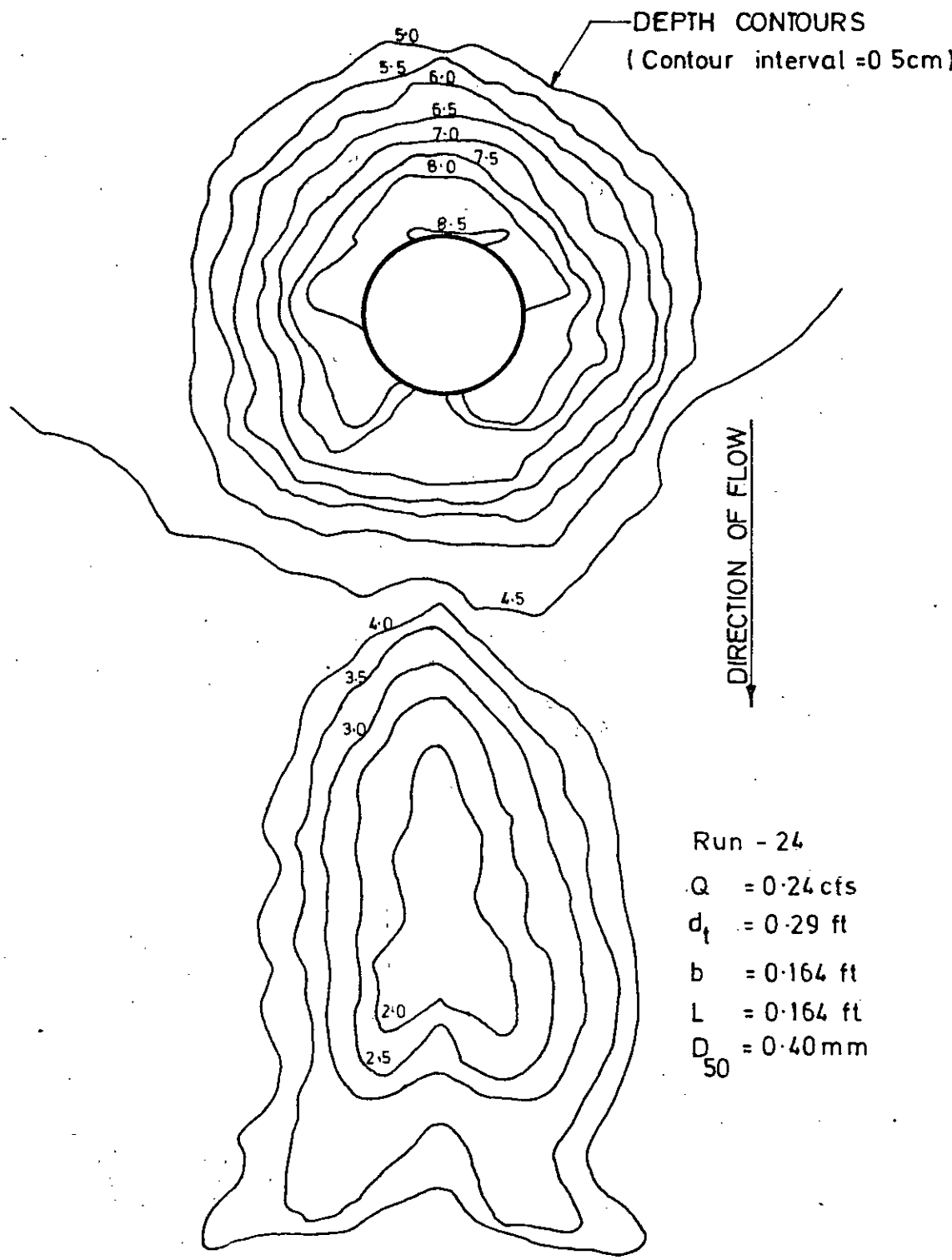
FIG. 5·12   SCOUR PATTERN AROUND CIRCULAR PIER

DEPTH CONTOURS

(Contour interval = 0·5 cm)

5·5

6·0

6·5

7·0

7·5

8·0

5·0

4·5

3·5   4·0

DIRECTION OF FLOW
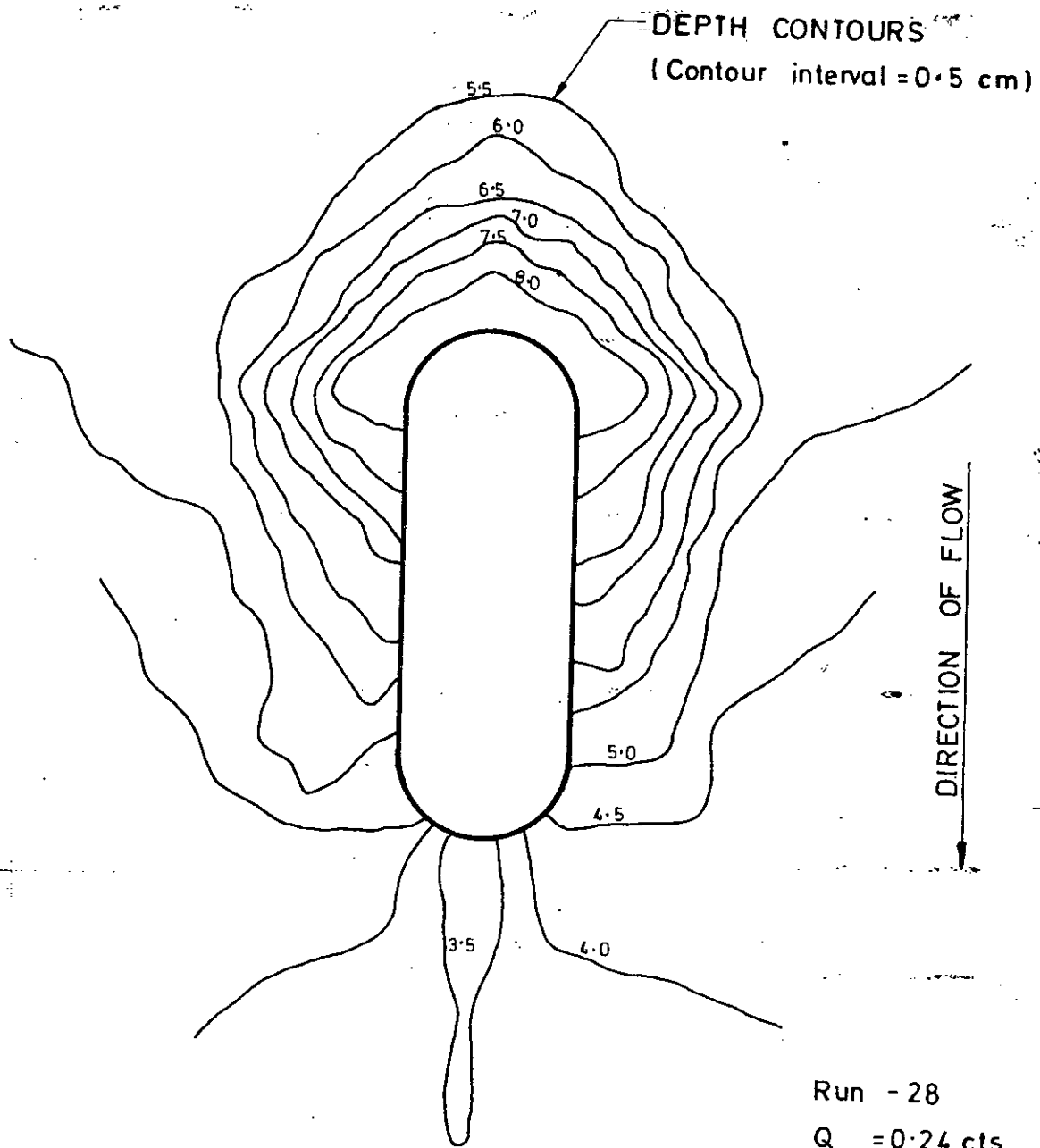
Run − 28

Q   = 0·24 cts

d_t = 0·28 ft

b   = 0·164 ft

L   = 0·492 ft

D_{50} = 0·40 mm

FIG. 5·13   SCOUR PATTERN AROUND ROUND-NOSE PIER

(Scale 1:2)

DEPTH CONTOURS
(Contour interval = 0·5 cm)

DIRECTION OF FLOW

6·5

6·0

5·5 5·0

4·5 4·0

3·5

Run -32

Q = 0·24 cts

d_t = 0·25 cft

b = 0·164 ft

L = 0·492 ft

D_{50} = 0·40 mm
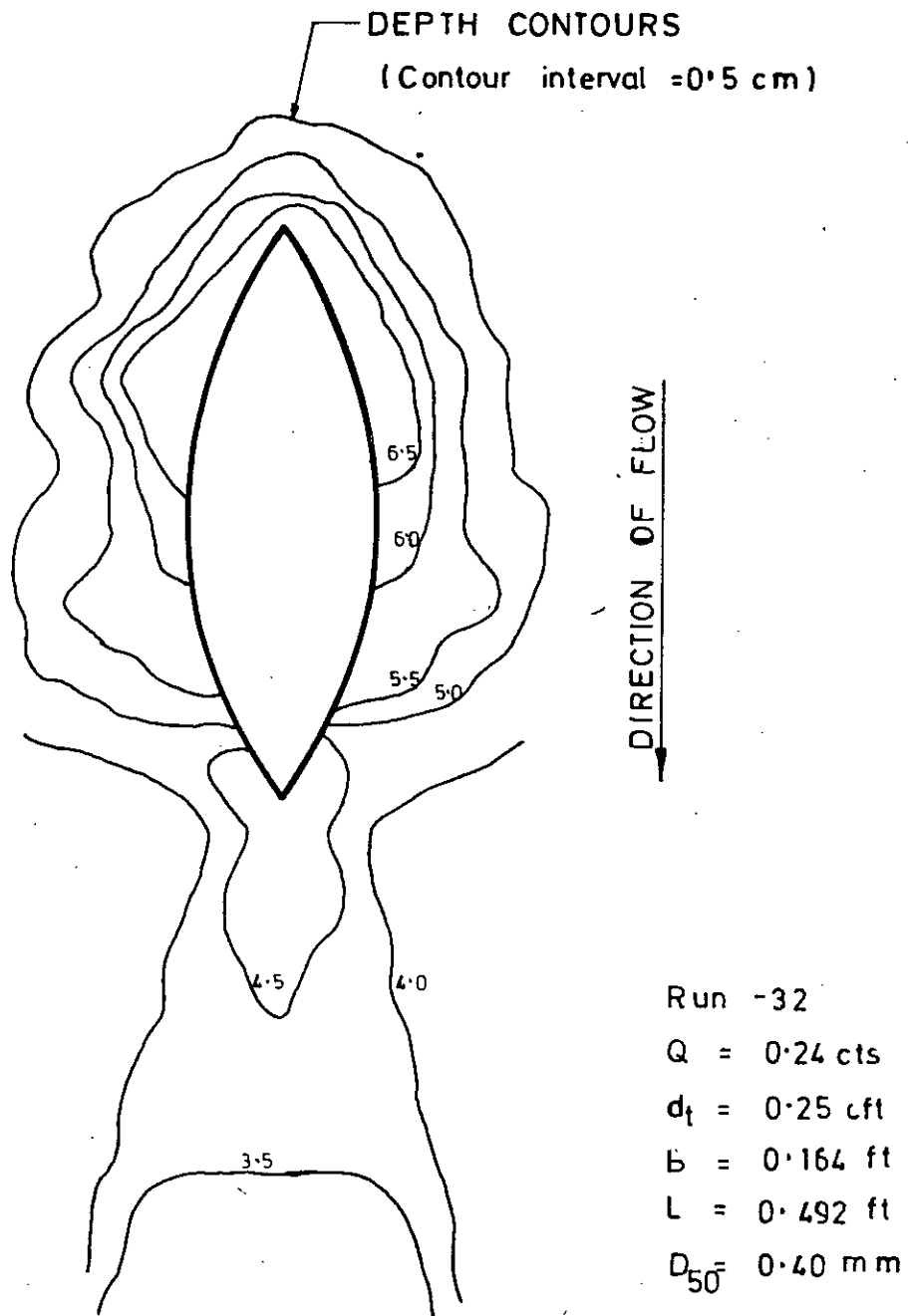
FIG. 5.14 SCOUR PATTERN AROUND SHARP-NOSE PIER
(Scale 1:2)

DEPTH CONTOURS
(Contour interval = 0·5 cm)

5·5
6·0
6·5
7·0
7·6
8·8
8·5
9·0
9·5
1 0

5·0
4·5
4·0

4·0   3·5   4·0

3·0

DIRECTION OF FLOW

Run ~36

Q   = 0·24 cts

d_t = 0·33 ft

b   = 0·164 ft
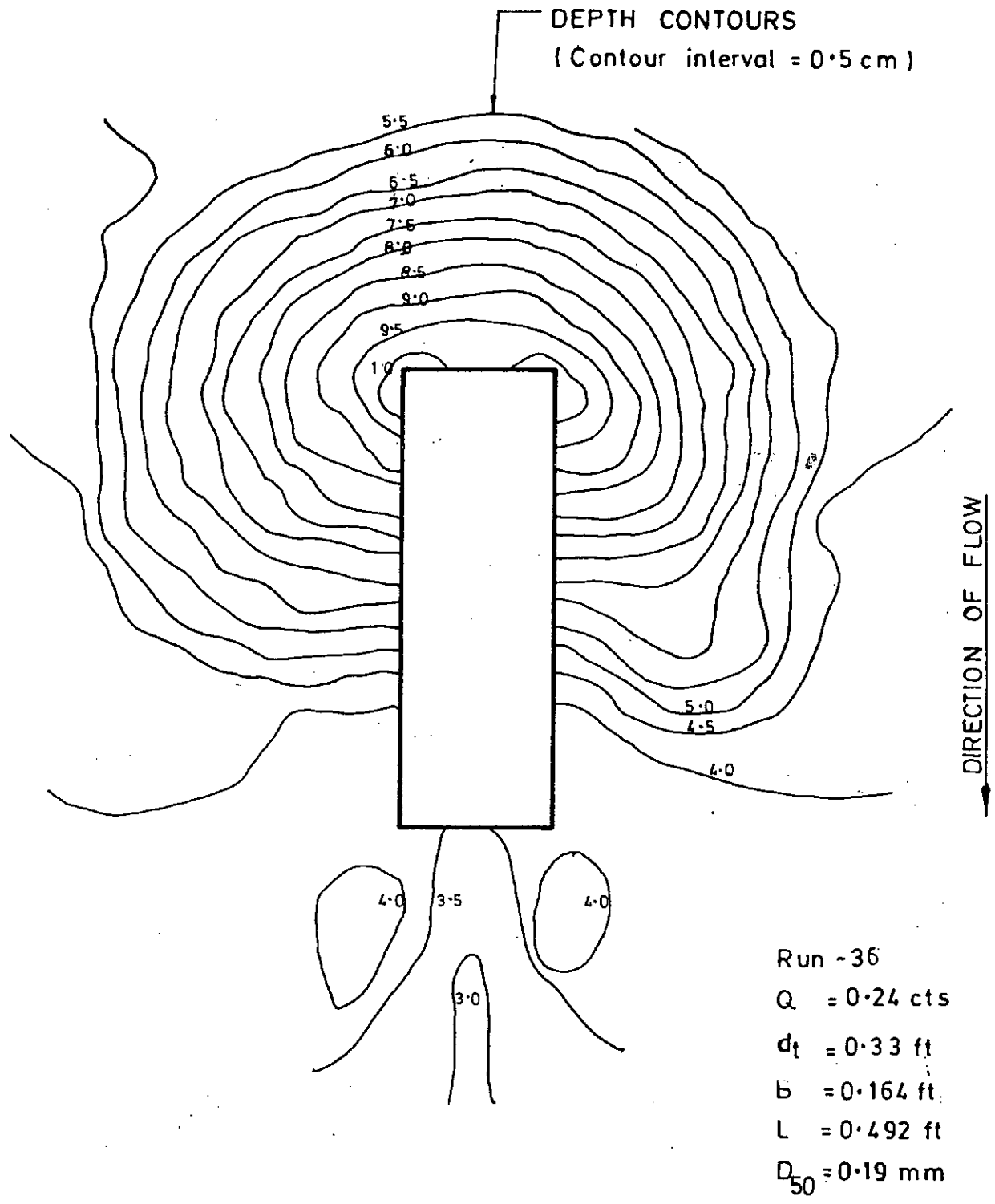
L   = 0·492 ft

D_{50} = 0·19 mm

FIG. 5·15   SCOUR PATTERN AROUND RECTANGULAR PIER
(Scale1:2)

DEPTH CONTOURS
(Contour interval = 0·5 cm)

DIRECTION OF FLOW
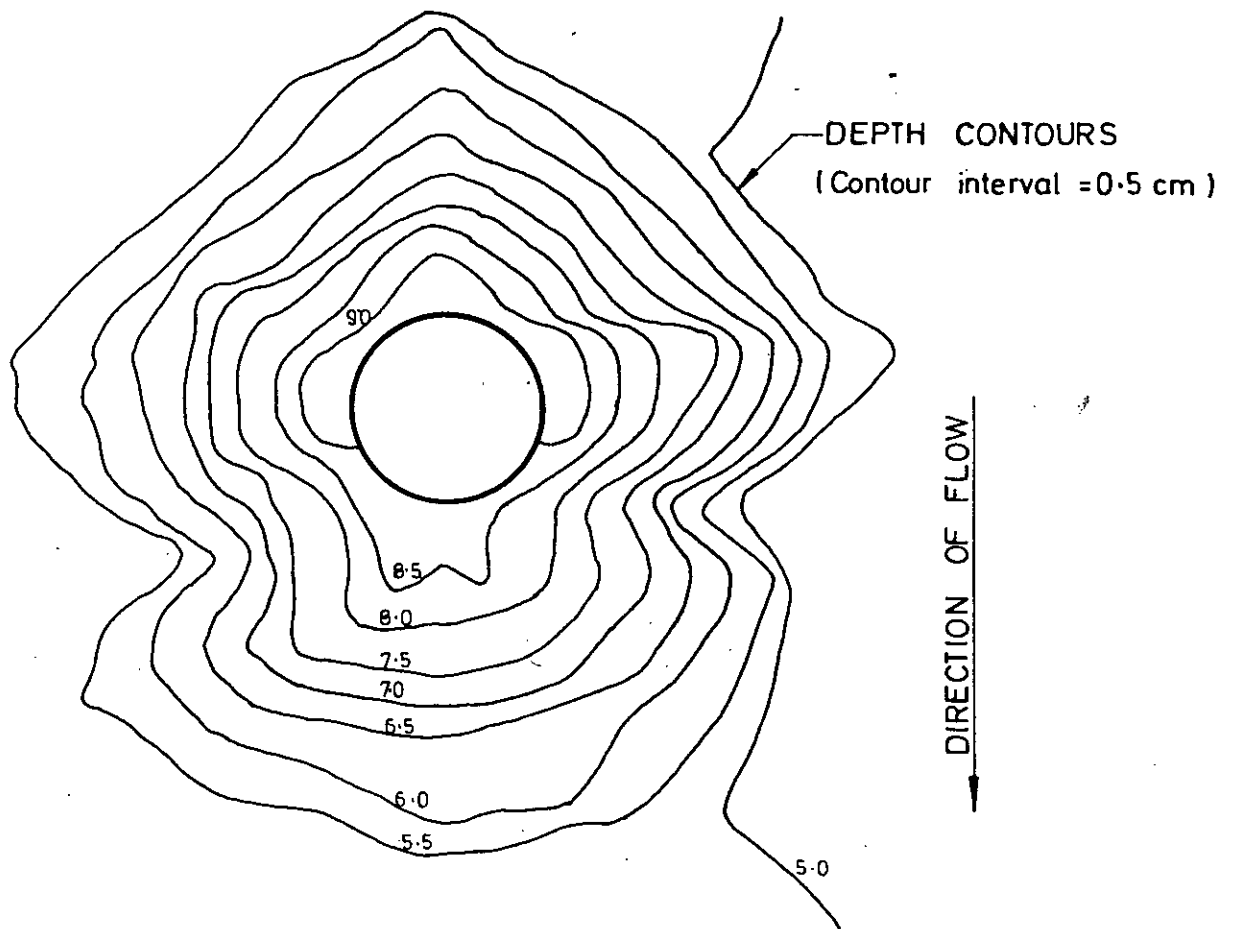
Run = 40

Q = 0·24 cfs

d_t = 0·31 ft

b = 0·164 ft

L = 0·164 ft

D_{50} = 0·19 mm

FIG. 5.16   SCOUR PATTERN AROUND CIRCULAR PIER
(Scale 1:2)
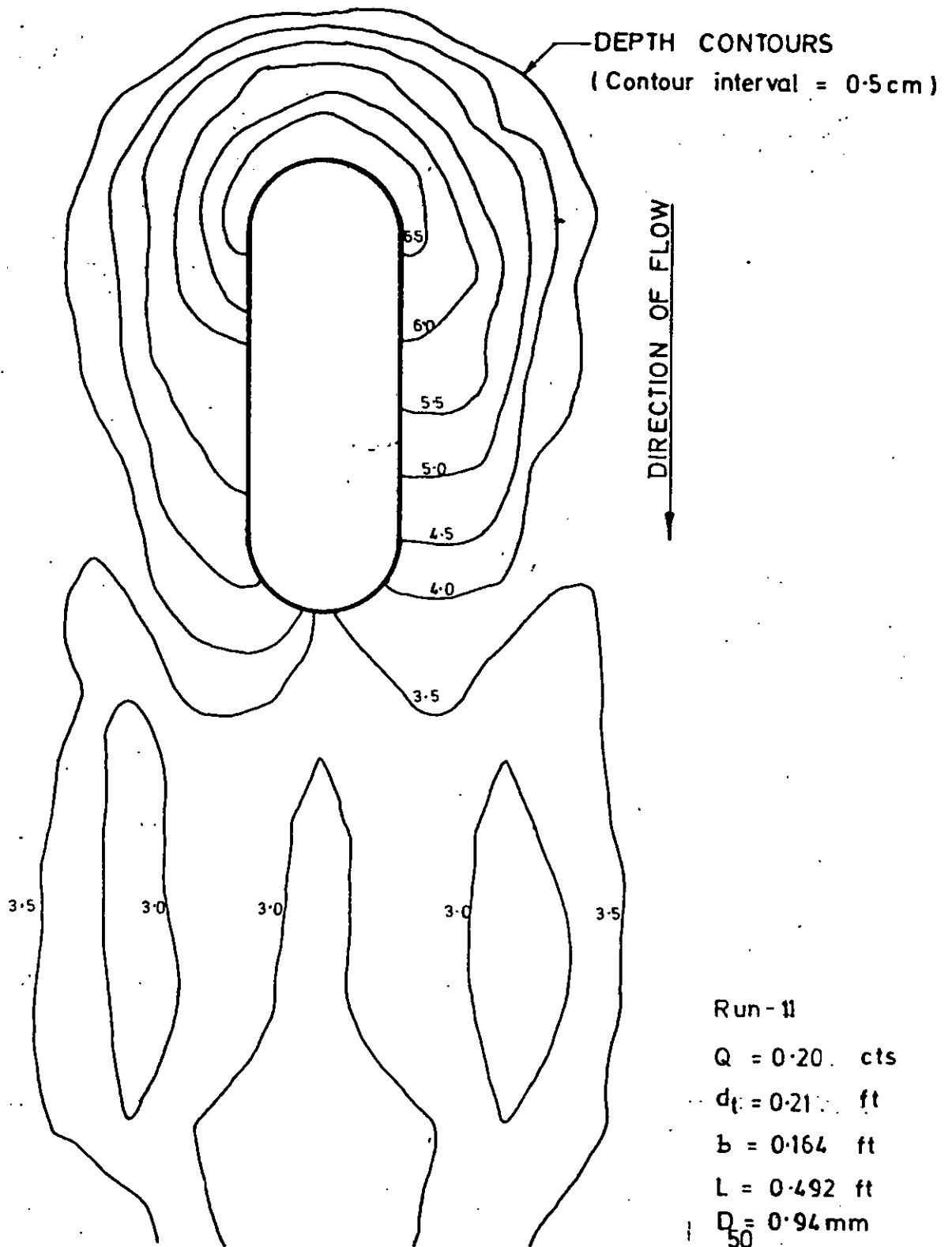
—DEPTH CONTOUR
(Contour interval =0·5cm)

6·0

9·0

8·5

8·0

7·5

7·0   6·5

DIRECTION OF FLOW

7·0

7·0

6·5

6·0
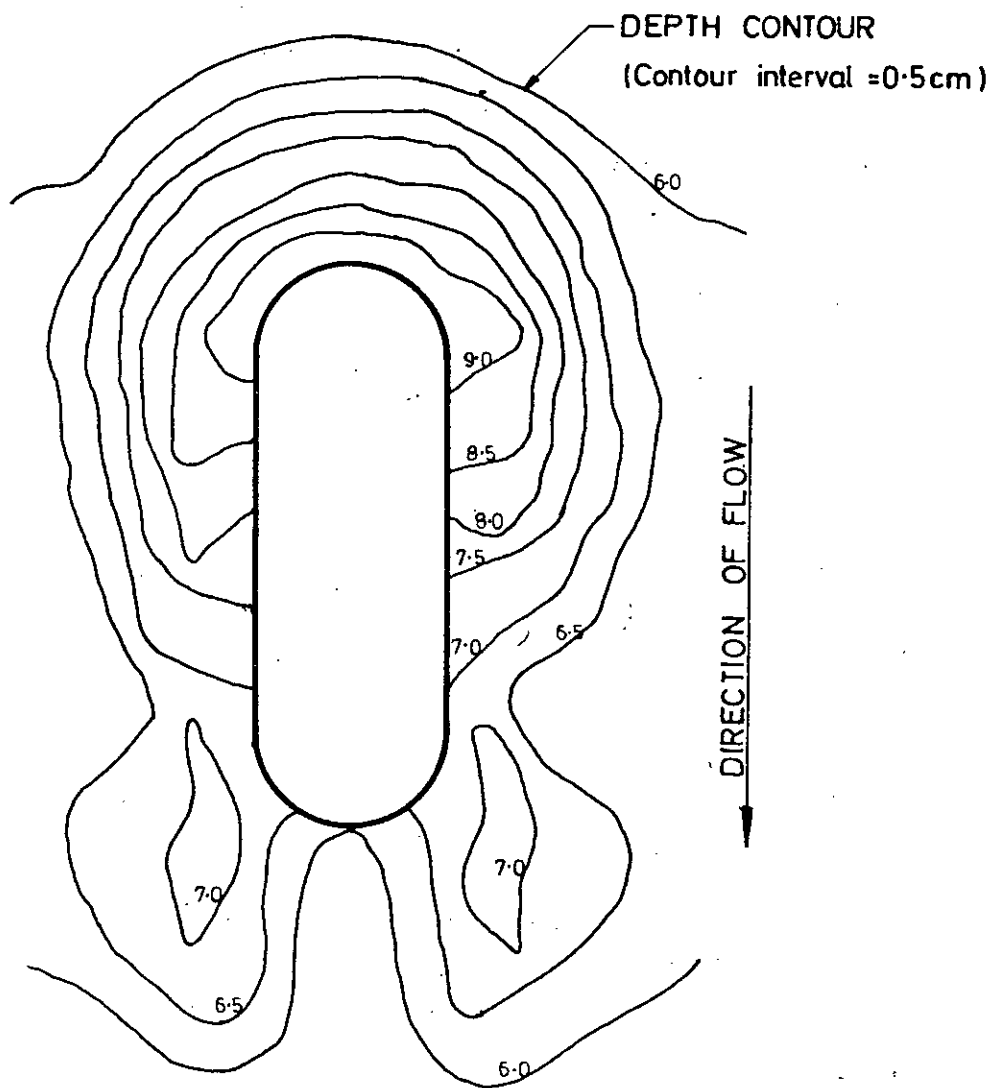
Run - 44

Q = 0·24 cts

d_t = 0·31 ft

b = 0·164 ft

L = 0·492 ft

D_{50}= 0·19 mm

FIG. 5·17   SCOUR PATTERN AROUND ROUND NOSE PIER
(Scale 1:2)

DEPTH CONTOUR
(Contour interval = 0·5 cm)

DIRECTION OF FLOW

5·5
5·0
4·5
4·0
3·5
3·0
2·5

3·0
3·0
3·5

Run - 46
Q = 0·17 cts
d_t = 0·18 ft
b = 0·164 ft
L = 0·49 ft
D_{50} = 0·19 mm
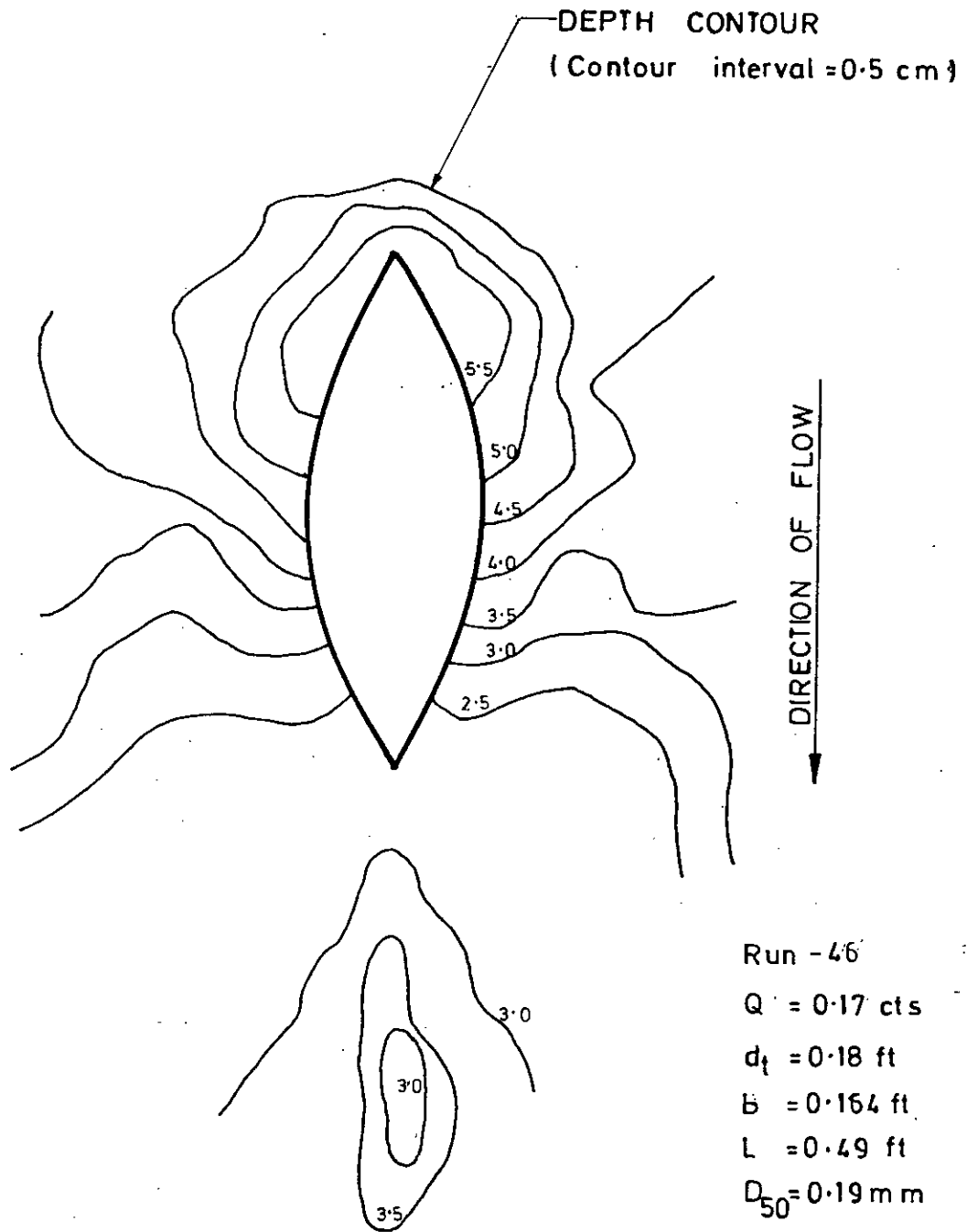
FIG. 5·18 SCOUR PATTERN AROUND SHARP NOSE PIER
(Scale 1:2)
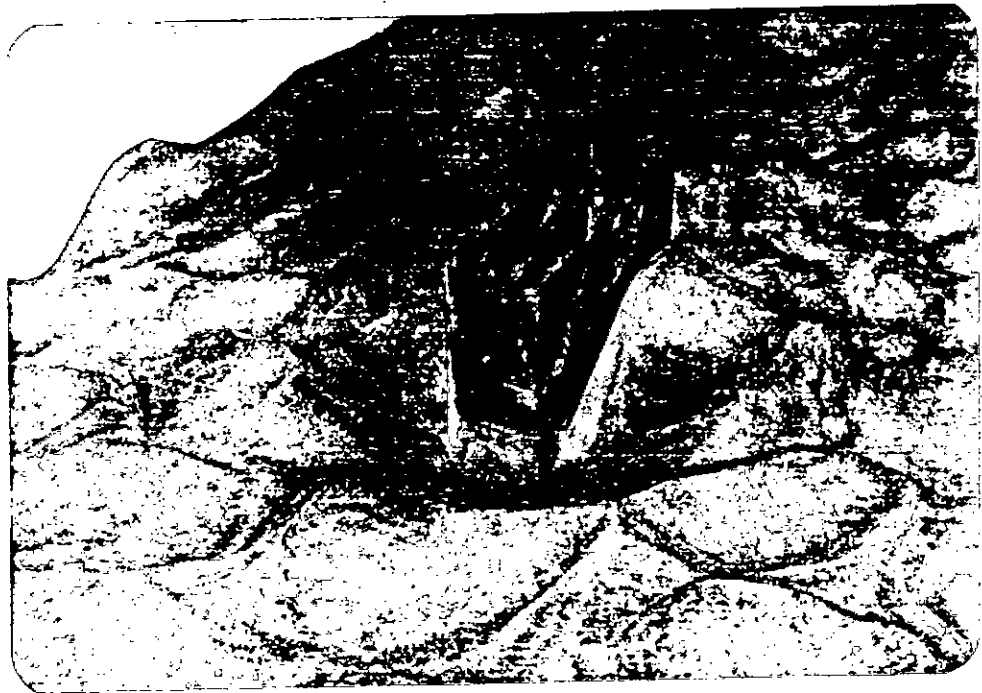
(a) RECTANGULAR PIER

(b) CYLINDRICAL PIER

FIG. 5·19 PHOTOGRAPHS OF SCOUR AROUND PIERS
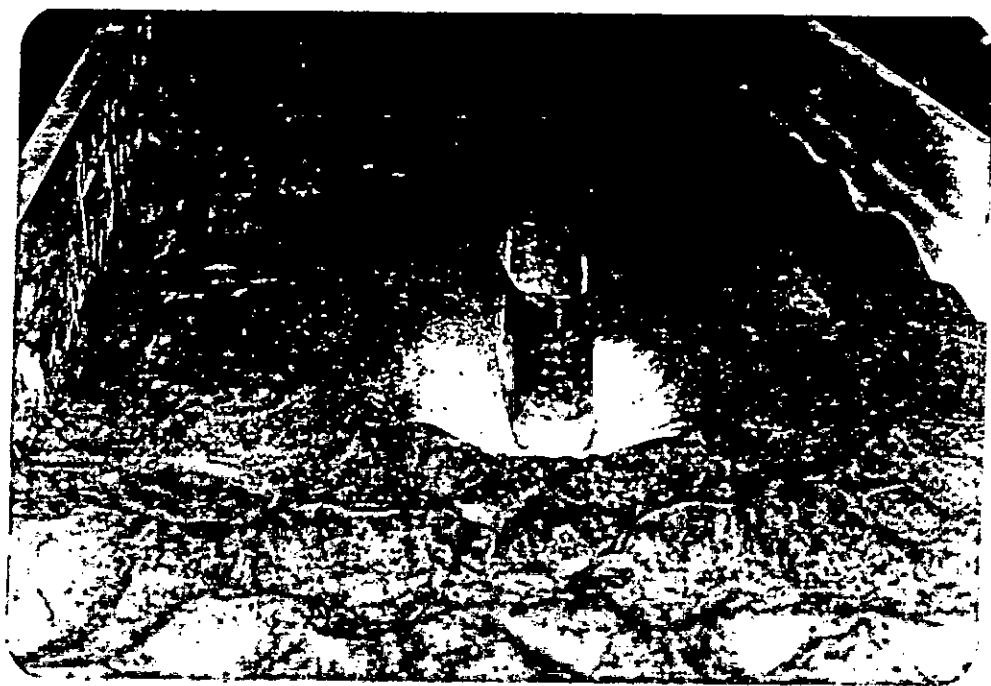
(a) ROUND-NOSE PIER.
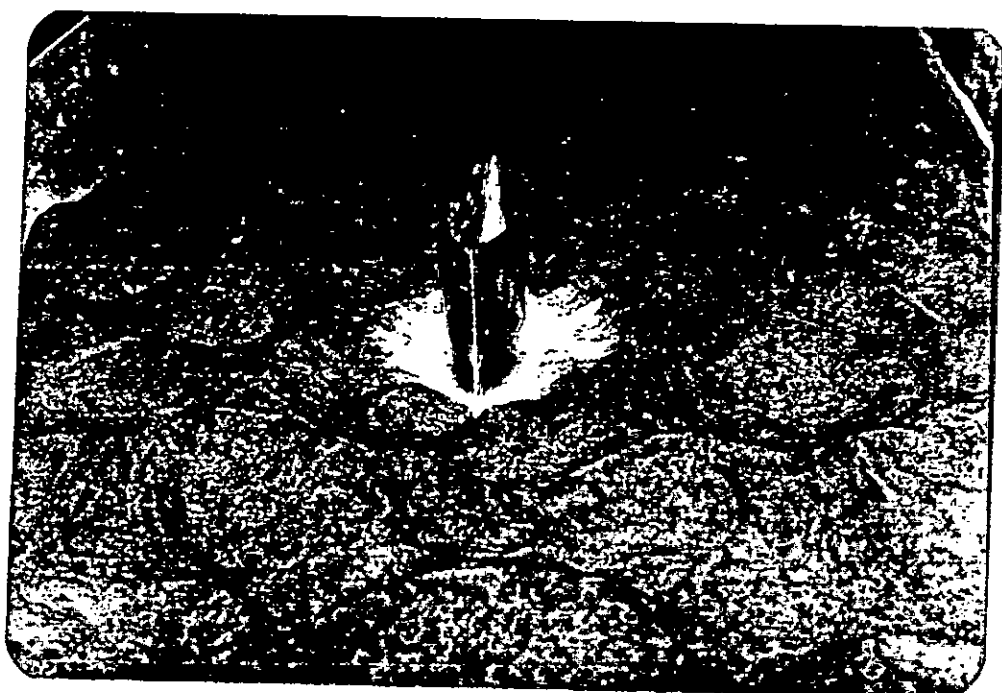
(b) SHARP NOSE PIER.

FIG. 5·20 PHOTOGRAPHS OF SCOUR AROUND PIERS
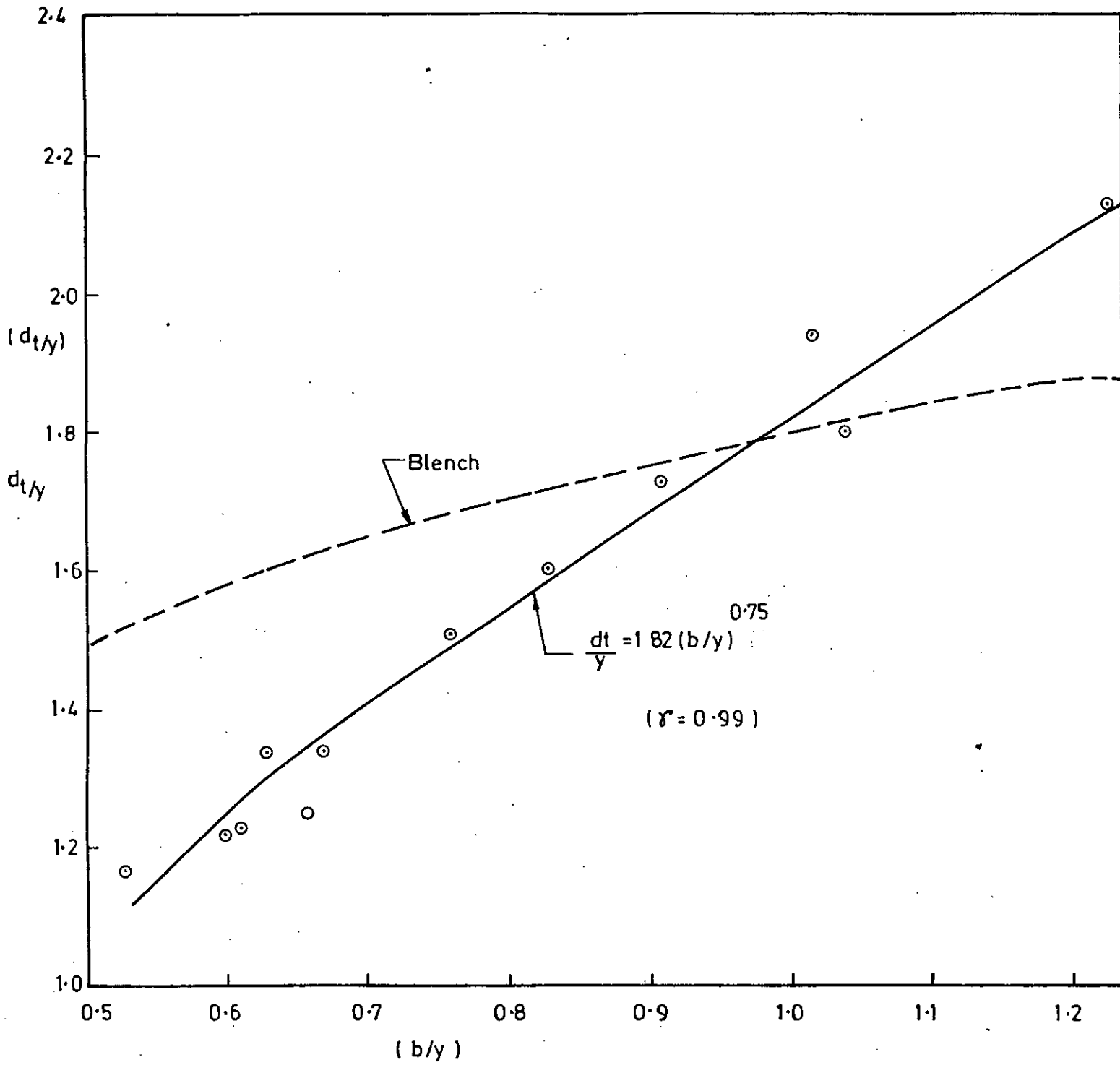
FIG. 5·21 <u>RELATION BETWEEN d_t/y AND b/y</u>
<u>OF HARDINGE BRIDGE</u>
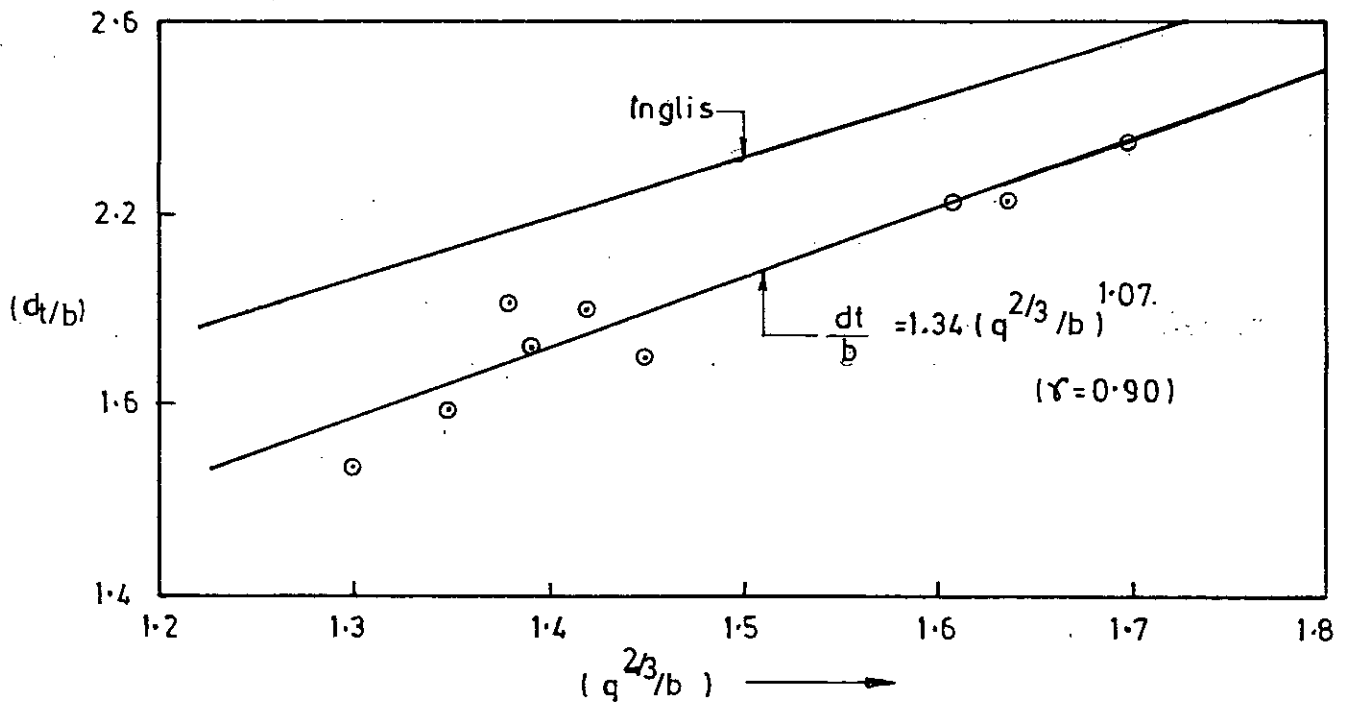
FIG. 5·22 <u>RELATION BETWEEN d_t/y AND $q^{2/3}/b$ OF HARDING BRIDGE</u>
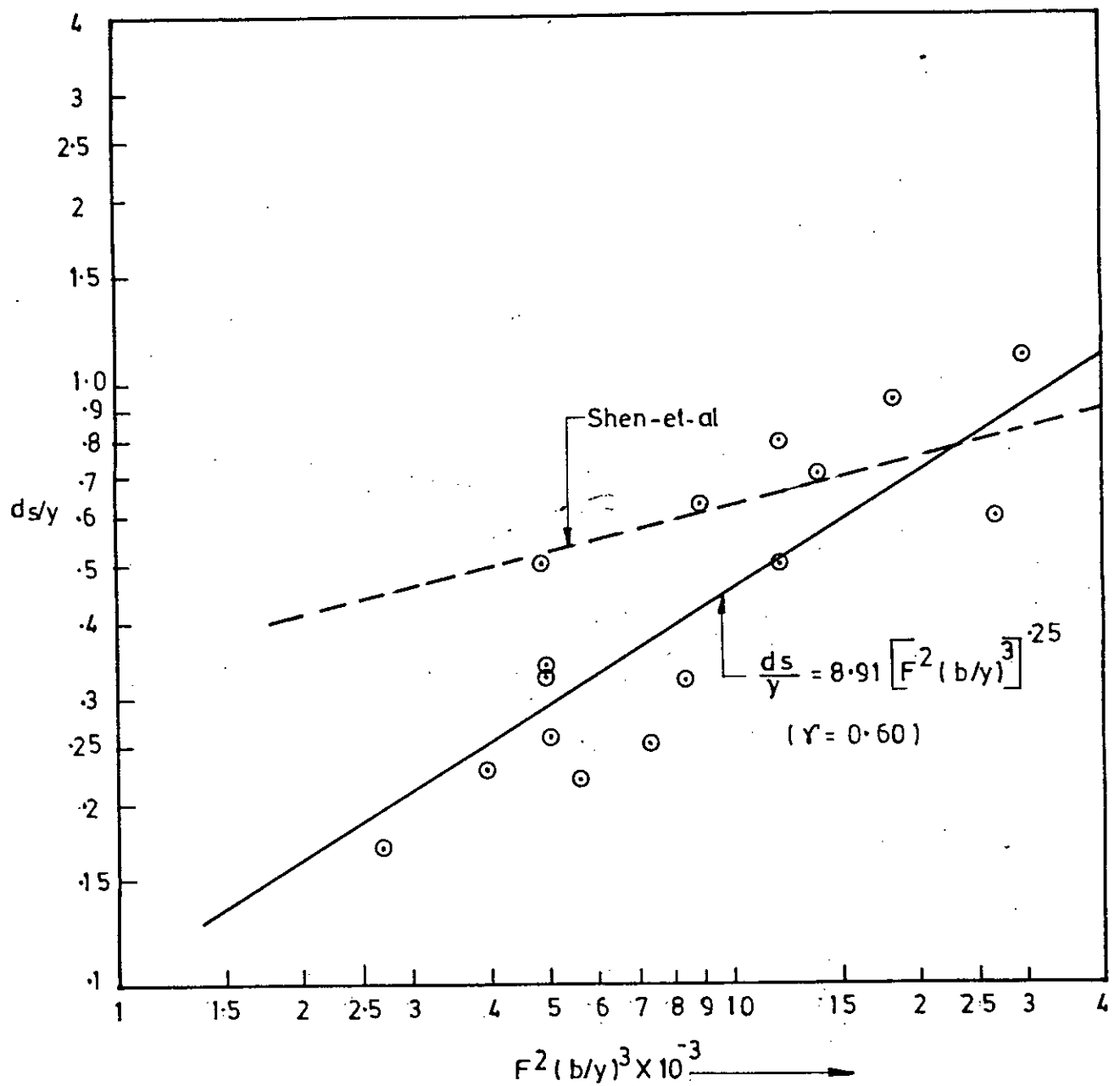
FIG. 5·23 RELATION BETWEEN RELATIVE SCOUR DEPTH d_s/y
AND FLOW PARAMETER $F^2(b/y)^3$ OF HARDING BRIDGE
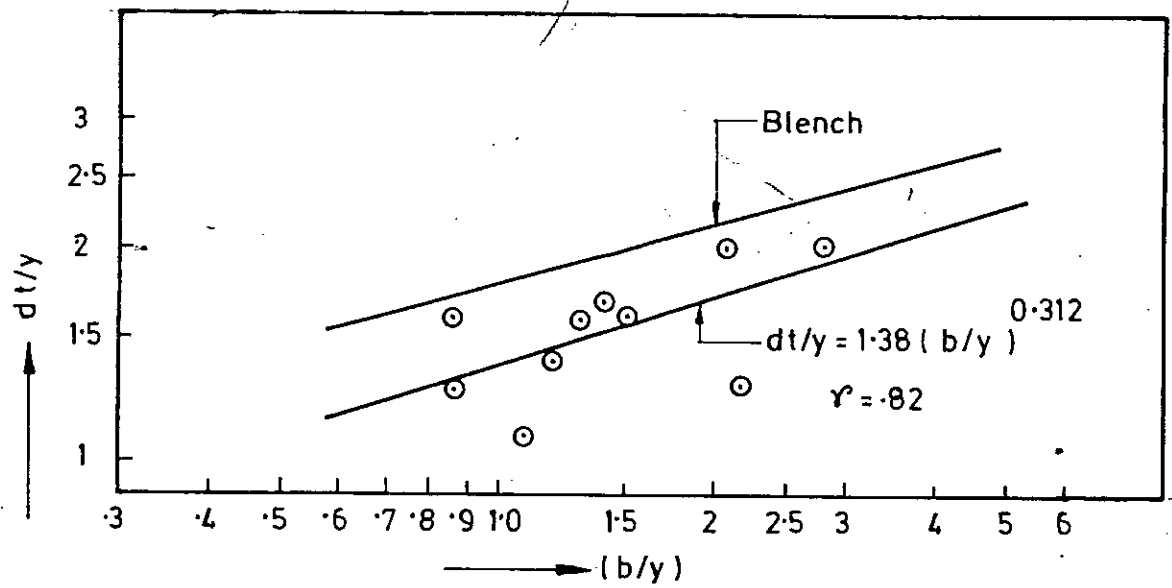
FIG. 5·24 RELATION BETWEEN dt/y AND b/y OF
EAST-WEST INTERCONNECTOR
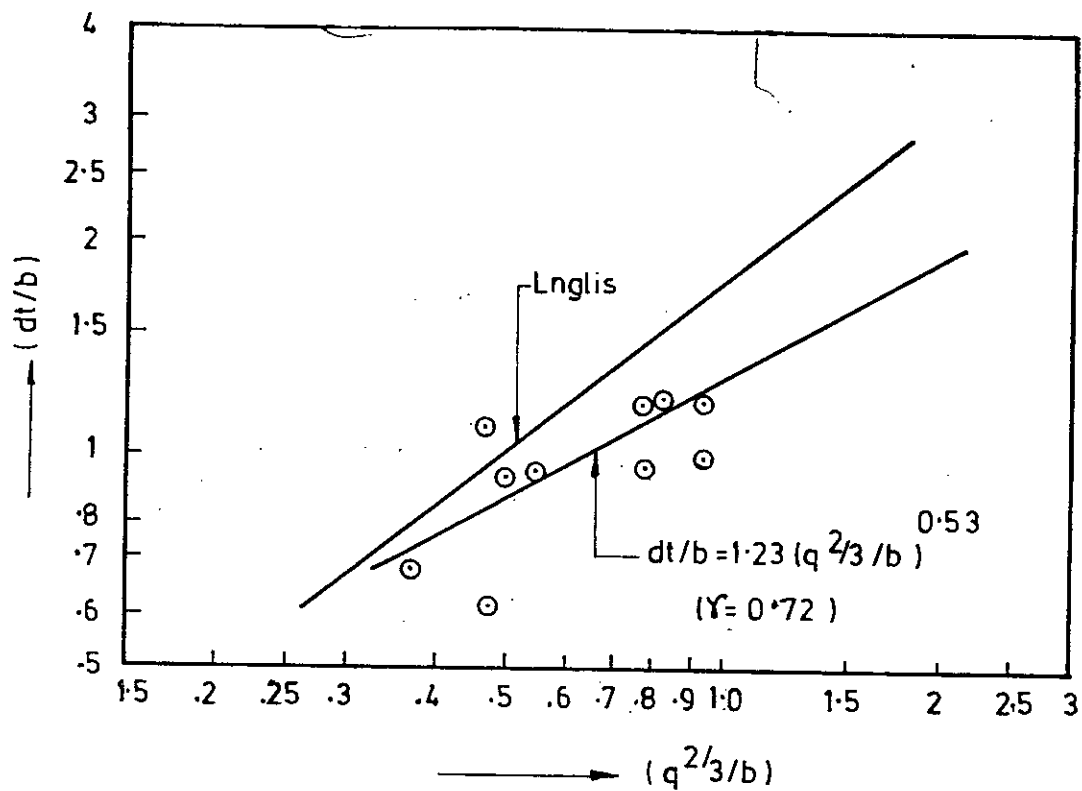
FIG. 5·25 RELATION BETWEEN $\dfrac{dt}{y}$ AND $\left(q^{2/3}/b\right)$ OF
EAST- WEST INTERCONNECTOR
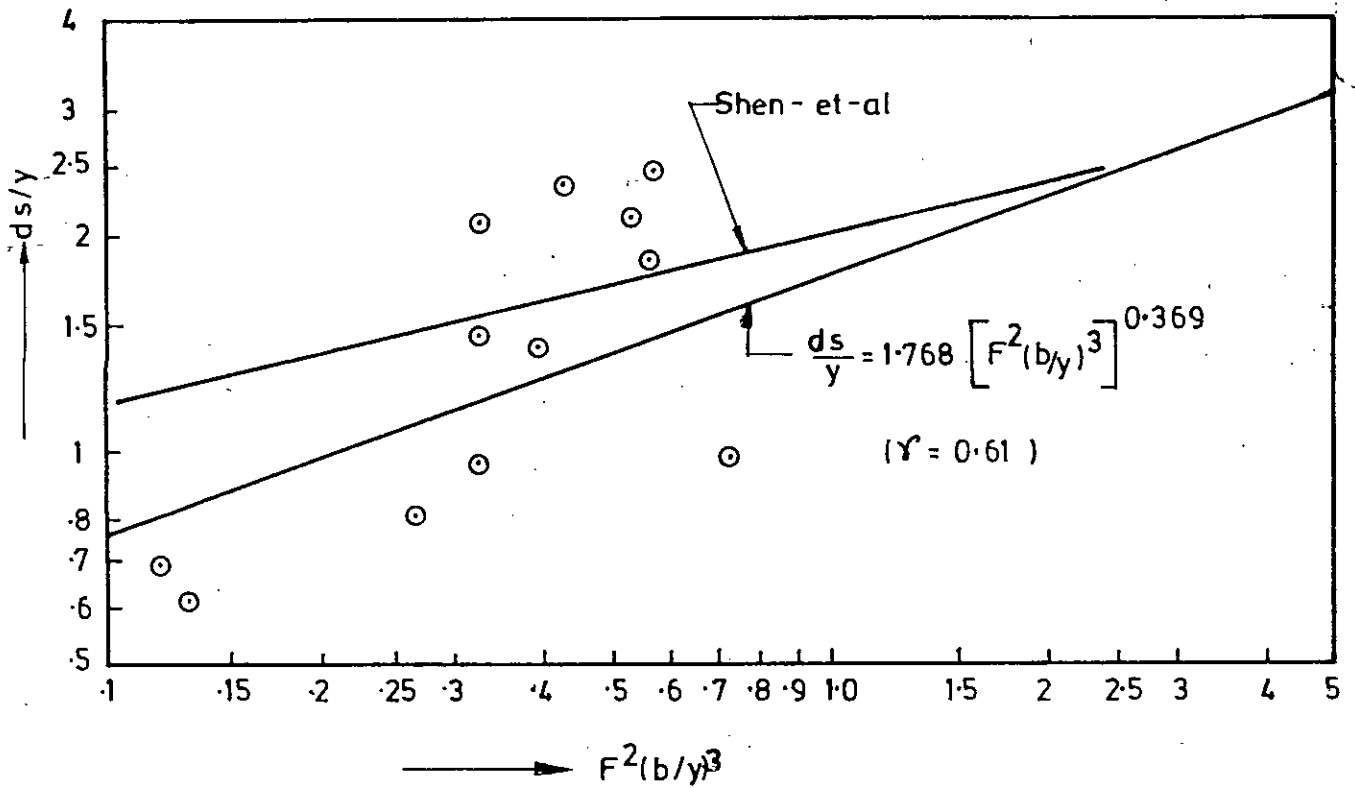
FIG. 5·26 RELATION BETWEEN RELATIVE SCOUR DEPTH ds/y AND FLOW PARAMETER $F^2(b/y)^3$ OF EAST–WEST INTERCONNECTOR

FIG. 5·27 COMPARISON OF BLENCH FORMULA WITH EXPERIMENTAL AND FIELD DATA

FIG. 5·28 COMPARISON OF INGLIS FORMULA WITH EXPERIMENTAL
AND FIELD DATA

Round-nose pier

- Field observation $D_{50} = 0.14$ mm
- Experimental data $D_{50} = 0.94$ mm
- Experimental data $D_{50} = 0.40$ mm
- Experimental data $D_{50} = 0.19$ mm

Shen-et-al, $(\gamma = 0.60)$
$$\frac{ds}{y} = 2\left[F^2(b/\gamma)^3\right]^{0.215}$$

Under-Prediction Zone

Line of Perfect Agreement

(d_s/y) observed

Over Prediction Zone

(d_s/y) predicted
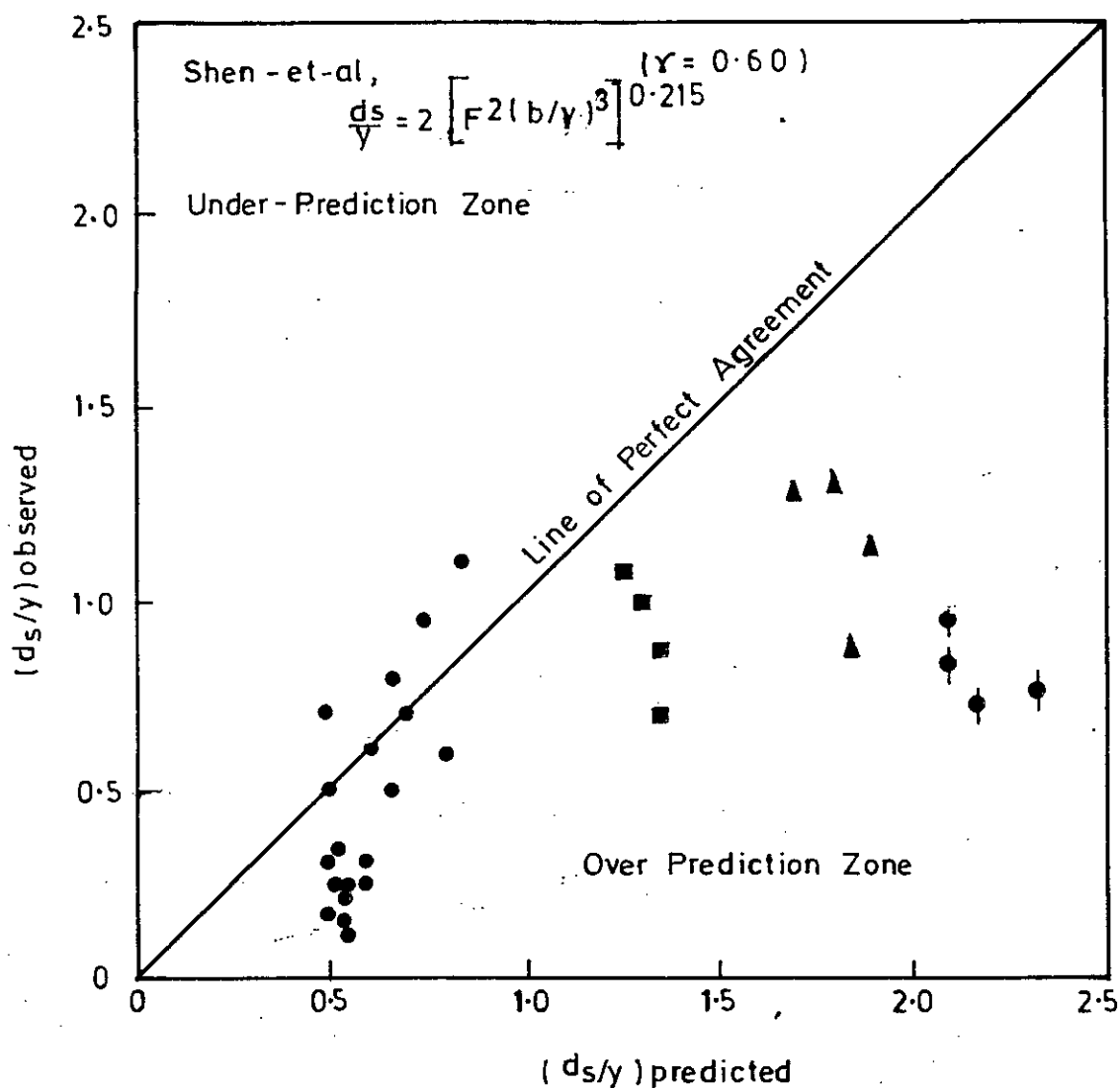
FIG. 5·29 COMPARISON OF SHEN-ET-AL FORMULA WITH EXPERIMENTAL AND FIELD DATA

FIG. 5·30 COMPARISON OF BLENCH FORMULA WITH EXPERIMENTAL AND FIELD DATA

Circular pier

●   Field   data $D_{50} = 0.19$ mm

⏺   Experimental data $D_{50} = 0.94$ mm

▲   Experimental data $D_{50} = 0.40$ mm

◼   Experimental data $D_{50} = 0.19$ mm

Inglis, $\dfrac{d_t}{b} = 1.7 \left(\dfrac{q^{2/3}}{b}\right)^{.78}$

Under-Predicted Zone

Line of Perfect Agreement

Over-Predicted Zone

(d_t/b) obseved

(d_t/b) predicted
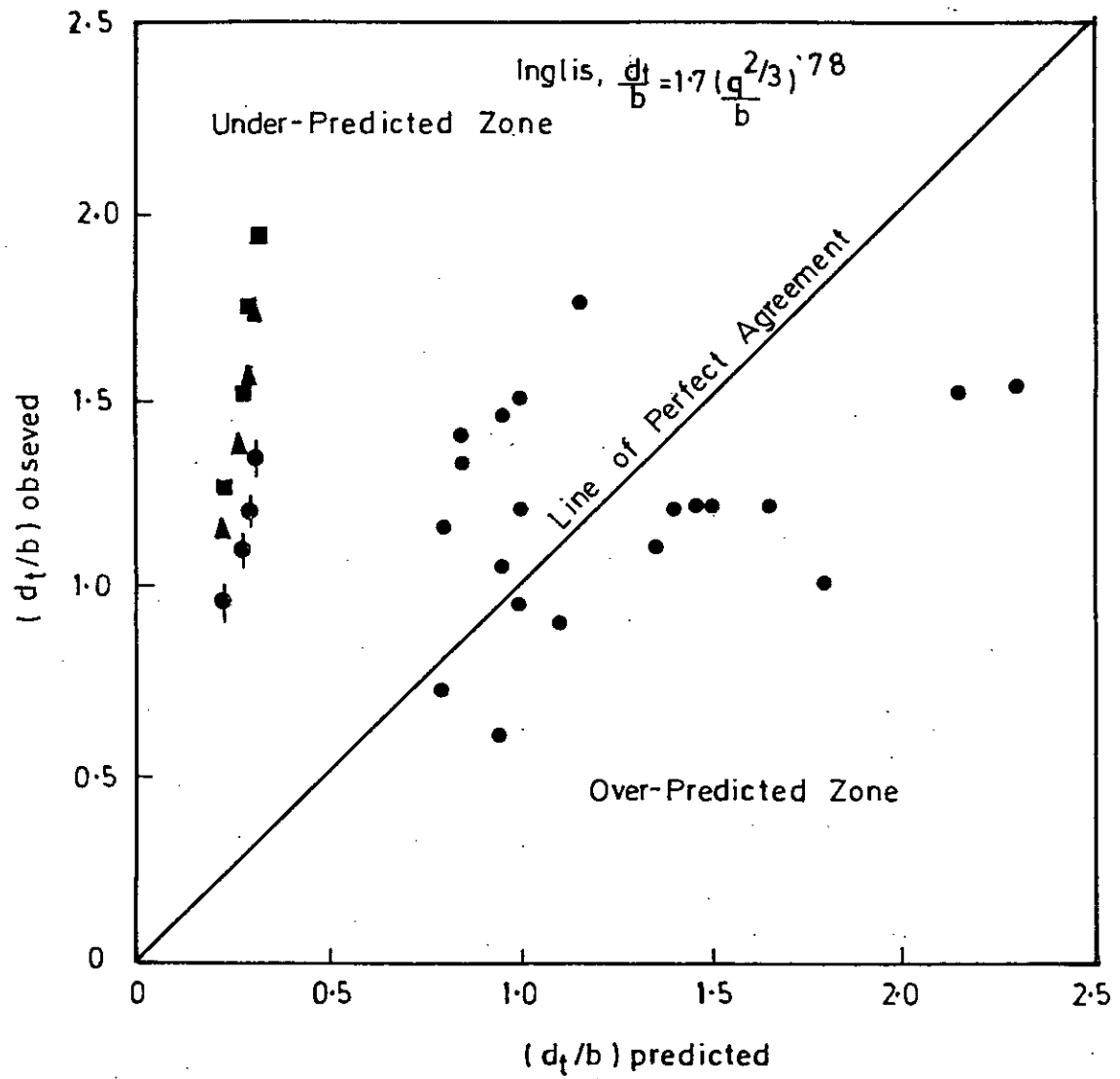
FIG. 5.31   COMPARISON OF INGLIS FORMULA WITH
EXPERIMENTAL AND FIELD DATA
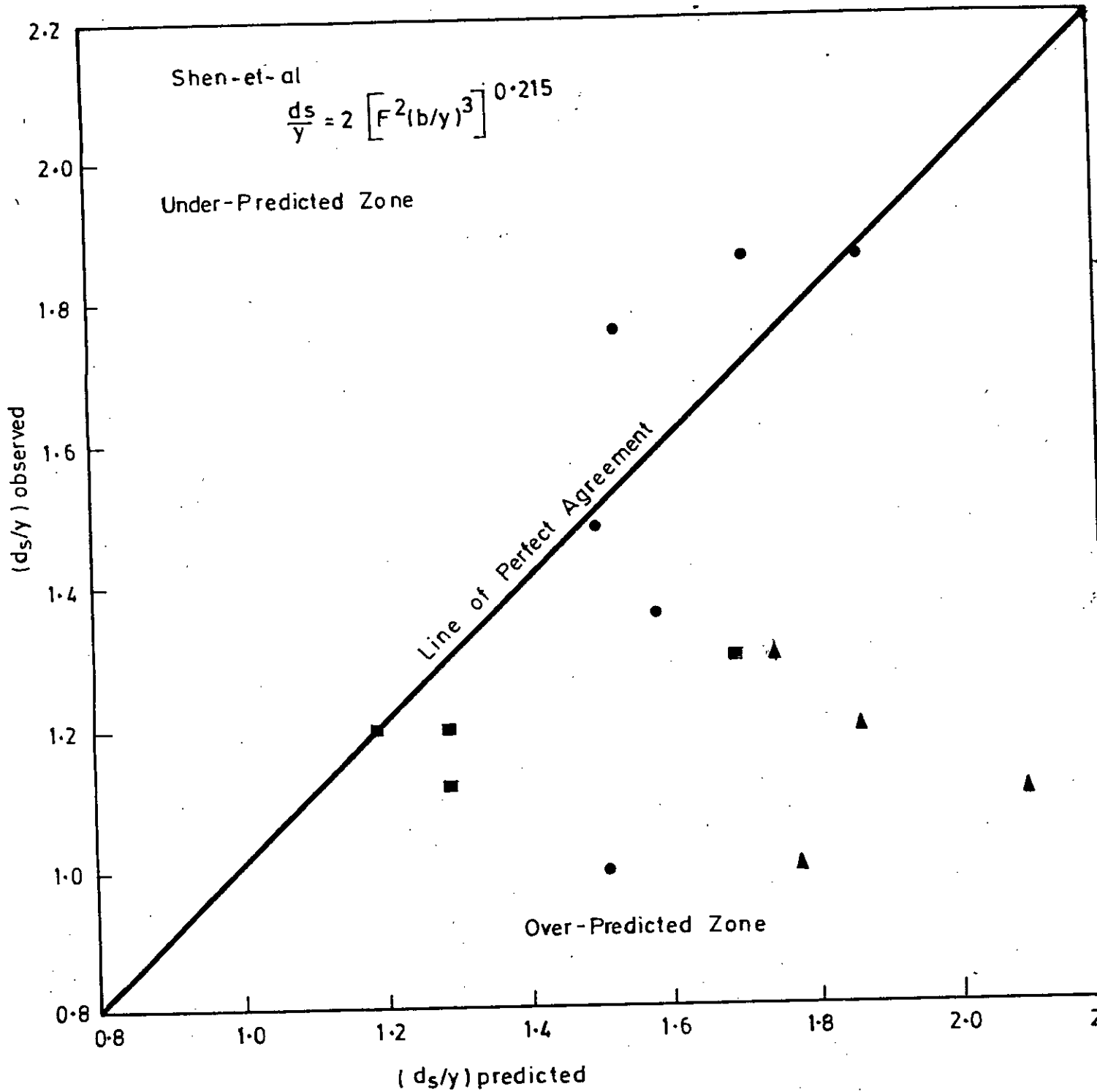
FIG. 5·32 COMPARISON OF SHEN-ET-AT FORMULA WITH EXPERIMENTAL
AND FIELD DATA

TABLE - 1

Type of Pier : Rectangular

b, Width of pier = 0.164 ft

l, Length of pier= 0.492 ft

Run No.	Sediment size D_{50}(mm)	Discharge Q_{max} (cfs)	Average Approach depth y (ft)	Channel width B,(ft)	Average velocity, V (ft/sec)	Maximum scour depth from W.L. d_t,(ft)	Critical velocity $V_c = \sqrt{gy}_c$
1	2	3	4	5	6	7	8
1	0.94	0.1295	.0837	2'-0"	0.7736	.1640	1.2775
2	0.94	0.1648	.0919	2'-0"	0.8966	.1877	1.3844
3	0.94	0.2001	.0991	2'-0"	1.0100	.2067	1.4769
4	0.94	0.2354	.1083	2'-0"	1.0870	.2329	1.5591
17	0.40	0.1295	.0978	2'-0"	0.6690	.2066	1.2775
18	0.40	0.1648	.1076	2'-0"	0.7658	.2362	1.3844
19	0.40	0.2001	.1165	2'-0"	0.8588	.2641	1.4769
20	0.40	0.2354	.1250	2'-0"	0.9439	.2914	1.5591
33	0.19	0.1295	.1148	2'-0"	0.5640	.2431	1.2775
34	0.19	0.1648	.1286	2'-0"	0.6407	.2756	1.3844
35	0.19	0.2001	.1381	2'-0"	0.7245	.3087	1.4769
36	0.19	0.2354	.1476	2'-0"	0.7974	.3326	1.5591

TABLE - 1(Contd.)

Froude No. $F = V/\sqrt{gy}$	Critical Froude No. $F_c = V_c/\sqrt{gy}$	Particle Froude No. $F_d = V/\sqrt{gD_{50}}$	Critical Partial Froude No. $F_{dc} = V_c/\sqrt{gD_{50}}$	d_t/b	Y/b	d_t/Y
9	10	11	12	13	14	15
0.4712	0.7782	2.4549	4.054	1.00	0.5	1.96
0.5212	0.8048	2.845	4.393	1.15	0.56	2.04
0.5654	0.8268	3.205	4.687	1.26	0.604	2.09
0.5821	0.8349	3.449	4.949	1.42	0.66	2.15
0.3790	0.7237	3.2545	6.2147	1.26	0.59	2.14
0.4114	0.7438	3.7253	6.7346	1.44	0.656	2.20
0.4434	0.7625	4.1778	7.1846	1.61	0.71	2.27
0.4711	0.7781	4.5917	7.5845	1.776	0.772	2.33
0.2933	0.6645	3.9809	9.0170	1.482	0.70	2.12
0.3149	0.6803	4.5223	9.7716	1.680	0.784	2.14
0.3436	0.7004	5.1138	10.4245	1.882	0.862	2.24
0.3658	0.7152	5.6283	11.0047	2.028	0.934	2.25

TABLE - 2

Type of Pier : Circular

b, Width of Pier = 0.164 ft

Run No.	Sediment Size D_{50} (mm)	Discharge Q_{max} (cfs)	Average approach depth, Y (ft)	Channel Width, B, ft	Average velocity, V ft/sec	d_t Maximum Scour depth from W.L. (ft)	Critical velocity $V_c = \sqrt{gy_c}$
1	2	3	4	5	6	7	8
5.	0.94	0.1295	0.0820	2'-0"	0.7894	0.1595	1.2775
6.	0.94	0.1648	0.0942	2'-0"	0.8747	0.182	1.3844
7.	0.94	0.2001	0.1011	2'-0"	0.9896	0.2001	1.4769
8.	0.94	0.2354	0.1073	2'-0"	1.0969	0.2221	1.5591
21.	0.40	0.1295	.0984	2'-0"	0.6580	.1926	1.2775
22.	0.40	0.1648	.1030	2'-0"	0.8000	.2280	1.3844
23.	0.40	0.2001	.1142	2'-0"	0.8761	.2592	1.4769
24.	0.40	0.2354	.1247	2'-0"	0.9239	.2871	1.5591
37.	0.19	0.1295	.1155	2'-0"	0.5606	.2083	1.2775
38.	0.19	0.1648	.1267	2'-0"	0.6504	.2510	1.3854
39.	0.19	0.2001	.1362	2'-0"	0.7346	.2887	1.4769
40.	0.19	0.2354	.1493	2'-0"	0.7883	.3199	1.5591

TABLE - 2 (Contd.)

Froude No. $F=V/\sqrt{gy}$	Critical Froude No. $F_c=V_c/\sqrt{gy}$	Particle Froude No. $F_d=V/\sqrt{gD_{50}}$	Critical Partial Froude No. $F_{dc}=V_c/\sqrt{gD_{50}}$	d_t/b	Y/b	$d_t/$
9	10	11	12	13	14	15
0.4858	0.7861	2.5052	4.0539	0.973	0.494	1.94
0.5022	0.795	2.776	4.393	1.11	0.574	1.93
0.5485	0.819	3.140	4.687	1.22	0.616	1.98
0.5901	0.839	3.481	4.948	1.35	0.654	2.07
0.3697	0.7177	3.2010	6.2147	1.17	0.60	1.96
0.4393	0.7602	3.8917	6.7346	1.39	0.628	2.15
0.4569	0.7702	4.2619	7.1846	1.58	0.607	2.27
0.4611	0.7781	4.4944	7.5845	1.75	0.780	2.30
0.2907	0.6624	3.9570	9.0170	1.27	0.704	1.80
0.3220	0.6854	4.5908	9.7716	1.530	0.798	2.01
0.3508	0.7052	5.1851	10.4245	1.76	0.856	2.12
0.3595	0.7111	5.5641	11.0047	1.95	0.938	2.14

TABLE - 3

Type of Pier : Round-nose

b, Width of Pier = 0.164 ft

l, Length of pier= 0.492 ft

Run No.	Sediment Size D_{50}(mm)	Discharge Q_{max} (cfs)	Average Approach depth,Y (ft)	Channel Width,b ft.	Average velocity, V ft/sec.	Maximum scour depth from W.L. d_t,(ft)	Critical velocity $V_c = \sqrt{gy}_c$
1	2	3	4	5	6	7	8
9.	0.94	0.1295	.0824	2'-0"	0.7858	.1469	1.2775
10.	0.94	0.1648	.0935	2'-0"	0.8813	.1624	1.3844
11.	0.94	0.2001	.1017	2'-0"	0.9838	.1870	1.4769
12.	0.94	0.2354	.1083	2'-0"	1.0868	.2100	1.5591
25.	0.40	0.1295	.0921	2'-0"	0.6514	.1854	1.2775
26.	0.40	0.1648	.1024	2'-0"	0.8047	.2231	1.3844
27.	0.40	0.2001	.1125	2'-0"	0.8894	.2575	1.4769
28.	0.40	0.2354	.1247	2'-0"	0.9439	.2831	1.5591
41.	0.19	0.1295	.1165	2'-0"	0.5558	.1985	1.2775
42.	0.19	0.1648	.1266	2'-0"	0.6509	.2369	1.3844
43.	0.19	0.2001	.1362	2'-0"	0.7346	.2759	1.4769
44.	0.19	0.2354	.1482	2'-0"	0.7942	.3084	1.5591

TABLE - 3 (Contd.)

Froude No. $F=V/\sqrt{gy}$	Critical Froude No. $F_c=V_c/\sqrt{gy}$	Particle Froude No. $F_d=V/\sqrt{gD_{50}}$	Critical partical Froude No. $F_{dc}=V_c/\sqrt{gD_{50}}$	d_t/b	Y/b	d_t/Y
9	10	11	12	13	14	15
0.4824	0.7843	2.4936	4.0539	0.88	0.502	1.76
0.5079	0.7979	2.7967	4.3932	0.99	0.57	1.74
0.5436	0.8161	3.1219	4.6867	1.14	0.62	1.84
0.5820	0.8349	3.4488	4.9475	1.28	0.66	1.94
0.3641	0.7141	3.1688	6.2147	1.13	0.562	1.86
0.4432	0.7624	3.9146	6.7346	1.36	0.624	2.14
0.4673	0.7760	4.3266	7.1846	1.57	0.686	2.29
0.4711	0.7781	4.5917	7.5845	1.726	0.76	2.27
0.2870	0.6596	3.9230	9.0170	1.21	0.71	1.70
0.3224	0.6857	4.5943	9.7716	1.444	0.792	1.87
0.3508	0.7052	5.1851	10.4245	1.682	0.86	2.03
0.3636	0.7137	5.6057	11.0047	1.880	0.942	2.08

TABLE - 4

Type of Pier : Sharp -nose

b, Width of pier = 0.164 ft

l, Length of pier = 0.492 ft

Run No.	Sediment Size D_{50}(mm)	Discharge Q_{max} (cfs)	Average Approach depth,Y (ft)	Channel Width,B (ft)	Average velocity, V (ft/sec)	Maximum scour depth from W.L. d_t(ft)	Critical velocity $V_c=\sqrt{gy_c}$
1	2	3	4	5	6	7	8
13.	0.94	0.1295	.0837	2'-0"	0.7736	.1329	1.2775
14.	0.94	0.1648	.0935	2'-0"	0.8813	.1493	1.3844
15.	0.94	0.2001	.1017	2'-0"	0.9838	.1614	1.4769
16.	0.94	0.2354	.1076	2'-0"	1.0939	.1837	1.5591
29.	0.40	0.1295	.0984	2'-0"	0.6578	.1706	1.2775
30.	0.40	0.1648	.1056	2'-0"	0.7803	.1969	1.3844
31.	0.40	0.2001	.1181	2'-0"	0.8472	.2228	1.4769
32.	0.40	0.2354	.1283	2'-0"	0.9174	.2452	1.5591
45.	0.19	0.1295	.1204	2'-0"	0.5378	.1575	1.2775
46.	0.19	0.1648	.1322	2'-0"	0.6233	.1843	1.3844
47.	0.19	0.2001	.1427	2'-0"	0.7011	.2133	1.4769
48.	0.19	0.2354	.1509	2'-0"	0.7799	.2356	1.5591

<center>TABLE - 4 (Contd.)</center>

Froude No. $F=V/\sqrt{gy}$	Critical Froude No. $F_c=V_c/\sqrt{gy}$	Particle Froude No. $F_d=V/\sqrt{gD_{50}}$	Critical Particle Froude No. $F_{dc}=V_c/\sqrt{gD_{50}}$	d_t/b	Y/b	d_t/Y
9	10	11	12	13	14	15
0.4712	0.7782	2.4549	4.0539	0.81	0.50	1.59
0.5079	0.7979	2.7967	4.3932	0.91	0.57	1.60
0.5437	0.8161	3.1219	4.6867	0.984	0.62	1.58
0.5877	0.8376	3.4713	4.9474	1.120	0.656	1.71
0.3695	0.7176	3.1999	6.2147	1.04	0.576	1.73
0.4232	0.7508	3.7959	6.7346	1.20	0.644	1.86
0.4345	0.7574	4.1213	7.1847	1.358	0.72	1.89
0.4514	0.7671	4.4628	7.5844	1.494	0.782	1.91
0.2731	0.6488	3.7960	9.0170	0.96	0.734	1.30
0.3021	0.6710	4.3995	9.7716	1.124	0.806	1.40
0.3271	0.6890	4.9486	10.4245	1.30	0.87	1.49
0.3538	0.7073	5.5048	11.0047	1.436	0.932	1.56

TABLE - 5

SCOUR DATA OF HARDINGE BRIDGE

Sl. No.	Date of scour.data observations	Mean surface velocity,	Mean Velocity (.85 times mean surface velocity), V(fps)	Maximum Scour depth from water level d_t(ft)	Maximum Scour depth below bed level, d_s(ft)	Approach depth Y, (ft)
1	2	3	4	5	6	7
1.	10.8.76	6.90	5.87	74.5	14.0	60.5
2.	24.7.76	5.97	5.08	66.6	13.6	53.0
3.	2.9.76	9.78	8.31	71.3	26.8	44.5
4.	9.9.77	7.67	6.52	82.4	11.9	70.5
5.	2.9.77	7.31	6.21	79.0	20.0	59.0
6.	25.8.77	7.19	6.11	66.1	8.6	57.5
7.	4.8.77	8.18	6.95	70.8	14.3	56.5
8.	21.7.77	7.14	6.07	61.8	6.8	55.0
9.	1.7.78	4.15	3.53	64.0	28.5	35.5
10.	9.7.78	4.69	3.99	63.8	33.8	30.0
11.	19.7.78	5.26	4.47	69.9	33.9	36.0
12.	19.7.78	5.73	4.87	69.9	29.4	40.5
13.	5.10.78	4.97	4.23	73.9	24.9	49.0
14.	12.10.78	3.91	3.32	80.5	33.0	47.5
15.	6.9.78	8.15	6.93	73.5	18.5	55.0
16.	13.9.78	10.08	8.57	82.5	27.5	55.0
17.	20.9.78	8.57	7.29	75.6	13.6	62.0
18.	2.8.78	6.72	5.71	79.3	30.3	49.0
19.	30.8.78	9.00	7.65	87.3	21.8	65.5

TABLE - 5(Contd.)

d_s/b	Y/b	Froude No. $F[= V/(gy)^{\frac{1}{2}}]$	Discharge per unit width, $q(= vy)$
8	9	10	11
0.378	1.635	0.1329	354.83
0.368	1.432	0.1228	268.95
0.724	1.203	0.2172	369.93
0.322	1.905	0.1368	459.625
0.541	1.595	0.1426	366.59
0.232	1.554	0.1420	351.41
0.386	1.527	0.1630	392.85
0.184	1.486	0.1442	333.79
0.770	0.959	0.1043	125.23
0.914	0.811	0.1283	119.59
0.916	0.973	0.1313	160.96
0.795	1.095	0.1349	197.26
0.673	1.324	0.1064	207.00
0.892	1.284	0.0850	157.87
0.500	1.486	0.1646	381.01
0.743	1.486	0.2036	471.24
0.368	1.676	0.1630	541.64
0.819	1.324	0.1438	279.89
0.589	1.770	0.1666	501.08

TABLE - 6

SCOUR DATA OF EAST-WEST INTERCONNECTOR

Caisson No.	Date of Scour depth observation	Maximum Water Surface level from Mean sea level	Velocity, V (fps)	Maximum Scour depth from top of the caisson	Maximum Scour below Water level d_t(ft)	Regime depth,Y (ft)
1	2	3	4	5	6	7
3	11-8-83	+27.60	4.50	45'-0"	33.10	16.82
3	29-7-83	+27.503	4.75	43'-0"	31.00	18.30
3	21-9-83	+31.60	3.75	33'-0"	25.10	12.65
4	8-6-83	+17.807	4.38	43'-0"	21.307	16.12
4	19-7-83	+25.960	6.00	53'-0"	39.46	26.36
4	11-8-83	+27.60	5.80	54'-0"	42.10	25.00
4	21-9-83	+31.60	2.25	53'-0"	45.10	5.69
5	8-6-83	+17.807	6.69	57'-0"	35.307	31.25
5	19-7-83	+25.960	6.50	56'-0"	42.46	29.87
5	29-8-83	+27.30	6.00	55'-0"	42.80	26.36
5	21-9-83	+31.60	4.50	60'-0"	52.10	16.82
6	19-7-83	+25.960	4.00	62'-0"	48.46	13.09
6	8-6-83	+17.807	4.32	59'-0"	37.307	15.78
6	17-8-83	+26.290	4.00	60'-0"	46.79	13.99
6	24-9-83	+30.50	1.50	35'-0"	26.00	3.02
7	4-6-83	+18.331	5.66	60'-0"	38.831	24.06
7	19-7-83	+25.96	8.00	66'-0"	52.46	41.32
7	13-8-83	+27.303	8.24	65'-0"	52.803	43.35
7	24-9-83	+31.11	5.00	70'-0"	61.61	19.82
8	29-7-83	+27.503	4.00	52'-0"	40.003	13.99
8	17-8-83	+26.23	4.50	55'-0"	41.73	16.82
8	26-9-83	+30.775	4.25	60'-0"	51.275	15.38

TABLE - 6(Contd.)

Scour depth below bed level d_s (ft)	d_s/b	Y/b	Froude Number F, $(=V/\sqrt{gy})$	Discharge per unit width $q(= vy)$
8	9	10	11	12
16.28	0.465	0.481	0.193	75.690
12.70	0.363	0.523	0.196	86.925
12.45	0.356	0.361	0.186	47.438
5.187	0.1482	0.461	0.192	70.606
13.10	0.374	0.753	0.206	158.160
17.10	0.489	0.714	0.204	145.00
39.41	1.126	0.163	0.166	12.803
4.057	0.116	0.893	0.211	209.063
12.59	0.360	0.853	0.210	194.155
16.44	0.470	0.755	0.206	148.160
35.28	1.008	0.471	0.193	75.690
34.470	0.985	0.399	0.188	55.960
21.527	0.615	0.451	0.192	68.170
32.800	0.937	0.399	0.188	55.960
22.98	0.657	0.086	0.152	4.53
14.771	0.422	0.687	0.203	136.180
11.140	0.318	1.181	0.219	330.650
9.453	0.270	1.239	0.221	357.638
41.790	1.194	0.566	0.198	99.100
26.013	0.743	0.399	0.188	55.960
24.910	0.712	0.481	0.193	75.690
36.350	1.039	0.439	0.191	65.365